Ultra-Lightweight Cement

Ninth Quarterly Technical Progress Report

September 30 to December 31, 2002

Fred Sabins

Issued January 31, 2003

DOE Award Number
DE-FC26-00NT40919

Submitted by Cementing Solutions, Inc.
4613 Brookwoods Drive
Houston, TX 77092

Disclaimer

Abstract

The objective of this project is to develop an improved ultra-lightweight cement using ultra-lightweight hollow glass spheres (ULHS). This report discusses testing that was performed for analyzing the alkali-silica reactivity of ULHS in cement slurries. DOE joined the Materials Management Service (MMS)-sponsored joint industry project "Long-Term Integrity of Deepwater Cement under Stress/Compaction Conditions." Results of the project contained in two progress reports are also presented in this report.

Table of Contents

Introduction

Oil well cementing involves placing a pumpable slurry of Portland cement, additives, and water into a wellbore. The slurry is pumped into the annular space between the borehole and a steel pipe (called a casing) that acts as a conduit from the reservoir to the surface. The setting of cement in place serves three important functions: (1) it supports the casing in the hole, (2) it isolates various formations from one another, and (3) it controls fluid movement within the well.

Typically, cement fluid density is anywhere from 12 to 17 lb/gal. Certain conditions that require the application of low-density cements can be encountered during the well construction process. Lower density is required (1) to limit hydrostatic pressure on the formation, and (2) to prevent the formation from fracturing and imbibing the well fluid. This phenomenon, known as lost circulation, increases drilling and completion times and increases construction cost because of the need for expensive remedial treatments. Lost circulation most commonly occurs in the upper sections of the well, where surface and intermediate casings are installed. Because formations covered by these casings are relatively close to the Earth's surface, application temperatures for these low-density cements are low.

The minimum density achievable with conventional cements and additives is approximately 11 lb/gal. At this density, the slurry's stability and set cement's strength and permeability are only marginally acceptable. Adding water to reduce the density of these conventional cements is impractical because additional water dilutes the cement, causing low strength and high permeability. Low temperatures, such as those in the upper well sections, delay strength development. To obtain a lower cement density or greater cement strength, ultra-lightweight materials must be mixed into the slurry.

Ultra-lightweight hollow spheres (ULHS) are excellent candidate materials for producing ultra-lightweight cements. These small hollow glass beads effectively trap air in the slurry, thereby lowering the slurry density without the addition of water. This project is designed to develop cementing systems using ULHS through a carefully designed program of modeling, design, laboratory testing, and field-testing.

The goals of this portion of the project are to study the long-term effects of the alkali-silica reaction in cements and to conduct a comprehensive evaluation of the ULHS from 3M and the potential for this product to be susceptible to ASR. The expansion and tensile strengths of 8 different cement specimens will be tested. The initial casting of the expansion specimens was unsuccessful, so the procedure has been modified to correct the existing flaws so that the expansion specimens can be recast successfully.

The DOE recently joined a Materials Management Service project that contains 14 oil and well service companies as sponsors and focuses on the performance of low-density cements used for controlling shallow water flows in deep water drilling conditions. The focus of this MMS JIP is on low density and low temperature, and it fits in with

lightweight cement project since both are concerned with long-term performance throughout the life of the well.

Executive Summary

Laboratory testing during the ninth quarter focused on evaluation of the alkali-silica reaction of 8 different cement compositions containing ULHS. The original laboratory procedure for measuring set cement expansion resulted in test specimen erosion that was unacceptable. This procedure has been modified and testing has been re-initiated.

This report provides the following information:

- ?? Alkali-Silica Reactivity Testing Progress
- ?? Presentation of MMS project data

Alkali-Silica Testing

Approval was made for a continuation of the current cooperative agreement with DOE. This extension consisted of a new task to study the long-term effects of the Alkali-Silica Reaction (ASR) in ULHS cements. The goal of this task is to determine procedures and methods from the construction industry that are applicable to oil well cements, and conduct long-term tests to verify if ASR is occurring and when and how it manifests itself. Compositions to be tested and test procedures in the ASR evaluation are listed in Appendix A.

ASR testing included preparation of tensile strength, compressive strength, and expansion specimens. The expansion specimens failed as they were originally poured. The ULHS cements experienced segregation and erosion while in the curing bath. All of the TXI lightweight cement specimens failed (broke) while in the curing bath, which may indicate expansion due to the alkali silicate reaction. The specimens were then recast with modified mold covers. Standard ASTM molds were used for all specimens with the exception of the TXI lightweight cement. The TXI lightweight cement used a non-standard volumetric expansion mold. While different specimen configurations are not directly comparable, two sets of other compositions were cast using each mold type to provide a comparison.

Preliminary compressive strength and tensile strength data were gathered. However, this testing was stopped when the expansion specimen failure was discovered, and this testing was re initiated also to be in sync with the expansion testing. It was decided to hold presentation of these initial data until the next report so that a more complete data suite would be available for analysis.

Contribution of the MMS Data

The data collected in the MMS JIP deals with the durability of various cements under thermal and pressure cycling. The major focus of the testing is the determination of the mechanical properties of the cement to obtain the durability. Cement compositions tested in the MMS project are outlined in Table 2. Reports 2 and 3 contain all of the data and are attached in Appendix B.

The major focus of current work is obtaining an accurate measurement of the Poisson's Ratio and the durability of the cement across soft formations during temperature and pressure cycling.

Conclusions

1. At this point in the project, usable ASR test specimens have been poured.
2. The testing regime is on schedule.
3. The MMS data will expand the database for the durability of lightweight cement.

1. List of Acronyms and Abbreviations

API—American Petroleum Institute
ASR—alkali-silica reactivity
ASTM—American Society for Testing and Materials
Bc—Bearden units of consistency
BHCT—bottomhole circulating temperature
BHST—bottomhole static temperature
BWOC—by weight of cement
$CaCl_2$—chemical formula for calcium chloride
cp—centipoise
gal—gallon
H_2O—chemical formula for water
hr—hour
ID—inner diameter
in.—inch
J—Joule
lb—pound
md—millidarcy
min—minute
MMS—Minerals Management Service
OD—outer diameter
psi—pound per square inch
rev—revolution
rpm—revolutions per minute
s—second
sk—sack of cement
QC—quality control
TXI—Texas Industries
TXI LW—manufactured lightweight cement available from TXI
ULHS—ultra-lightweight hollow (glass) spheres
3K—3,000-psi designation
6K—6,000-psi designation

References

1. API Recommended Practice 10B: "Recommended Practices for Testing Well Cements," 22nd Edition, American Petroleum Institute, Washington, D.C., December 1997.

Appendix A—Alkali-Silica Reactivity (ASR) Testing

Objective

The goals of this project are to study the long-term effects of the alkali-silica reaction in cements and to conduct a comprehensive evaluation of the ULHS from 3M and the potential for this product to be susceptible to ASR.

Alkali-silica reactivity (ASR) is a chemical reaction that occurs between alkali and reactive silica present in cement and concrete mixes. When this reaction occurs, a gel is formed that absorbs available water and increases internal pressure, eventually causing the cement to fracture. This fracturing renders the cement vulnerable to several hazardous materials that can severally weaken the structure of the cement matrix causing it to fail.

Testing Procedures

A variation of the Length Change of Hardened Hydraulic-Cement Mortar and Concrete (ASTM C157-93) methods was used to test expansion in the slurries. An expansion measurement is taken at 24 hours, 7 days, 14 days, 28 days and every consecutive month for the duration of the project. For statistical purposes, six replicates of each slurry are made.

A variation of Splitting Tensile Strength of Cylindrical Concrete Specimens (ASTM C496-90) methods were used to determine a change in the tensile strength of specimens as a result of ASR. A tensile strength measurement is performed at 24 hours, 7 days, 28 days, 2 months, 4 months, and 6 months. For statistical purposes, nine replicates of each slurry are made.

Test Slurry Composition

As a baseline for testing, neat Class H cement with a density of 16.4 lb/gal and TXI Lightweight cement with a density of 13.5 lb/gal will be used. Ultra-light hollow sphere (ULHS) slurries with similar bead concentrations and a density of 9.0 lb/gal will also be used. Several 0.5% sodium chloride slurries will be used to evaluate accelerated ASR.

Neat Slurries (Baseline)

- Class H cement mixed with 4.3 gal of fresh water per sack to achieve a density of 16.4 lb/gal
- TXI Lightweight cement mixed with 6.0 gal of fresh water per sack to achieve a density of 13.5 lb/gal

Ultra-Light Hollow Sphere (ULHS) Slurries

- Class H cement plus 42.14% BWOC 3M 6K (6,000 psi) beads mixed with 11.81 gallons of fresh water per sack for a density of 9.0 lb/gal
- TXI Lightweight cement plus 37.19% BWOC 3M 6K (6,000 psi) beads mixed with 12.63 gallons of fresh water per sack for a density of 9.0 lb/gal

Salt Slurries

- Class H cement plus 0.5% BWOC NaCl mixed with 4.3 gallons of fresh water sack for a density of 16.4 lb/gal
- TXI Lightweight cement plus 0.5% BWOC NaCl mixed with 6.0 gallons of fresh water per sack for a density of 13.5 lb/gal
- Class H cement with 42.14% BWOC 3M 6K (6,000 psi) beads plus 0.5% BWOC NaCl mixed with 11.81 gallons of fresh water per sack for a density of 9.0 lb/gal
- TXI Lightweight cement with 37.19% BWOC 3M 6K (6,000 psi) beads plus 0.5% BWOC NaCl mixed with 12.63 gallons of fresh water per sack for a density of 9.0 lb/gal

Testing Conditions

- Application No. 3 – 128°F / 174°F (BHCT/BHST)
- Slurries were tested for a minimum of 200 days.

Mixing Procedures

Prepare a ULHS slurry as follows.

1. Weigh the appropriate amounts of the cement sample, additives, water, and ULHS into separate containers.
2. Mix the cement slurry according to Appendix A of API RP 10B.
3. Pour the slurry into a metal mixing bowl and slowly add ULHS while continuously mixing by hand with a spatula. Mix thoroughly.
4. Place this slurry in a Waring blender and mix at 4,000 rpm for 15 seconds. Then, return each specimen to lime-saturated water.

Alkali-Silica Reactivity (ASR) Testing for Expansion

Curing the Specimens

One of the test slurries (containing six replicates) is prepared per day until all samples for the project have been made. Cure each test specimen in a heated, circulating water bath containing saturated-lime curing water, as described in the procedure below.

1. Remove specimens from the molds at an age of 23 1/2 hours. Age of each specimen is measured from the moment when water is added to the cement during the mixing operation.
    - Never strike or jar a specimen during removal.
    - Never exert pressure directly against the gage studs.
    - Make sure the gage stud holder remains attached to the stud during specimen removal.

Important—To avoid damaging the specimens during removal from the molds, it may be necessary to leave the specimens in the molds for more than 24 hours. This is especially true for certain slow-hardening cements. If the curing schedule must be extended, make sure that the same curing time is used for all other specimen to be compared, and that all

comparison specimens are within ±1/2 hour of the same age at the time the initial comparator reading is performed.

2. Mark specimens for identification or positioning as required with a soft graphite pencil, a graphite liquid that deposits graphite without binder, or waterproof, indelible ink. Never use any other writing instrument.
3. Place the specimens in lime-saturated water maintained at 73.4 ±°F (23.0 ± 0.5°C) for a minimum of 15 min. This helps minimize variation in length measurements due to variation in temperature of the specimens.
4. When the specimens are 24 ± ½ hours in age, remove them from water storage one at a time, wipe with a damp cloth, and immediately take a comparator reading. Then, return each specimen in lime-saturated water.

Important—Monitor the curing water weekly to ensure that the lime concentration of the saturated aqueous solution is at 1,600 mg/L, +/- 300 mg/L.

Apparatus

Molds for cement specimen curing have one section and are constructed as shown in Fig. 6. Molds for test specimens used in determining the length change of cement pastes and mortars produce 1 ? 1 ? 11 ¼-in. prisms with a 10-in. gage length. The gage length is the nominal length between the innermost ends of the gage studs. The parts of the molds should fit tightly and firmly together when assembled, and their surfaces should be smooth and free of pits.

The molds are made of steel not readily attacked by the cement paste, mortar, or concrete. The sides of the molds should be sufficiently rigid to prevent spreading or warping. For the molds shown in Fig. 6, the tolerance on dimension A is ±0.03 in. Each end plate of the mold is equipped to hold properly in place during the setting period.

The gage studs are of American Iron and Steel Institute (AISI) 3 Type 316 stainless steel. To prevent restraint of the gage studs before the specimen is removed, the device for holding the gage studs in position is arranged such that it can be partially or completely released after the slurry compacts in the mold. The gage studs are set so their principal axes coincide with the principal axis of the test specimen. For the molds shown in Fig. D-1, gage studs extend into the specimen 0.625 ± 0.025 in. and the distance between the inner ends of the gage studs is 10.00 ± 0.10 in. Ten inches is the gage length for calculating length change.

Test Measurement

The comparator for the molds shown in Fig. D-1 features a dial micrometer or other measuring device graduated to read in 0.0001-in. units, accurate within 0.0001 in. in any 0.0010-in. range, and within 0.0002 in. in any 0.0100-in. range, and sufficient range (at least 0.3 in.) in the measuring device to allow for small variations in the actual length of specimens. The terminals of the comparator are plane, polished, and heat-treated, and are fitted with collars held in place with set screws. The collars extend 0.062 ± 0.003 in.

beyond the plane face of the terminal and have an inside diameter 0.02 in. greater than the average diameter of the portion of the gage studs that must fit into the collars.

The comparator must allow the checking of the measuring device against a reference bar at regular intervals. The reference bar has an overall length of 11 5/8 ±1/8 in. for the specimen in use. The bar is made of a steel alloy with a coefficient of thermal expansion not greater than two millionths per degree Celsius. Each end of the reference bar is fitted with heat-treated, hardened, and polished tips machined to the same shape as the contact end of the gage studs used in test specimens.

Reference Bar

Place the reference bar (Fig. D-2) in the instrument in the same position each time a comparator reading is taken. Check the dial gage setting of the measuring device by taking a comparator reading of the reference bar at least at the beginning and end of a series of specimen readings to span no more than a half-day, provided the apparatus is kept in a room maintained at constant temperature.

To obtain a comparator reading, perform the following steps.

1. Clean the hole in the base of the comparator into which the gage stud on the lower end of the bar fits.
2. Read and record the comparator indication of the length of the reference bar.
3. Take one bar out of immersion, blot the pins, place the bar in the comparator, read, and record the indication.
4. Return the bar to immersion and clean the hole in the base of the comparator.
5. Repeat the procedure with second and subsequent bars until all bars have been read, returned to immersion, and the readings recorded.
6. After reading the last bar, clean the hole in the comparator base and read and record the reference-bar indication. Blot only around the pins.

Calculate the specimen length change at any age as follows:

$$L = \frac{(L_x - L_i)}{G} ? 100$$

Where:
L = change in length at *x* age, %
Lx = comparator reading of specimen at *x* age minus comparator reading of reference bar at *x* age;
Li = initial comparator reading of specimen minus comparator reading of reference bar at that same time
G = nominal gage length, 10 in.

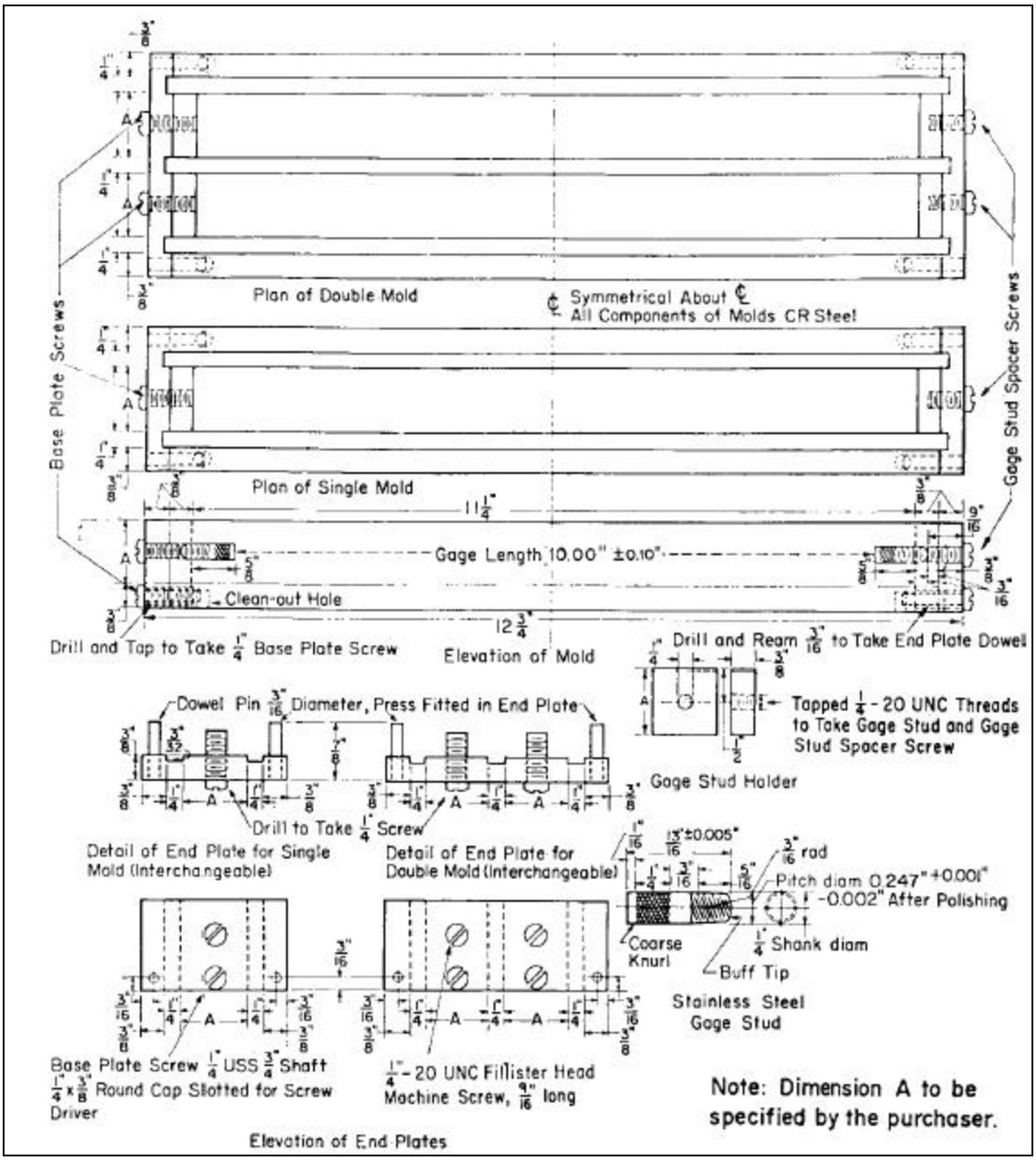

Figure D-1—Test specimen mold schematics

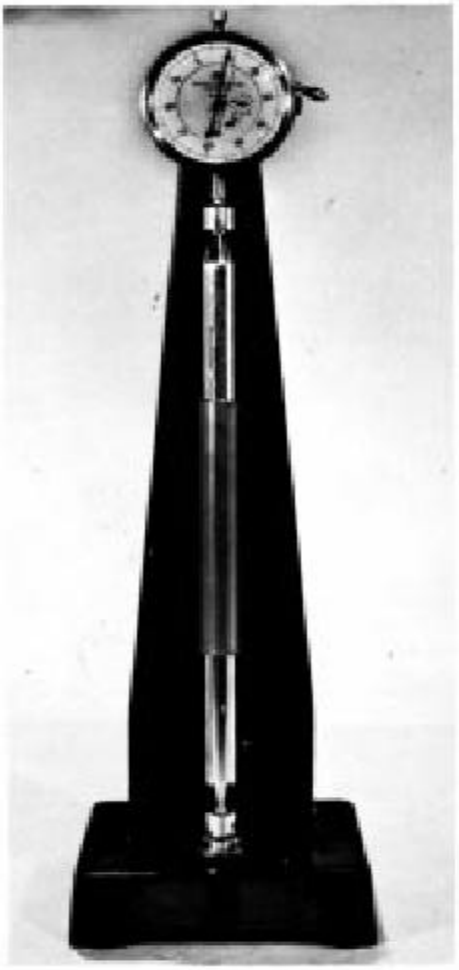
Type of Suitable Apparatus for Measurement of Length Changes

Figure D-2—Reference bar

Alkali-Silica Reactivity (ASR) Testing for Tensile Strength

The testing method used is similar to that described in ASTM C496-90 (Standard Test Method for Splitting Tensile Strength of Cylindrical Concrete Specimens). For this testing, the slurry is placed in a 1.5 ? 5-in. mold sealed at both ends.

Curing the Cement Specimens

One of the test slurries (containing six replicates) is prepared per day until all samples for the project have been made.

Prepare the molds as follows.

1. Place slurry in a mold, filling to approximately one-half of the mold depth, and puddle it.
2. Stir the remaining slurry by hand and place into additional molds and repuddle it.

3. Seal the molds and place them upright in a heated, circulating water bath at the appropriate curing temperature.
4. Remove specimens from the molds at an age of 23 1/2 hours. Age of each specimen is measured from the moment when water is added to the cement during the mixing operation.

Important—To avoid damaging the specimen during removal, it may be necessary to leave specimens in the molds for more than 24 hours. This is especially true for certain slow-hardening cements. If the curing schedule must be extended, make sure that the same curing time is used for all other specimen to be compared, and that all comparison specimen are within ±1/2 hour of the same age at the time the initial comparator reading is performed.

Test Measurement

After curing, the sample is extracted from the mold and cut into 1-in. ±1/8 in. sections in length. The density of each sample is measured before it is measured for tensile strength.

A ¼-in. section of the top surface of the sample is cut first. Next, the three 1-in.sections to be measured are cut. Each 1-in. ±1/8 in. section is identified as top, middle, and bottom and is measured for tensile strength in the test machine. The remaining sample pieces are discarded. Fig. D-3 shows a general schematic of how each specimen is oriented on its side during testing. The force applied to the specimens is automatically controlled and applied at a constant rate of approximately 0.025mm/hr. This testing is carried out at Westport Technology Center.

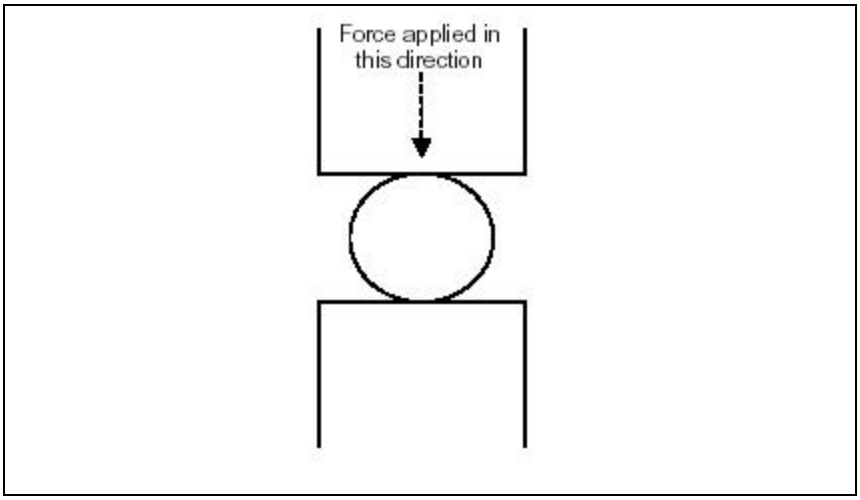

Figure D-3—Tensile Strength Crush Diagram

Appendix B

FINITE ELEMENT ANALYSIS OF CEMENT SYSTEMS UNDER STRESS CONDITIONS

The following system configurations have been studied (as described in the MMS project report) using 3D finite element modeling (Fig.1):

1. Pipe-in-pipe (Inner Steel Pipe + Cement + Outer Steel Pipe)
2. Pipe-in-soft (Inner Steel Pipe + Cement + Outer Plastisol layer)

The following stress conditions have been studied:

1. Normal production operation
2. Internal casing pressure (Pressure cycling)
3. Subsidence, Compaction (Confining pressure)
4. Thermal stress (Temperature cycling)

Parametric study for a variety of cement types (Young's modulus and Poisson ratio) and cement thickness have also been performed.

Assumptions

1. The system can be modeled using linear elastic theory.
2. The composite system retains continuity at the interfaces (Fig.2).
3. The system is axi-symmetric because of the boundary conditions.
4. All materials are homogeneous and continuous.
5. Plastisol has the same material properties as that of rubber.
6. Plane stress condition is valid.

I. PIPE-IN-PIPE

1. Casing Pressure

Casing pressure is varied from 100 psi to 10000 psi.
Young's Modulus = 5000 psi
Poisson Ratio = 0.35
Confining Pressure = 0 psi
Cement Thickness = 1"
No temperature gradient.

Discussion

The principal stress and displacement profiles are shown in Fig.3 through Fig.7, for casing pressures of 100, 500, 1000, 5000 and 10,000 psi. In all the above cases, no confining pressure or temperature gradient is applied to isolate the effect of casing pressure on the stress distribution. As a result, most of the stress distribution is within the high modulus inner pipe. Comparatively, the cement layer in series with the inner pipe experiences reduced loads and hence smaller displacements. The axi-symmetry of the loading conditions uniformly stresses the composite system in the same direction, due to which no tensile forces are experienced.

2. Confining Pressure

Confining pressure is varied from 100 psi to 1000 psi.
Young's Modulus = 5000 psi
Poisson Ratio = 0.35
Casing Pressure = 500 psi
Cement Thickness = 1"
No temperature gradient.

Discussion

Fig. 8 through Fig. 10 shows the stress and displacement fields for confining pressures of 100, 500 and 1000 psi. No temperature gradient is present. The high modulus inner and outer pipes reduce the effect of the load felt by the cement in each case, as a result of which very little stress variation is observed in the cement layer. Also, the compressive stress produces displacements in opposite directions at the two peripheries, with a stationary front in between.

3. Cement Thickness

Cement thickness is varied from 1" to 7.5"
Young's Modulus = 5000 psi
Poisson Ratio = 0.35
Confining Pressure = 500 psi
Casing Pressure = 500 psi
No temperature gradient.

Discussion

Fig. 11 through Fig. 13 shows the stress and displacement fields for varying cement thickness (1, 3.5, 5.5 and 7.5"). No temperature gradient is included. Again, most of the stress variation is within the higher modulus inner and outer pipes. As the cement thickness is increased, the displacement values are observed to rise as a result of more flexible material present to accommodate the stress. This suggests that the cement may actually lose contact with the steel pipe at the interface and hence the annular seal, when large displacements are observed. It is required to study this system with appropriate large displacement interface elements with sufficient description of interface bonding.

4. Young's Modulus

Young's Modulus is varied from 1000 psi to 7000 psi.
Poisson Ratio = 0.35
Confining Pressure = 500 psi
Casing Pressure = 500 psi
Cement Thickness = 1.5"
No temperature gradient.

Discussion

The cement's Young's modulus is varied (1000, 3000, 5000 and 7000 psi) and the stress/displacement profiles are shown in Fig. 14 through Fig. 16. Due to the high modulus inner and outer pipes sandwiching the low modulus cement, very little stress variation is seen in the cement for different Young's moduli. The change in displacement fields is also marginal. However, if one of the adjacent layers is of comparable or lesser Young's modulus than the cement (as in the Pipe-in-Soft case), a significant stress contrast will be observed.

5. Poisson Ratio

Poisson Ratio is varied from 0.15 to 0.45.
Young's Modulus = 5000 psi
Confining Pressure = 500 psi
Casing Pressure = 500 psi
Cement Thickness = 1.5"
No temperature gradient.

Discussion

The cement's Poisson ratio is varied (0.15, 0.25, 0.35 and 0.45) and the stress/displacement profiles are shown in Fig. 17 through Fig. 19. As in the previous case, very little stress variation is seen within the cement layer itself. However, the arrest of continuity of plane stress is observed sharply at the interfaces. Negligible effect is felt due to an increase in Poisson ratio as it not the limiting property under these simulation conditions.

6. Thermal Stress

Young's Modulus = 5000 psi
Poisson Ratio = 0.35
Confining Pressure = 500 psi
Casing Pressure = 500 psi
Cement Thickness = 1"

T_{out} = 68? F

T_{in} is varied from 80? F to 180? F.

Discussion

The stress and displacement profiles are shown in Fig.20 through Fig.23 for varying internal temperature (80, 110, 150 and 180? F). The thermal stress and the compressive stress act in opposite directions (especially near the outer boundary) and as a result, the net displacement is along the more dominant stress direction. As the internal temperature increases, the thermal stress dominates close to the inner boundary.

II. PIPE-IN-SOFT

1. Casing Pressure

Casing pressure is varied from 500 psi to 5000 psi.
Young's Modulus = 5000 psi
Poisson Ratio = 0.35
Confining Pressure = 500 psi
Casing Pressure = 500 psi
Cement Thickness = 1"
Plastisol Thickness = 0.5"
No temperature gradient.

Discussion

Fig.24 through Fig.26 show the stress and displacement profiles for varying casing pressure (500, 1000 and 5000 psi). For the range of casing pressures considered here and the simulation conditions, significant variation is seen in the stress distribution due to an increase in the casing pressure. Most of the casing pressure load is transferred across the cement layer and consequently to the low modulus plastisol (soft formation).

Fig.1. 3-D Finite element modeling

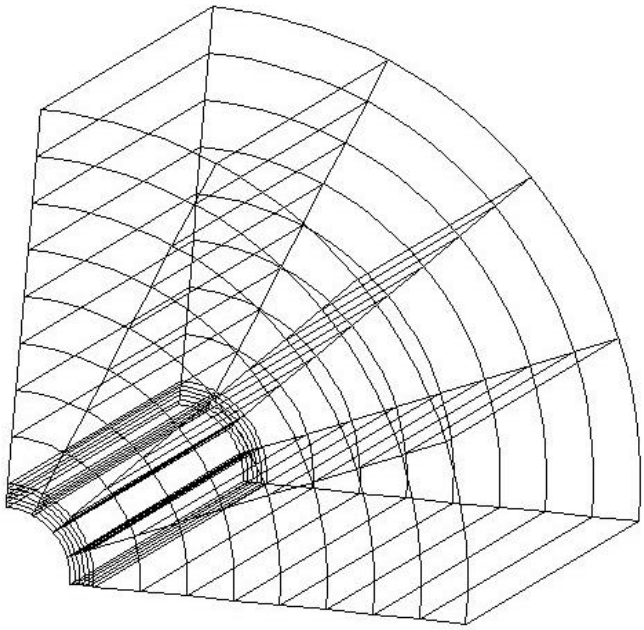

Fig.2. Total mesh displacement (normal operation)

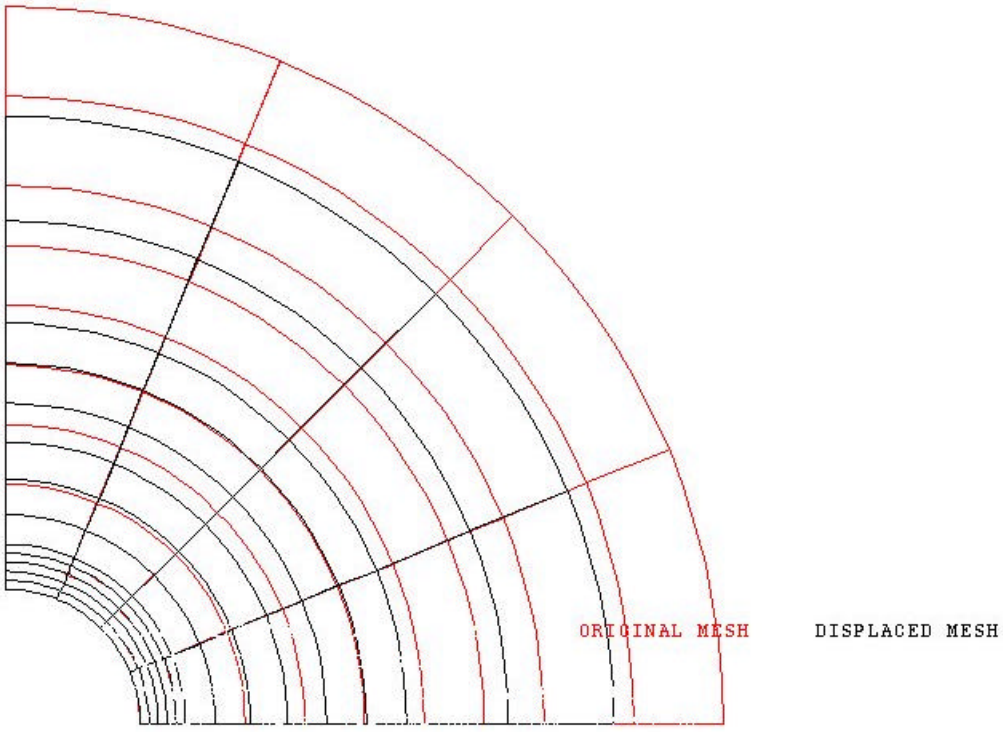
ORIGINAL MESH
DISPLACED MESH

Fig.3a First principal stress profile (Casing Pressure = 100 psi)

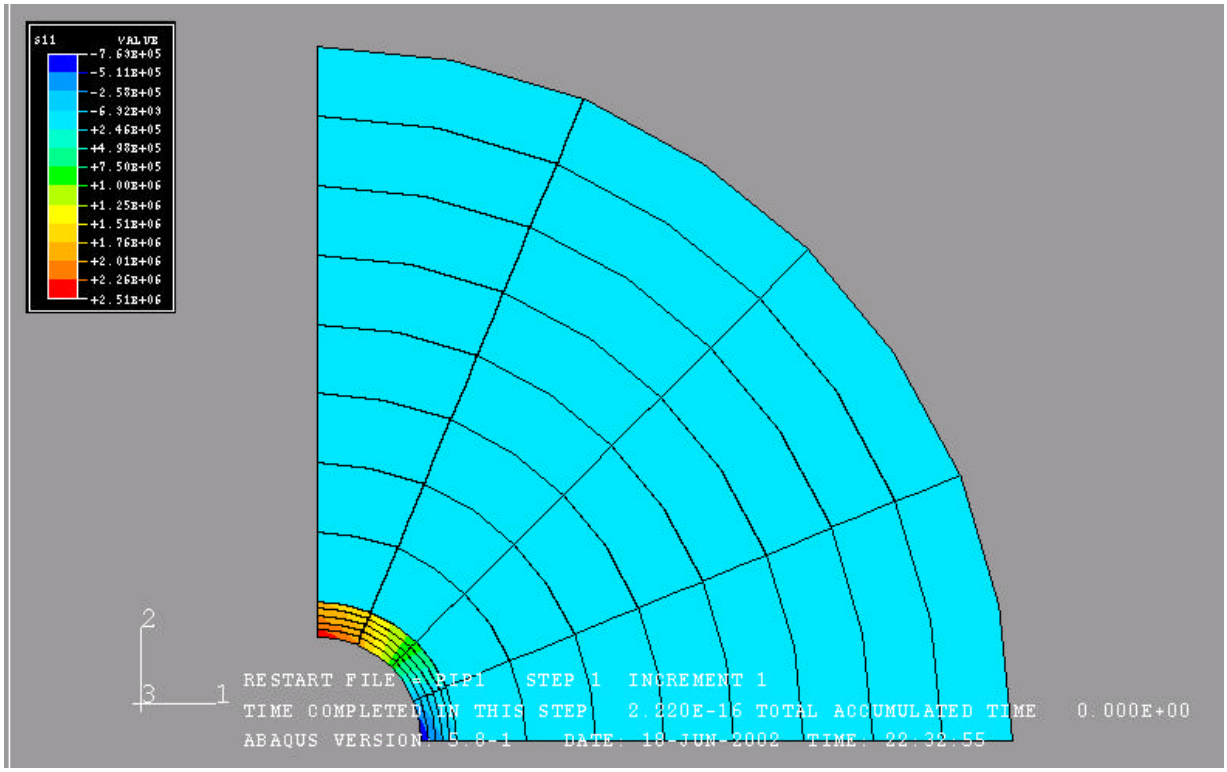

Fig.3b Second principal stress profile (Casing Pressure = 100 psi)

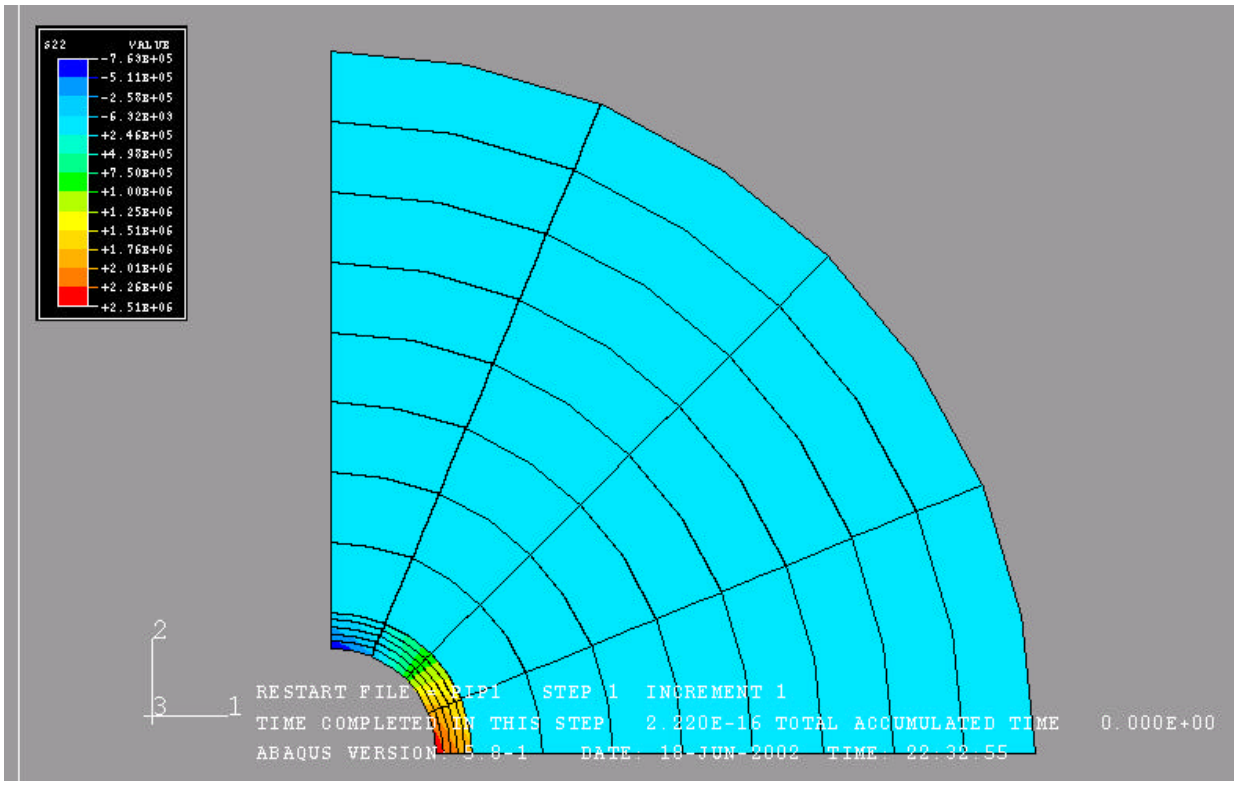

Fig.3c Horizontal displacement field (Casing Pressure = 100 psi)

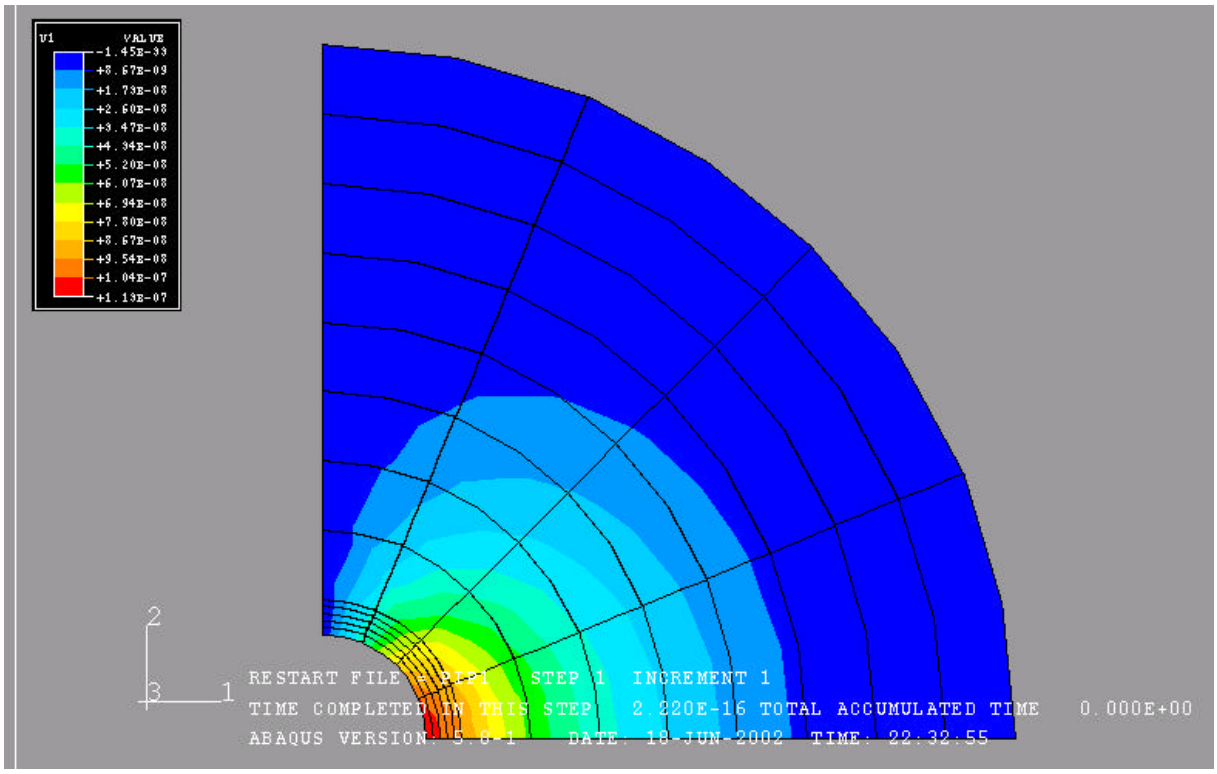

Fig.3d. Vertical displacement field (Casing Pressure = 100 psi)

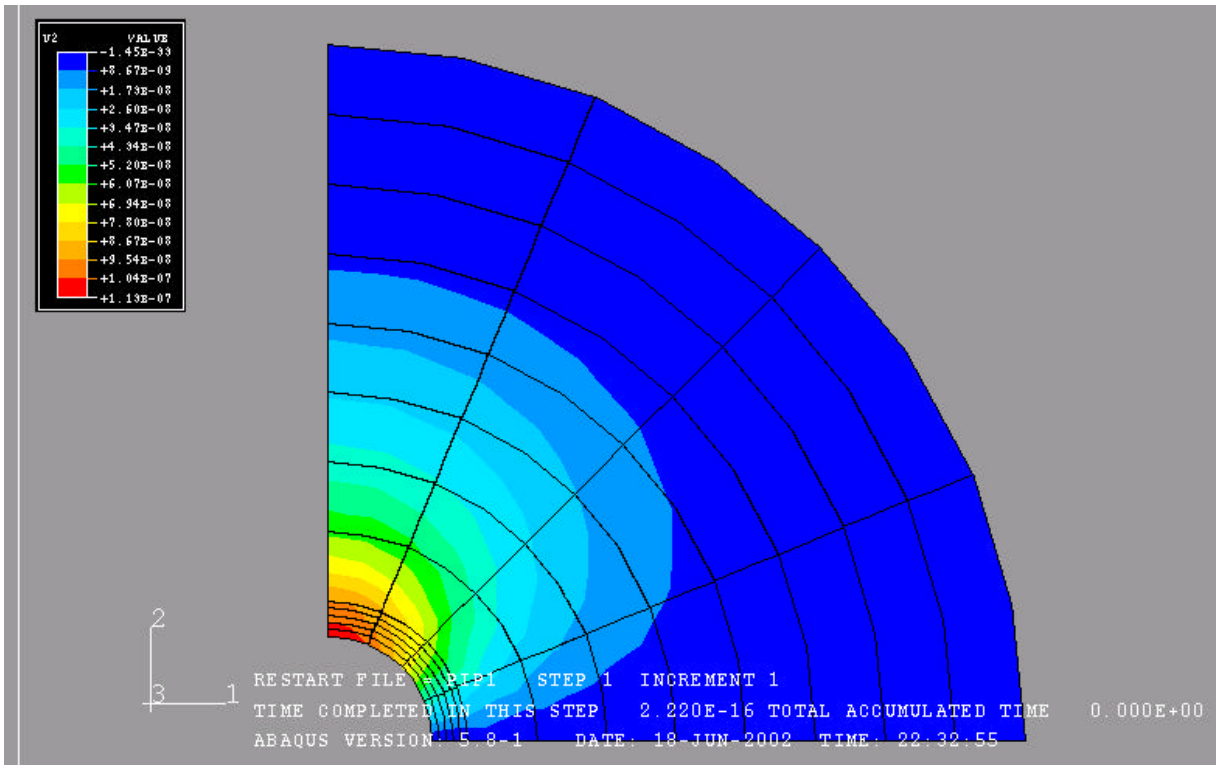

Fig.4a First principal stress profile (Casing Pressure =500 psi)

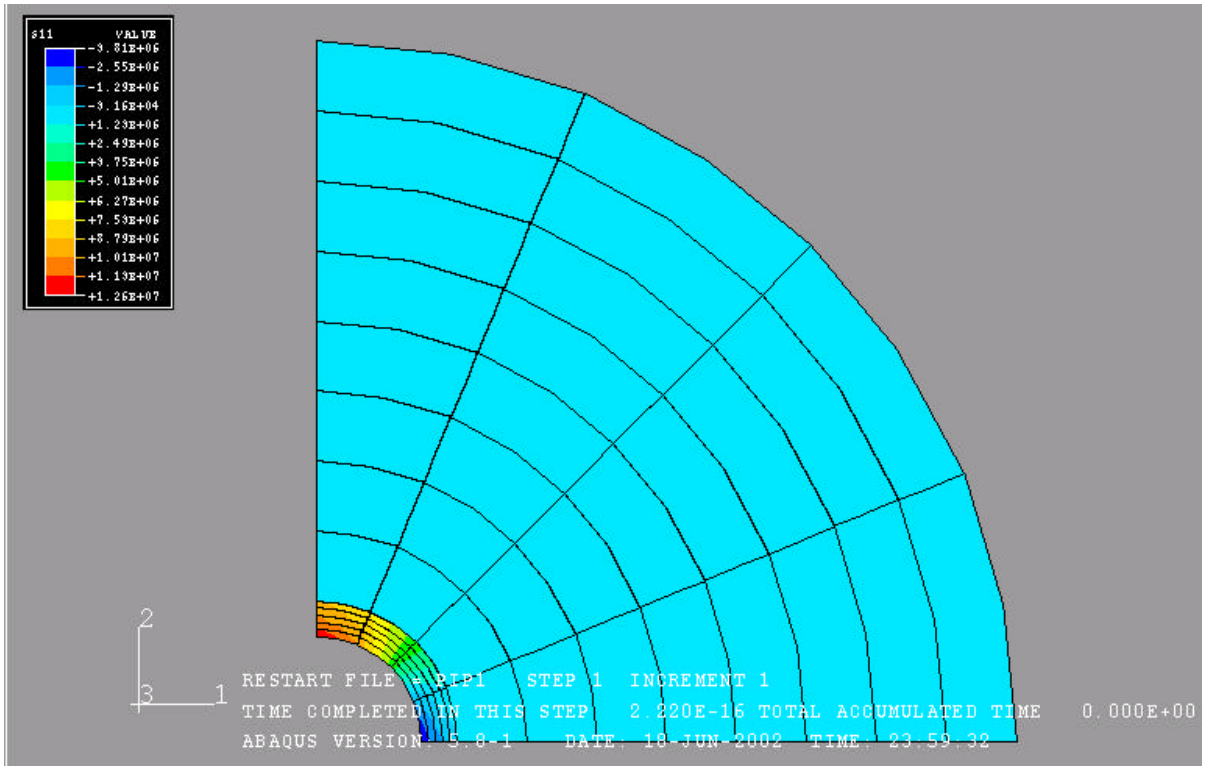

Fig.4b Second principal stress profile (Casing Pressure = 500 psi)

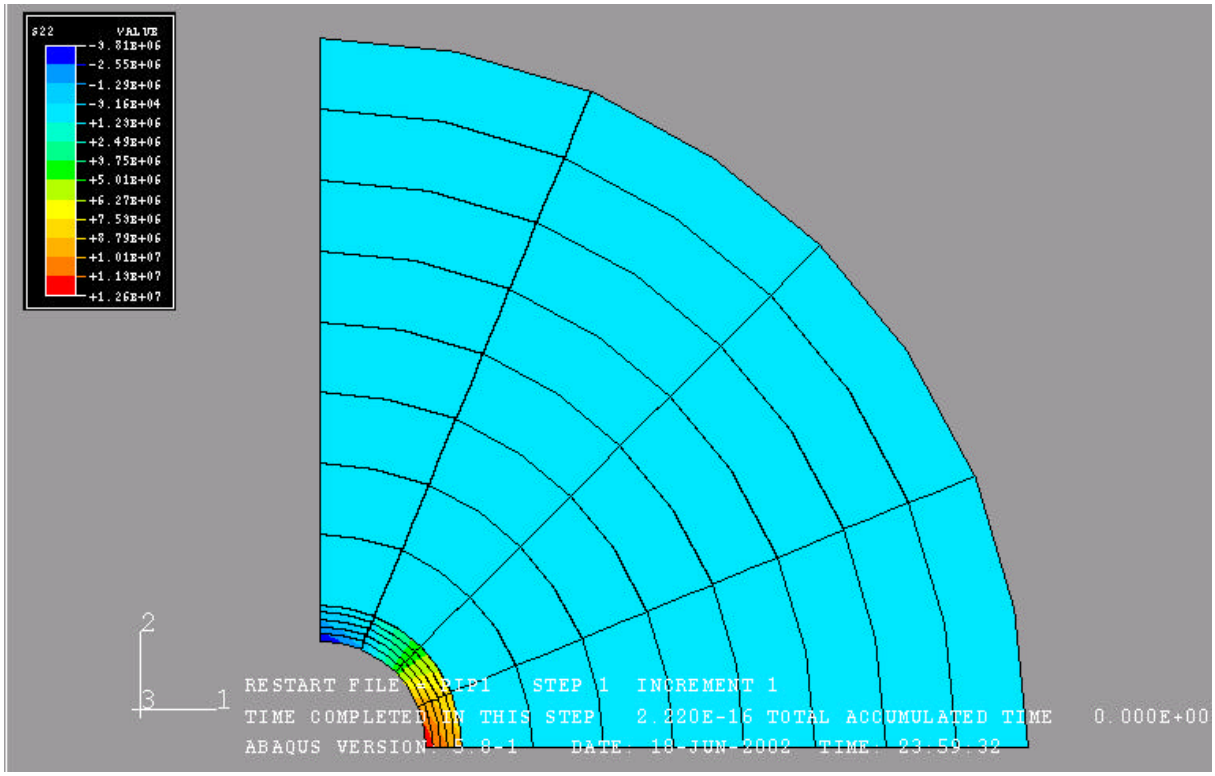

Fig.4c Horizontal displacement field (Casing Pressure = 500 psi)

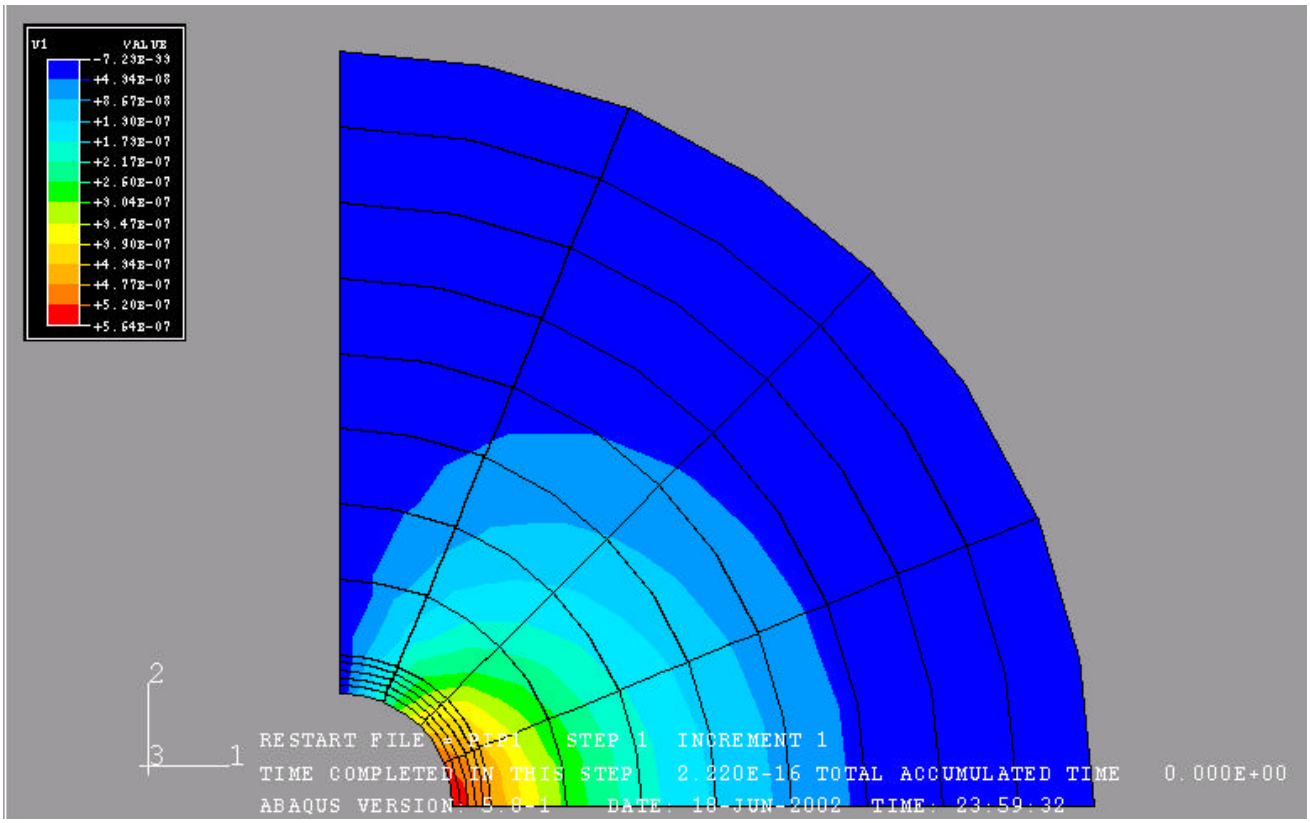

Fig.4d Vertical displacement field (Casing Pressure = 500 psi)

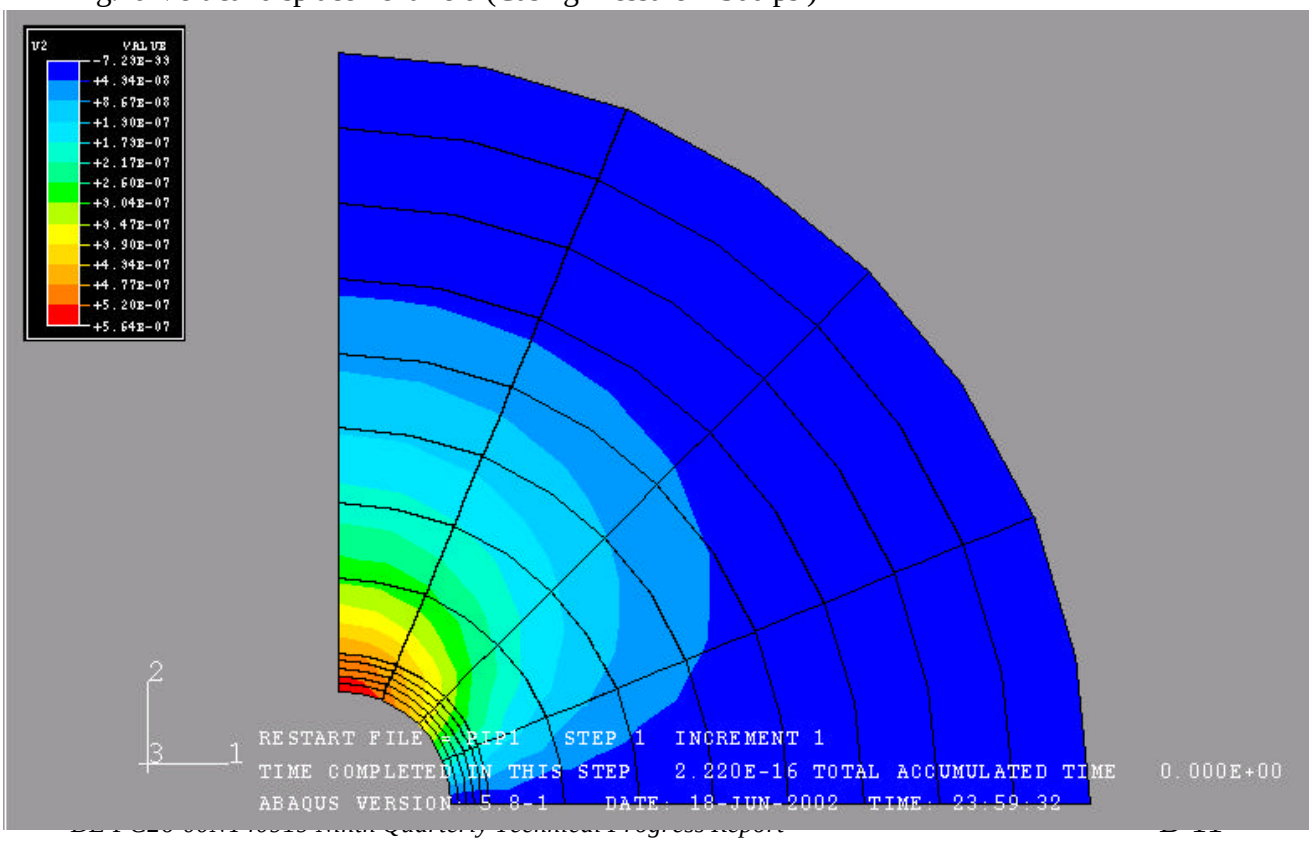

Fig.5a First principal stress profile (Casing Pressure = 1000 psi)

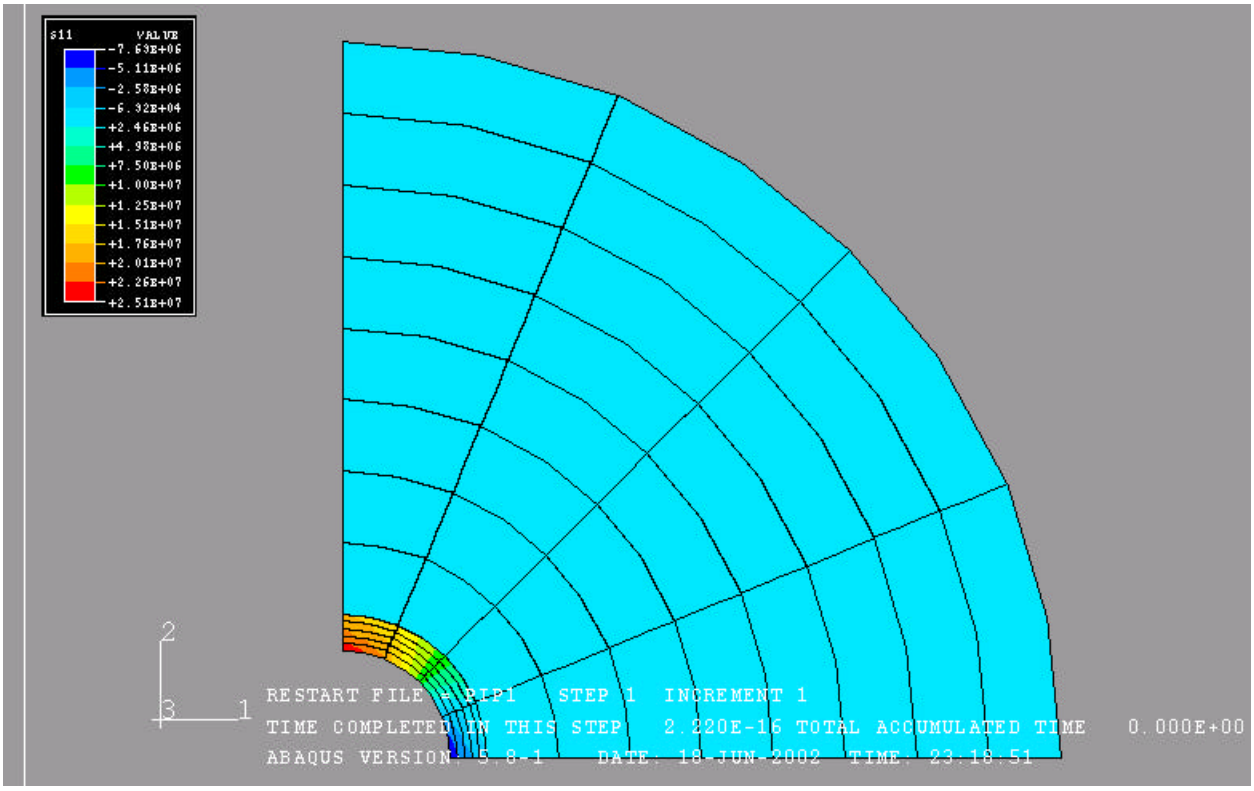

Fig.5b Second principal stress profile (Casing Pressure = 1000 psi)

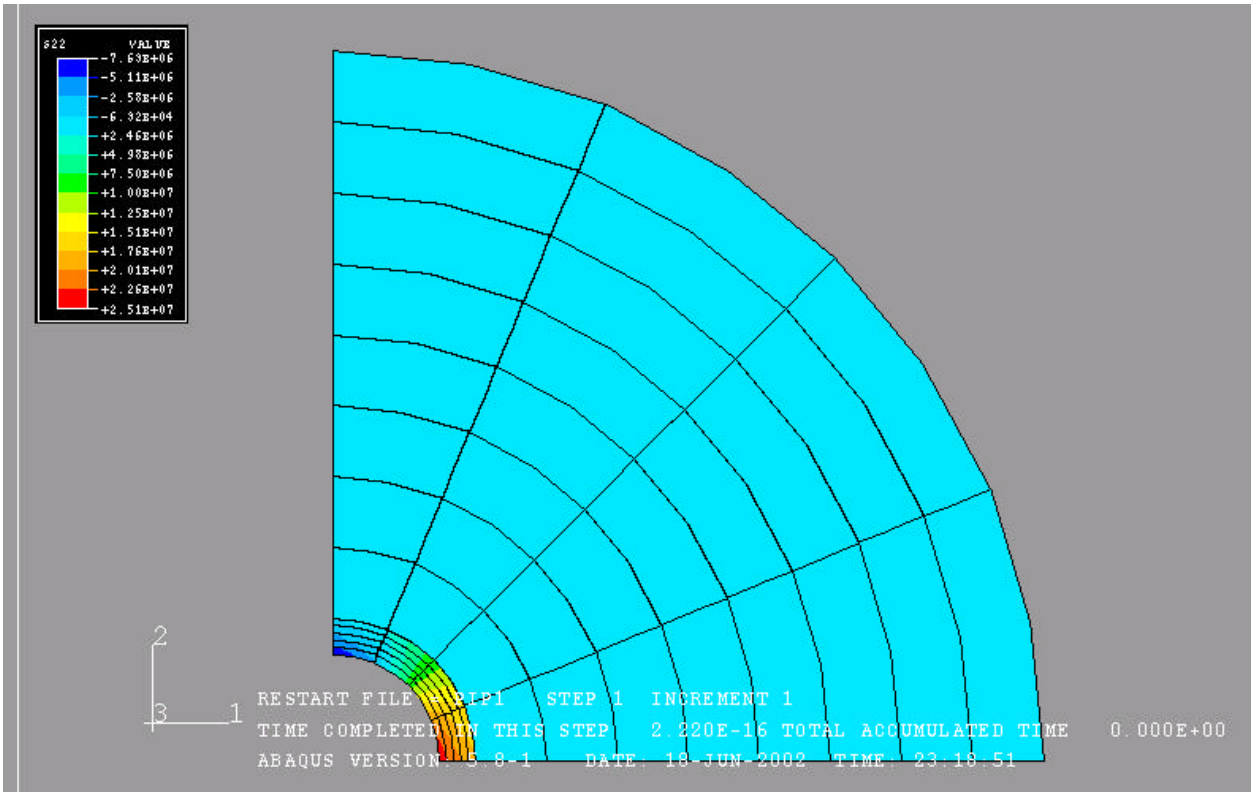

Fig.5c Horizontal displacement field (Casing Pressure = 1000 psi)

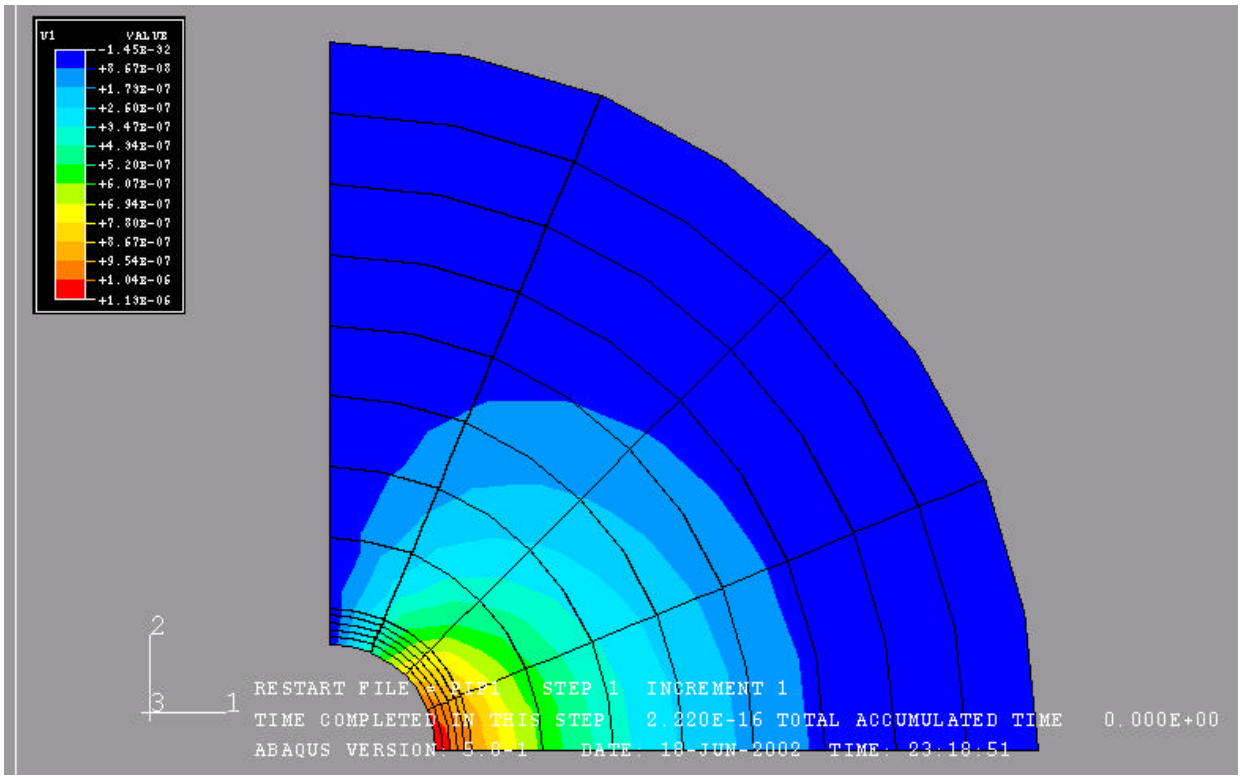

Fig.5d Vertical displacement field (Casing Pressure = 1000 psi)

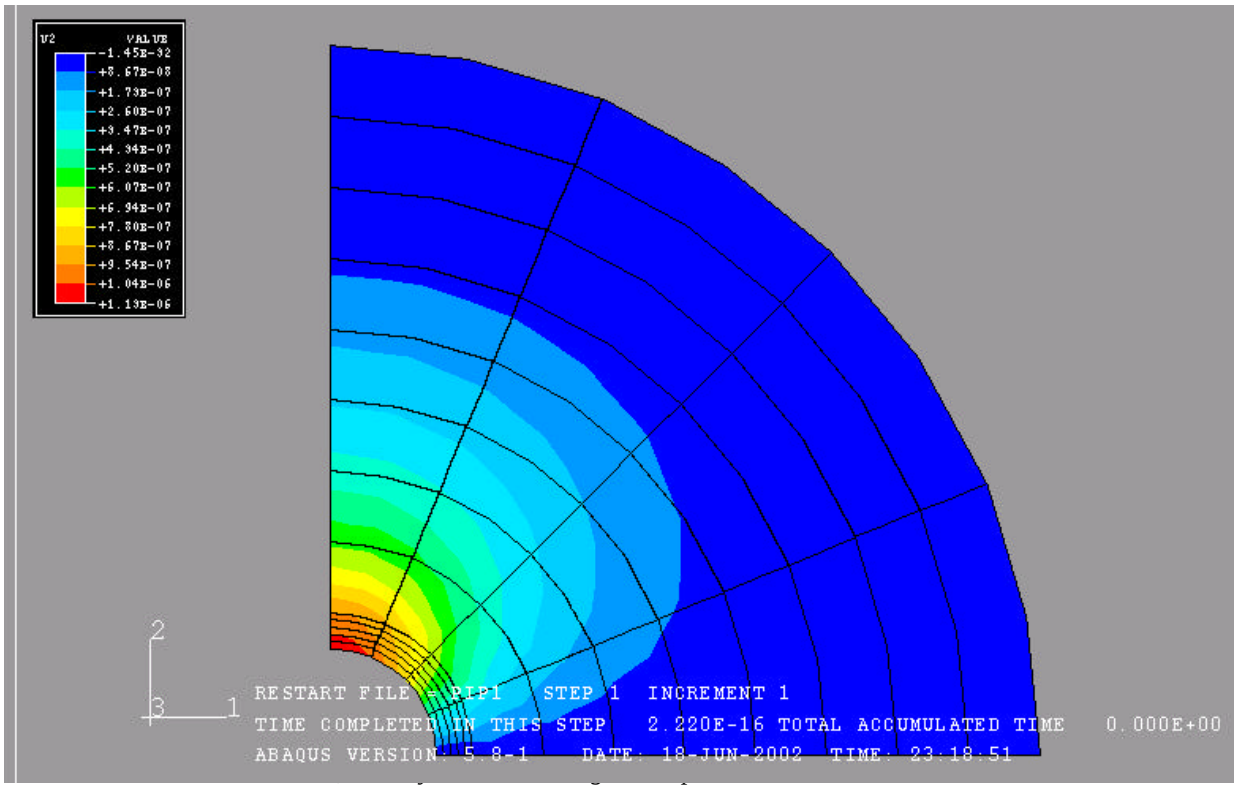

Fig.6a First principal stress profile (Casing Pressure = 5000 psi)

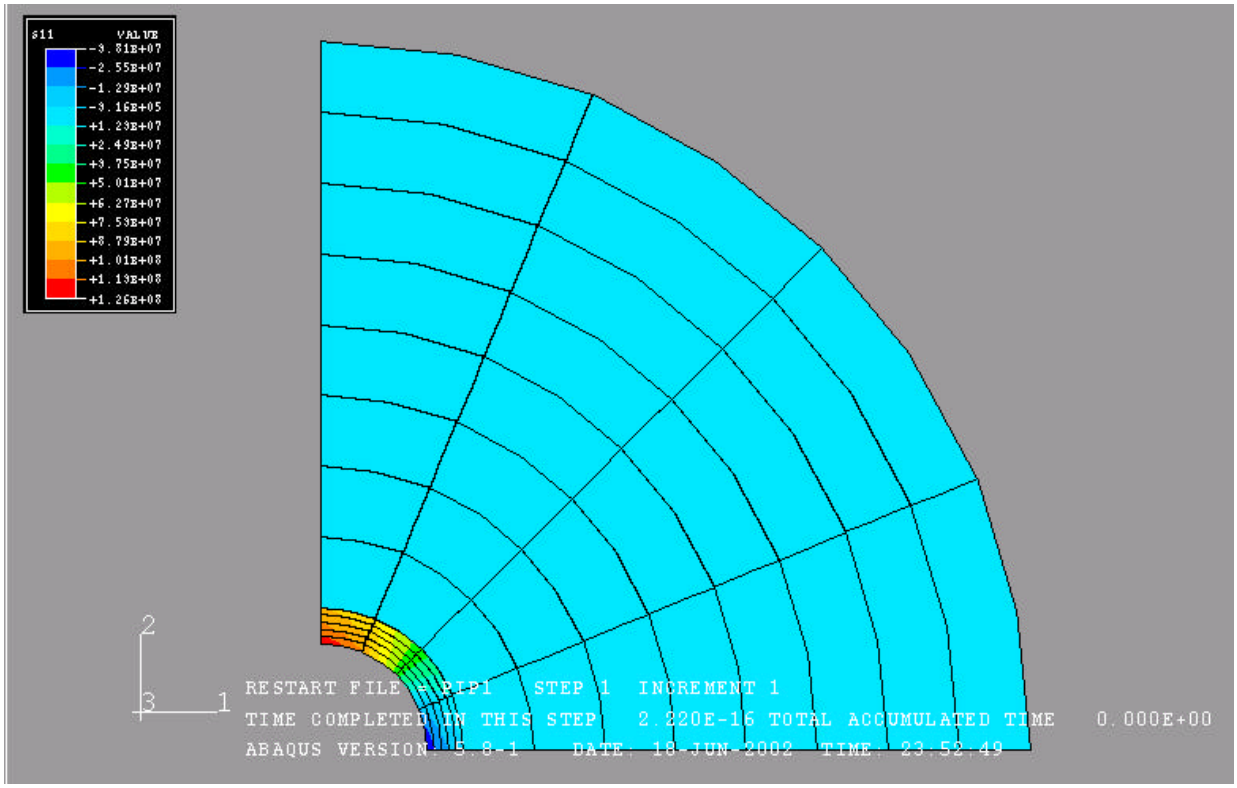

Fig.6b Second principal stress profile (Casing Pressure = 5000 psi)

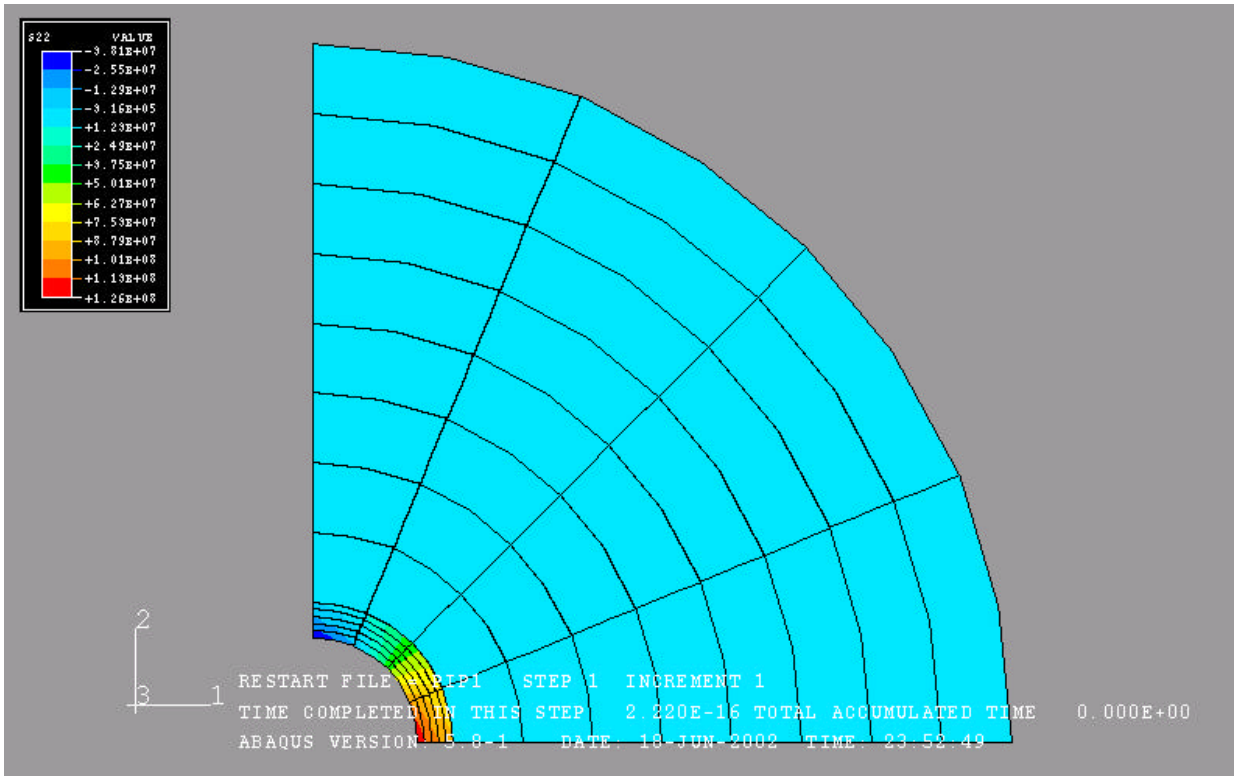

Fig.6c Horizontal displacement field (Casing Pressure = 1000 psi)

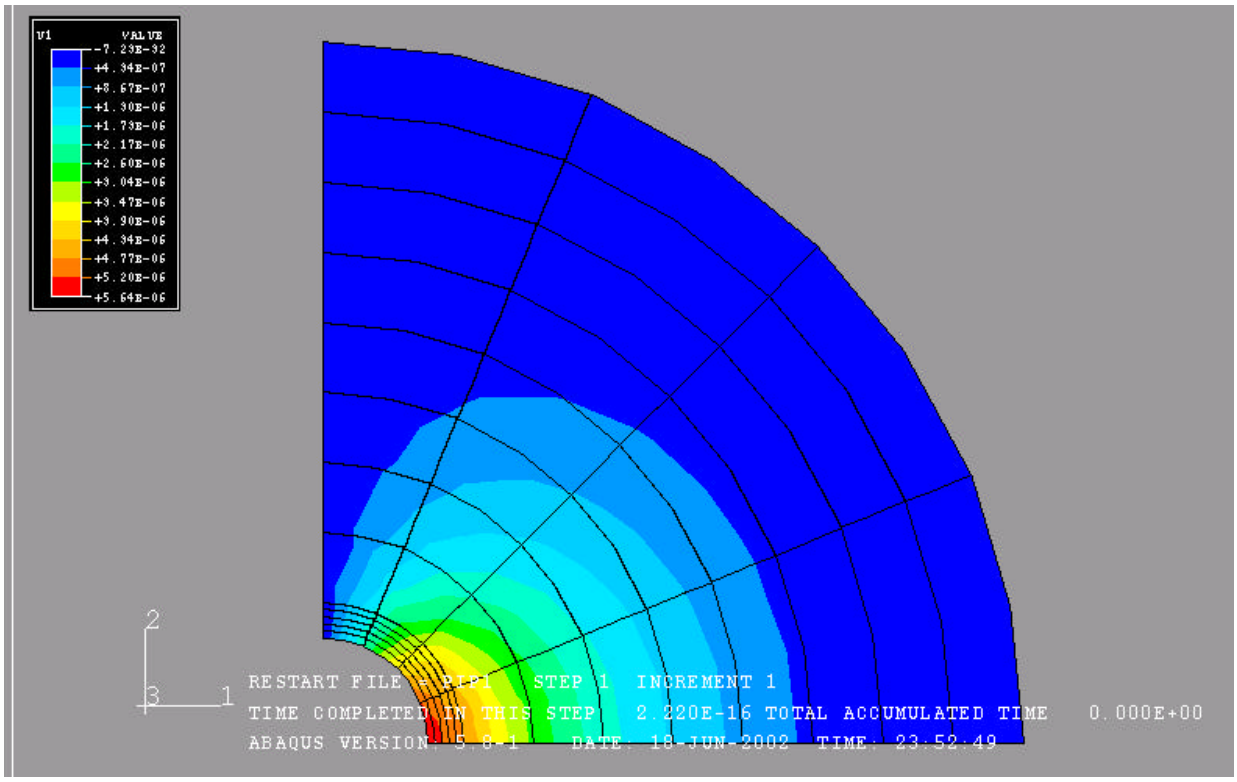

Fig.6d Vertical displacement field (Casing Pressure = 1000 psi)

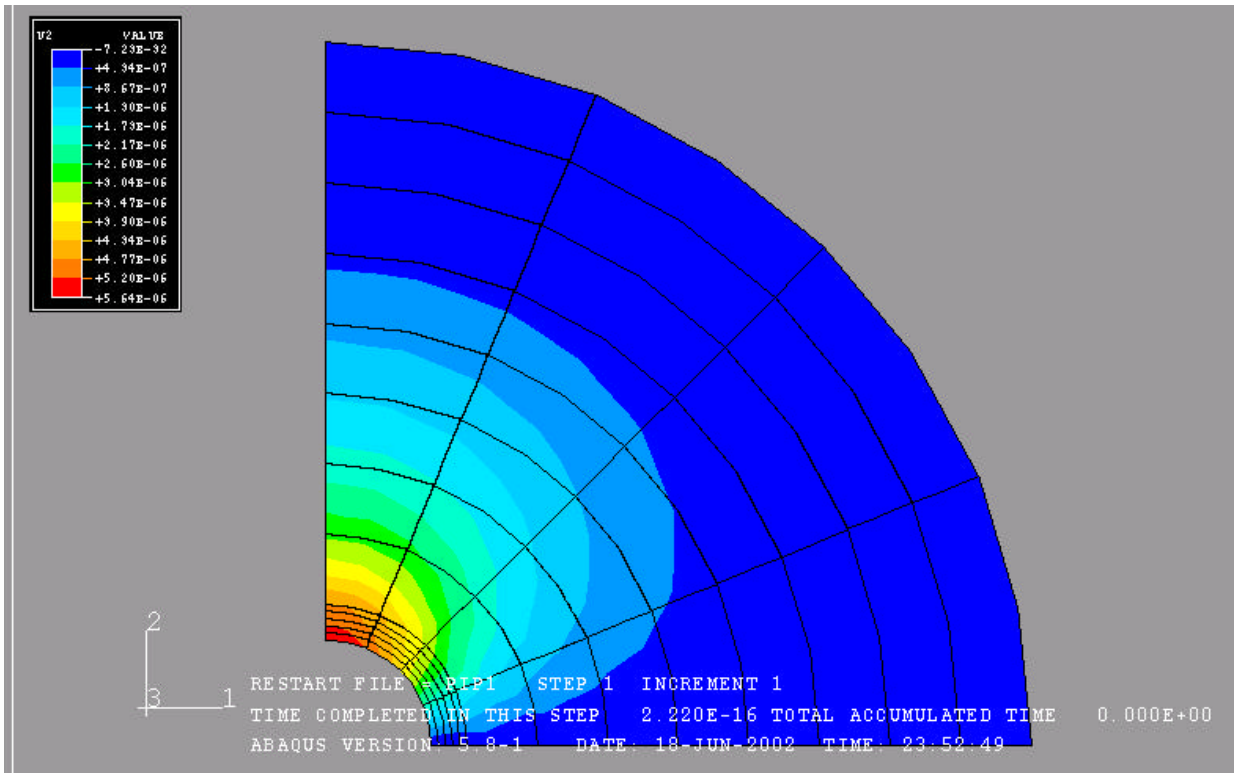

Fig.7a First principal stress profile (Casing Pressure = 10000 psi)

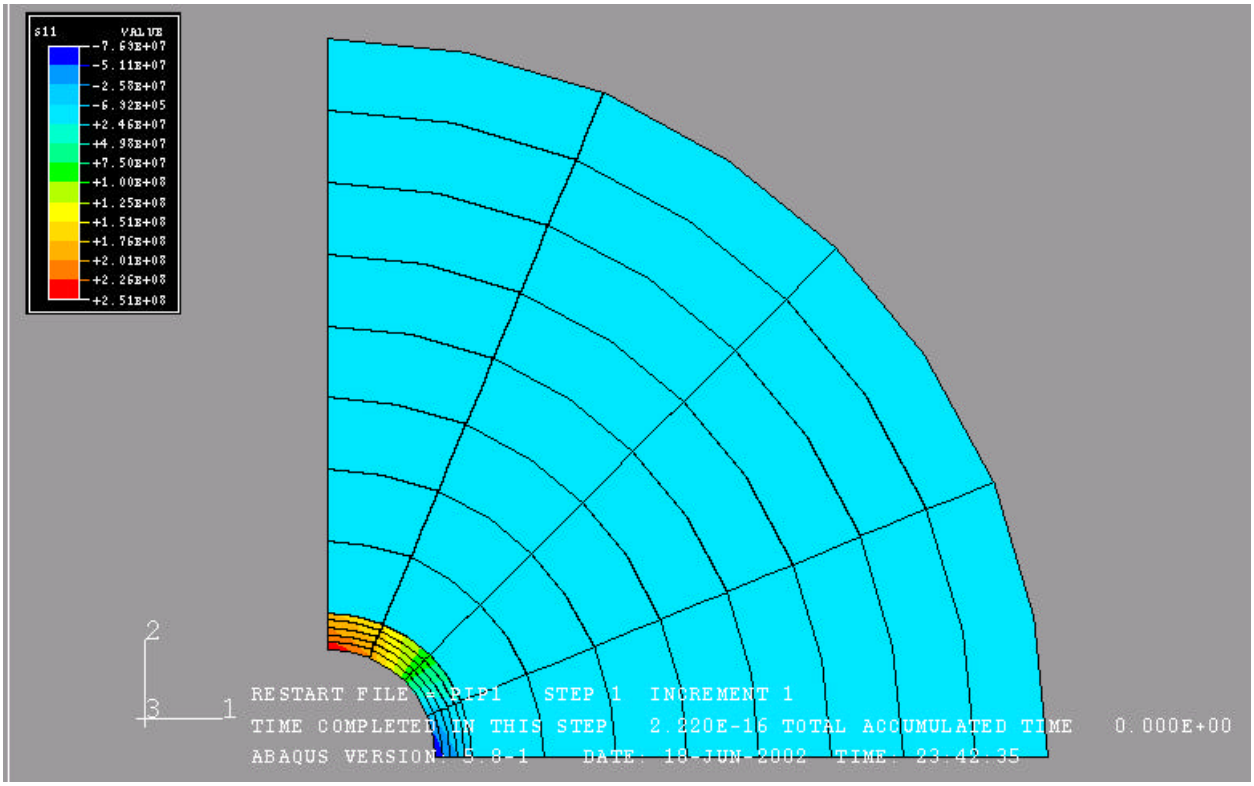

Fig.7b Second principal stress profile (Casing Pressure = 10000 psi)

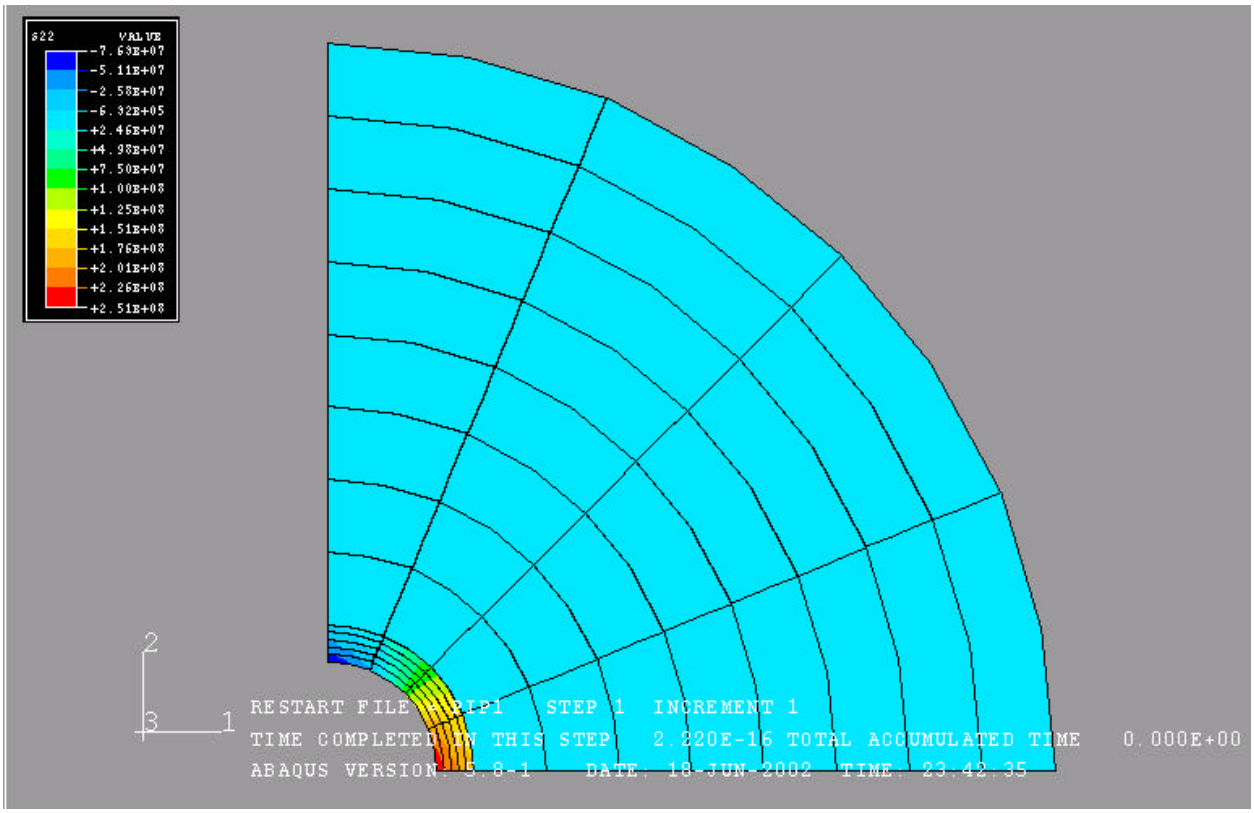

Fig.7c Horizontal displacement field (Casing Pressure = 10000 psi)

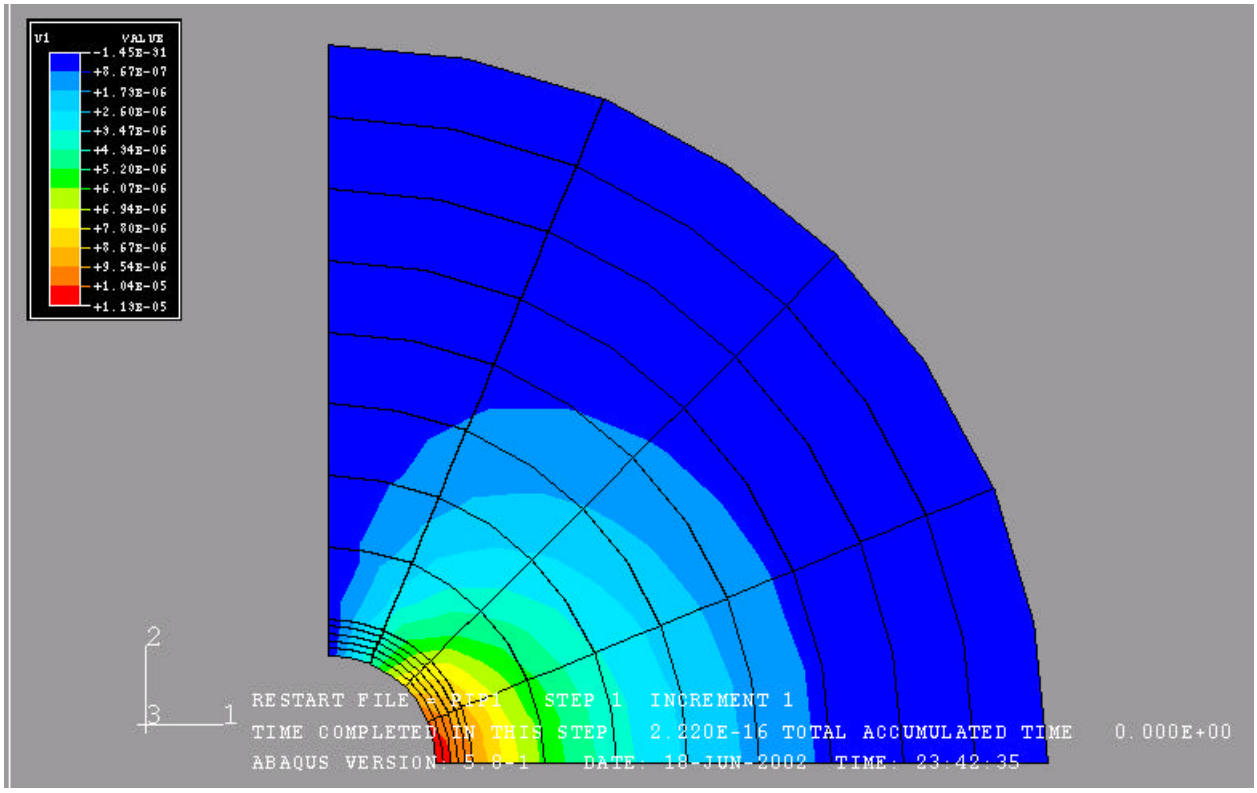

Fig.7d Vertical displacement field (Casing Pressure = 10000 psi)

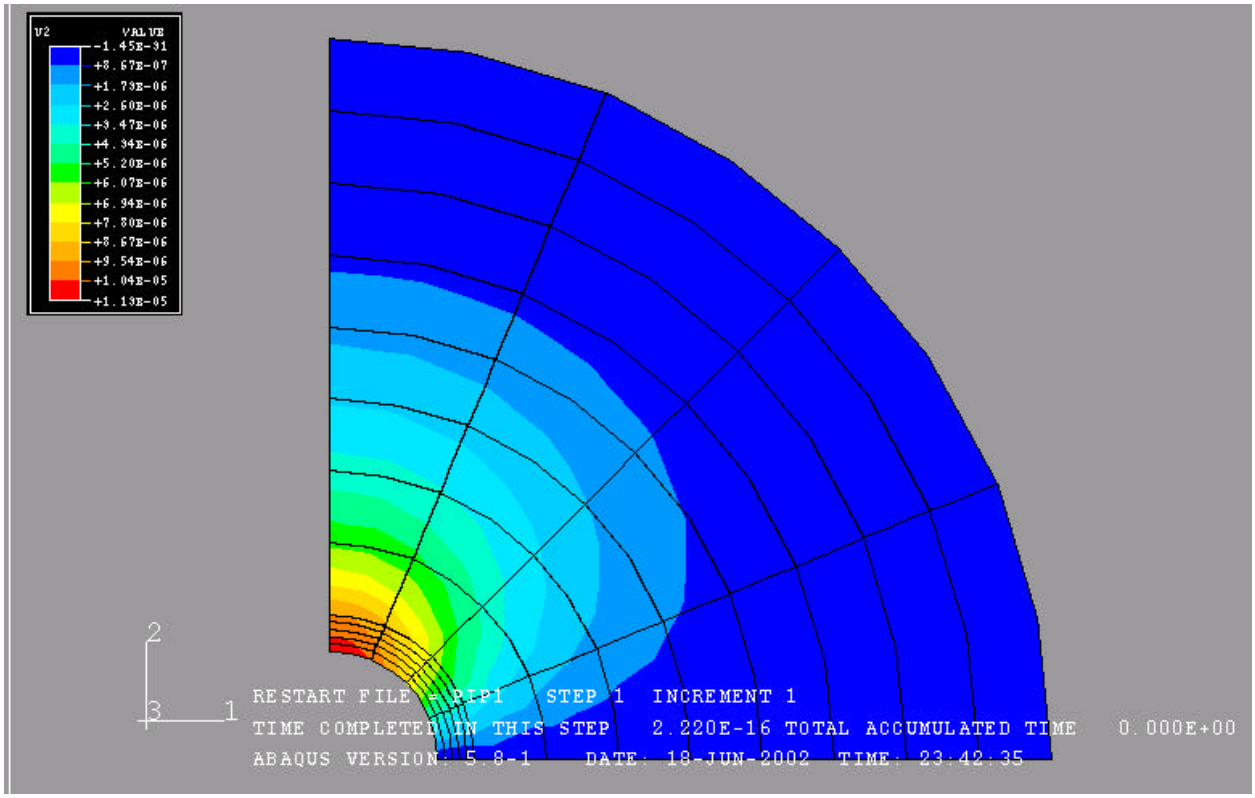

Fig.8a First principal stress profile (Confining Pressure = 100 psi)

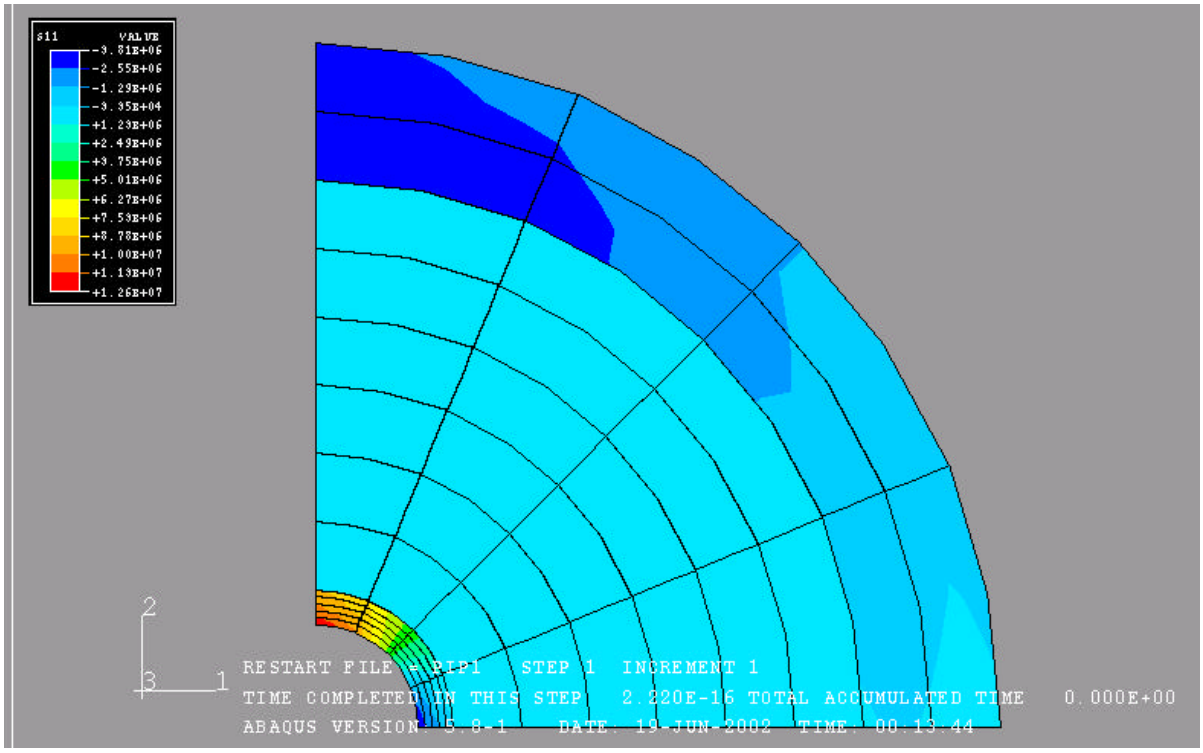

Fig.8b Second principal stress profile (Confining Pressure = 100 psi)

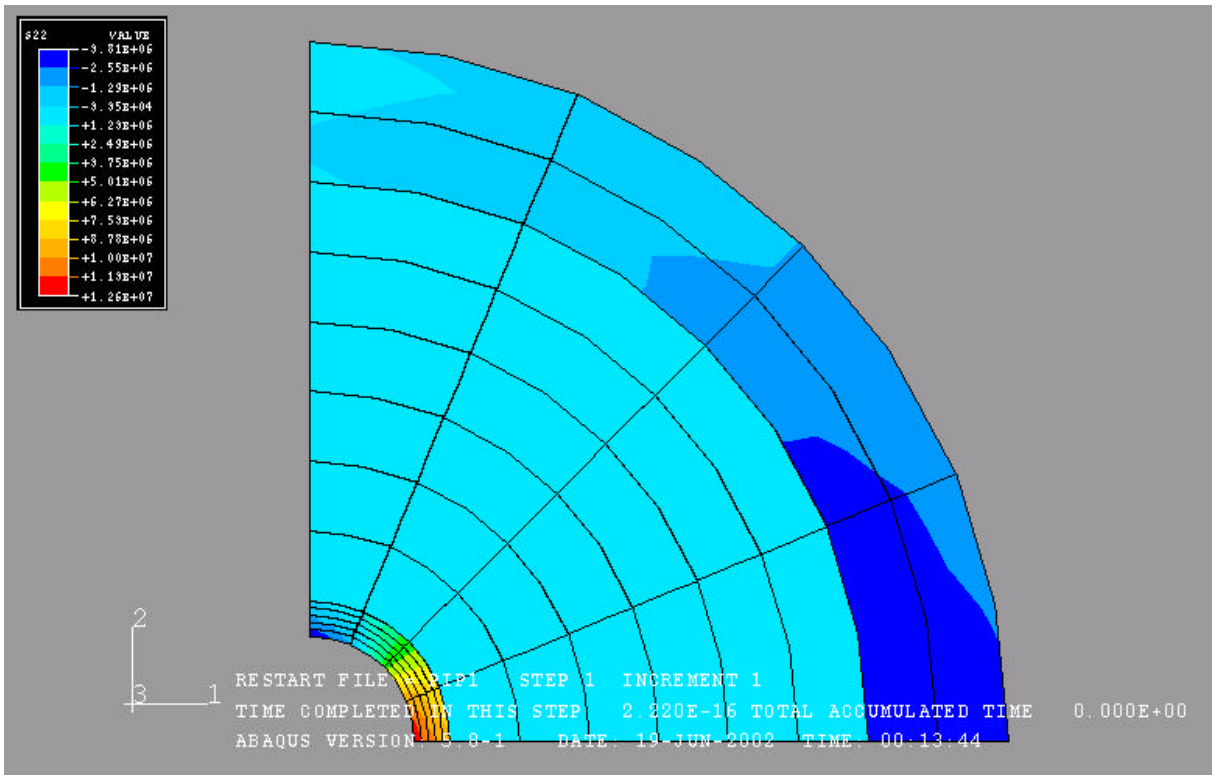

Fig.8c Horizontal displacement field (Confining Pressure = 100 psi)

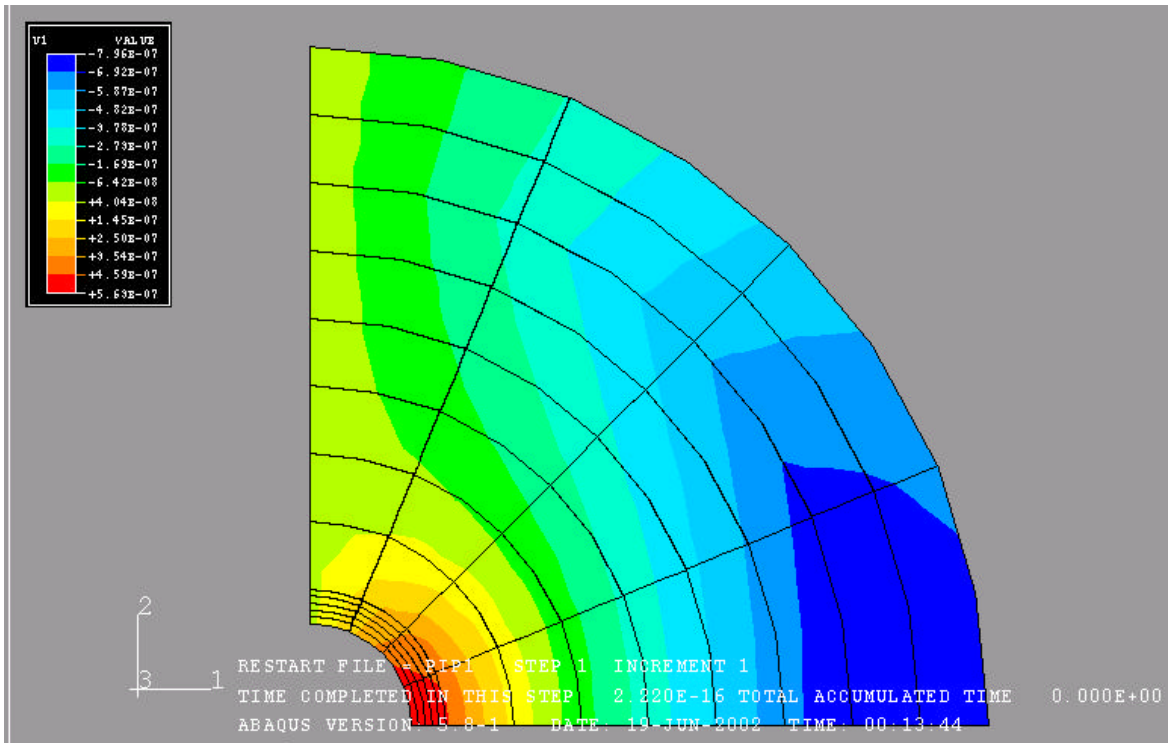

Fig.8d Vertical displacement field (Confining Pressure = 100 psi)

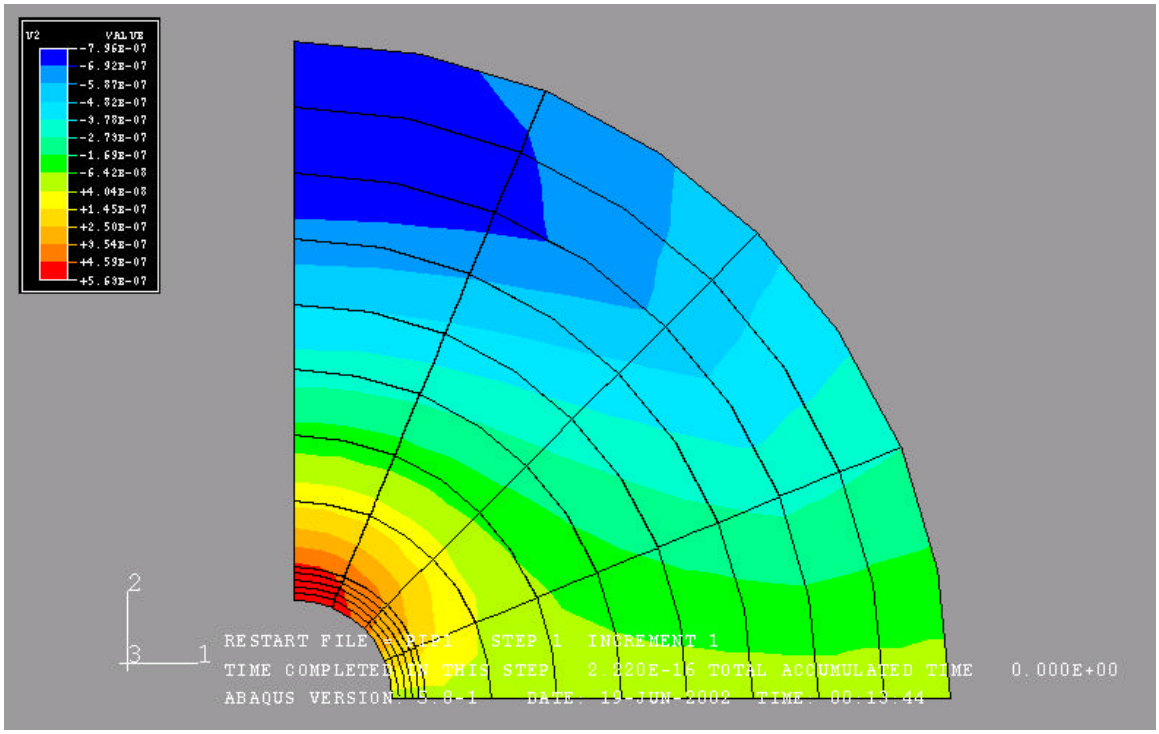

Fig.9a First principal stress profile (Confining Pressure = 500 psi)

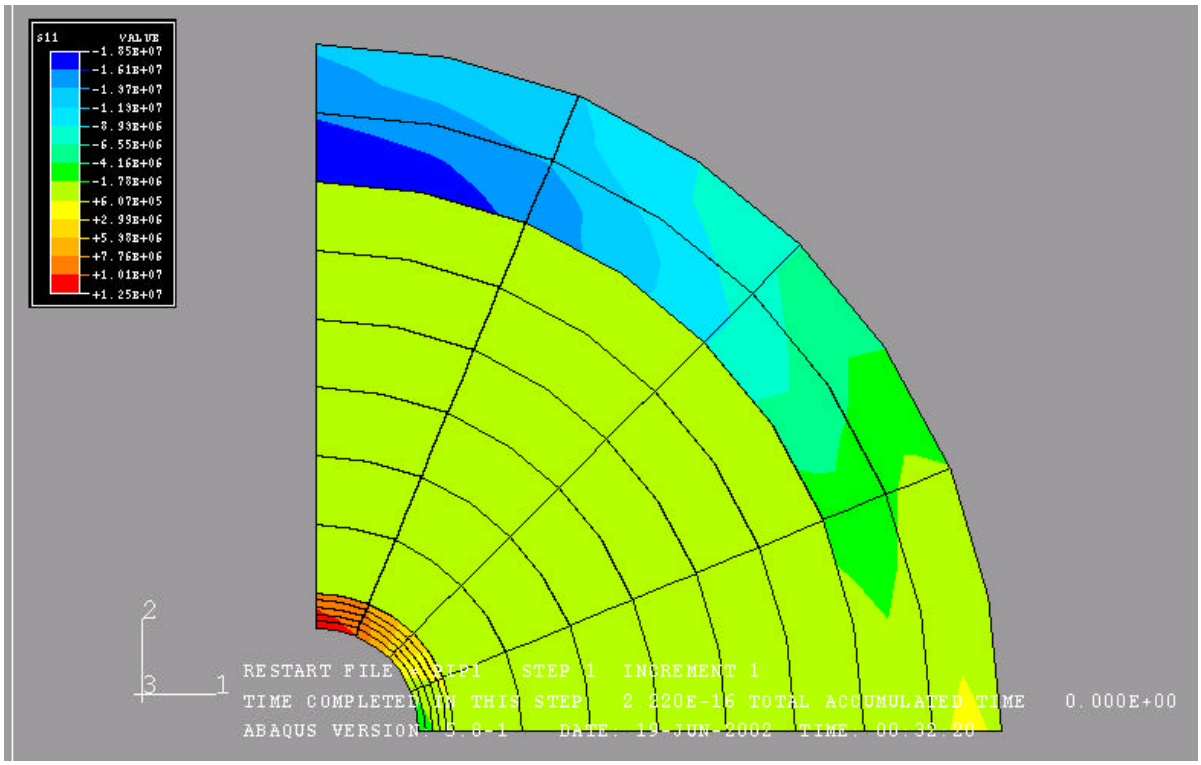

Fig.9b Second principal stress profile (Confining Pressure = 500 psi)

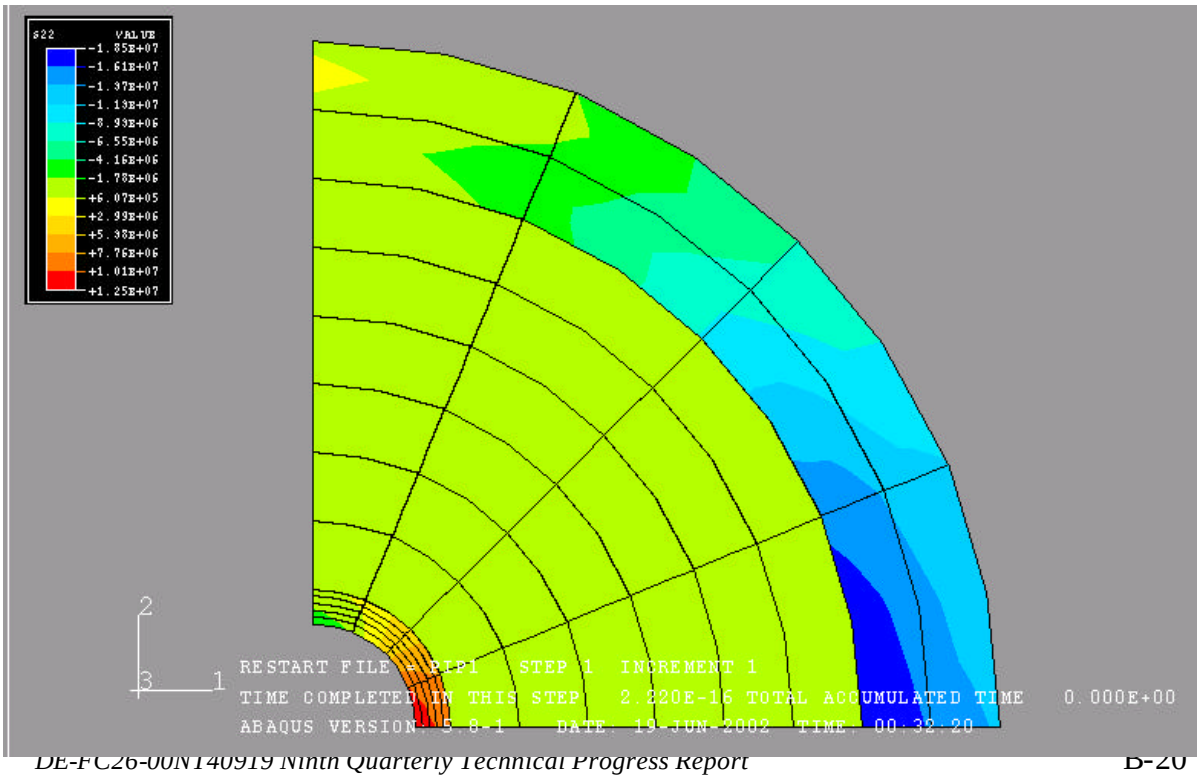

Fig.9c Horizontal displacement field (Confining Pressure = 500 psi)

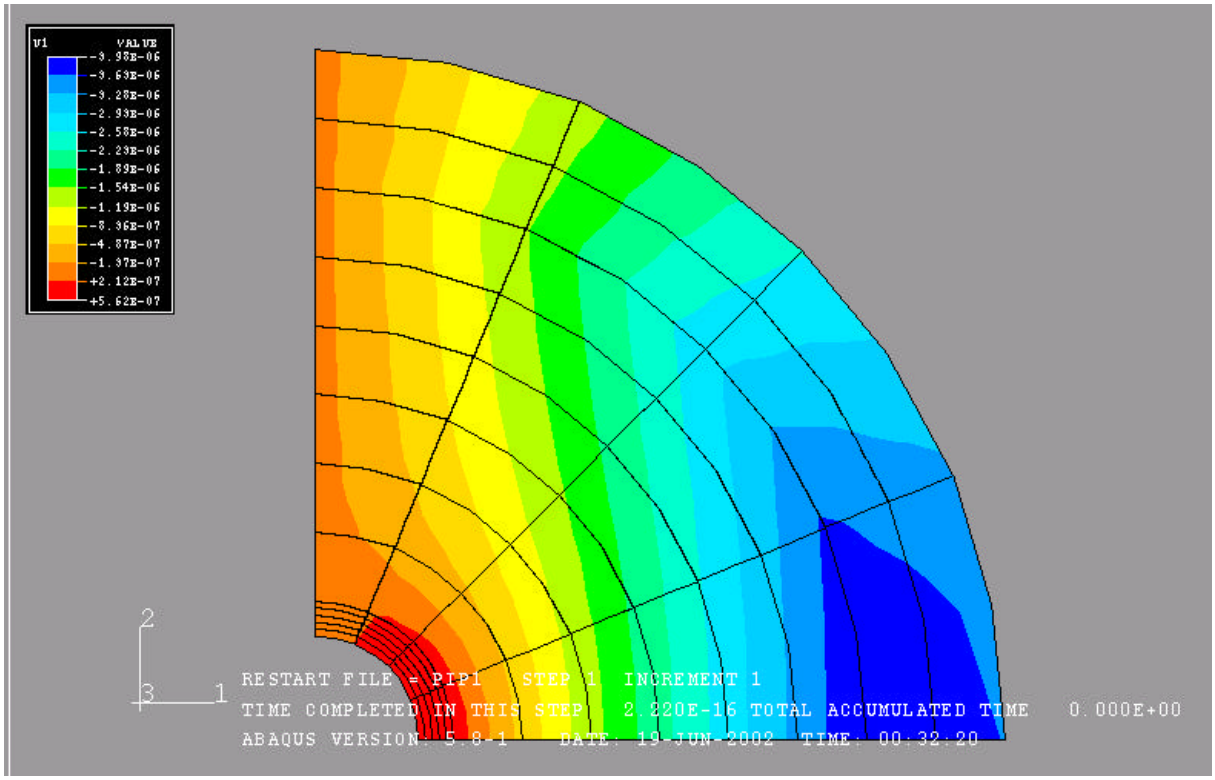

Fig.9d Vertical displacement field (Confining Pressure = 500 psi)

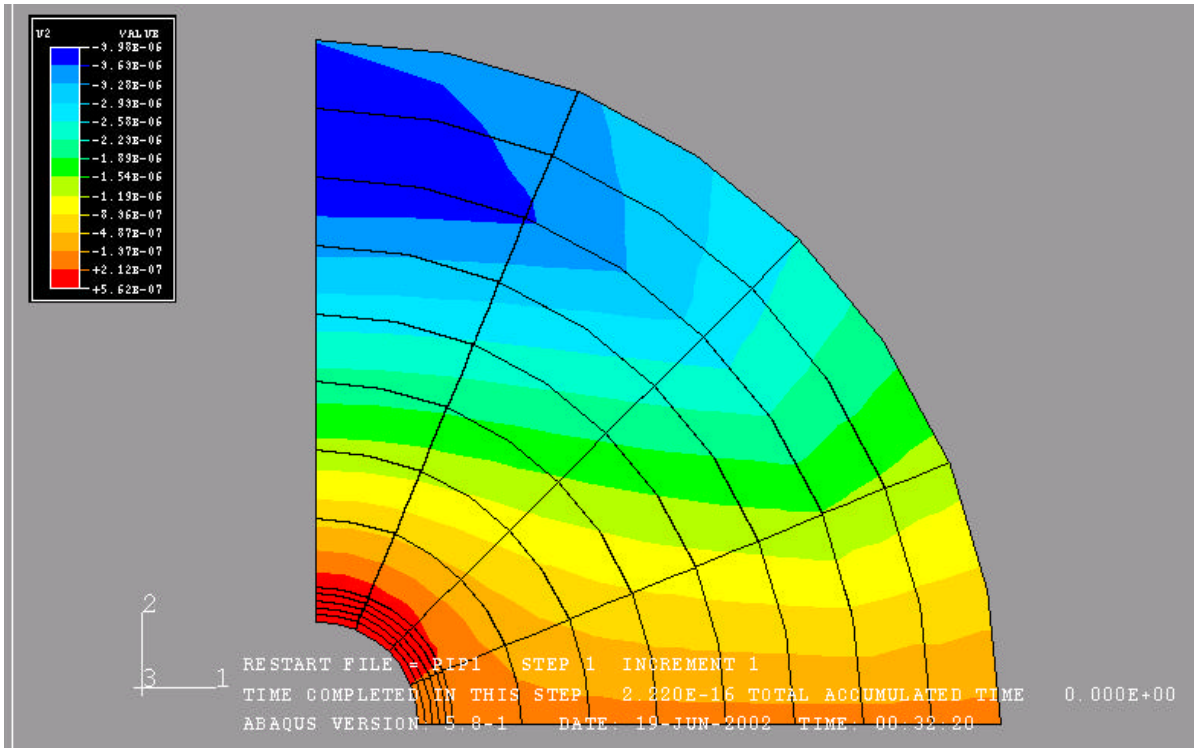

Fig.10a First principal stress profile (Confining Pressure = 1000 psi)

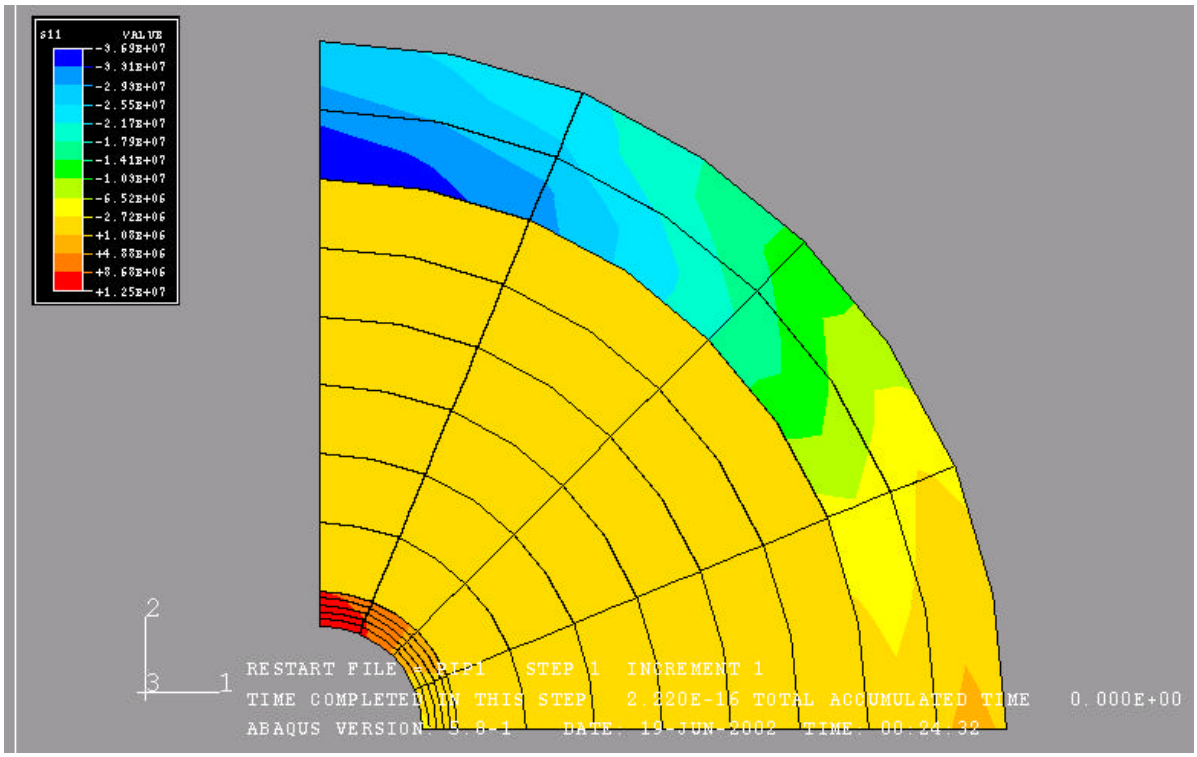

Fig.10b Second principal stress profile (Confining Pressure = 1000 psi)

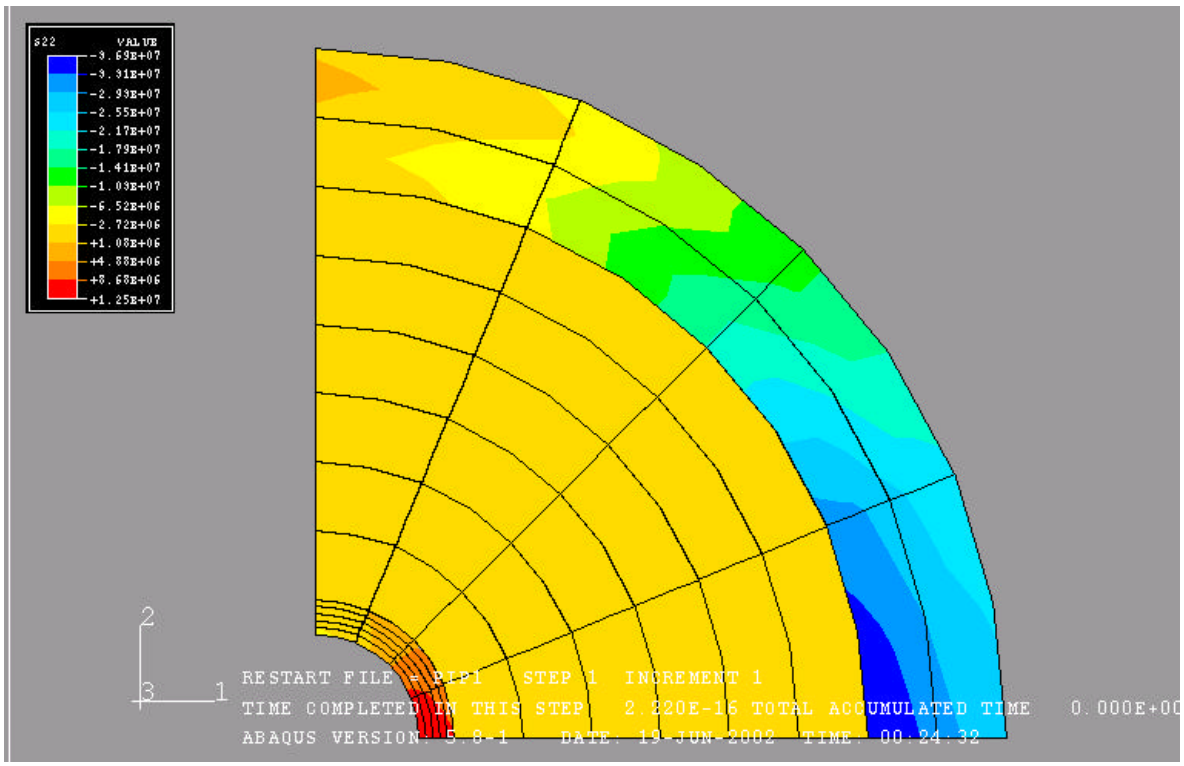

Fig.10c Horizontal displacement field (Confining Pressure = 1000 psi)

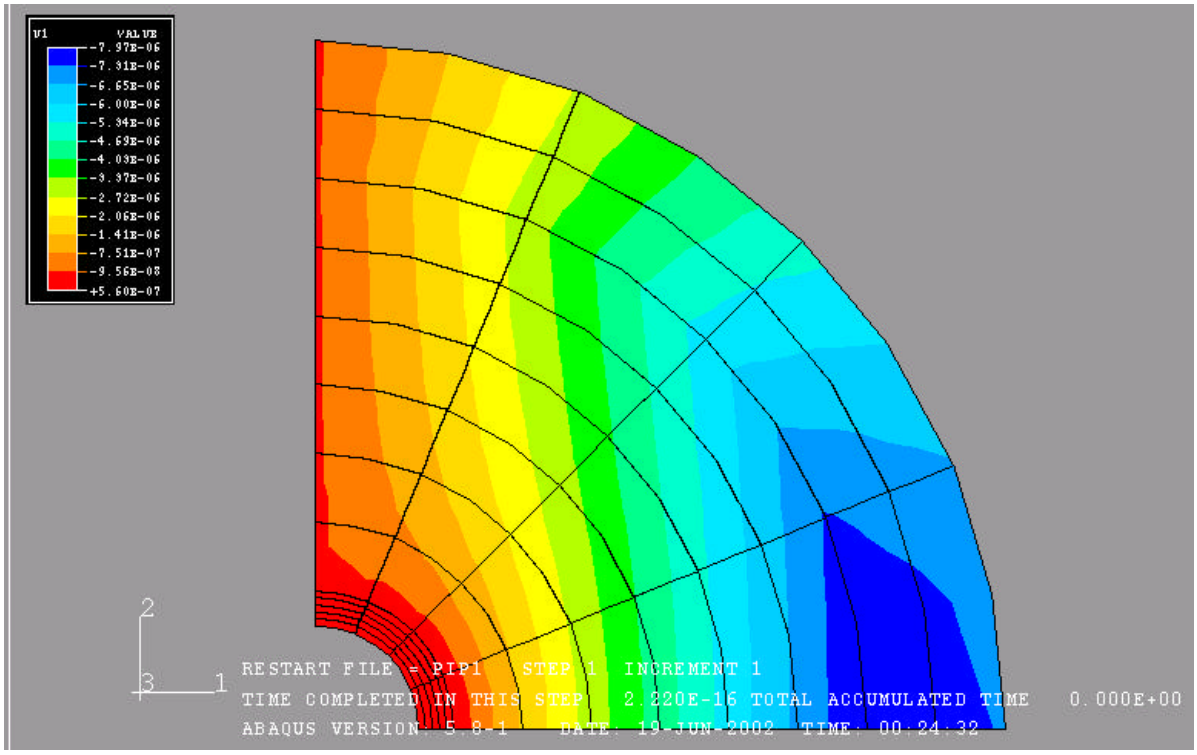

Fig.10d Vertical displacement field (Confining Pressure = 1000 psi)

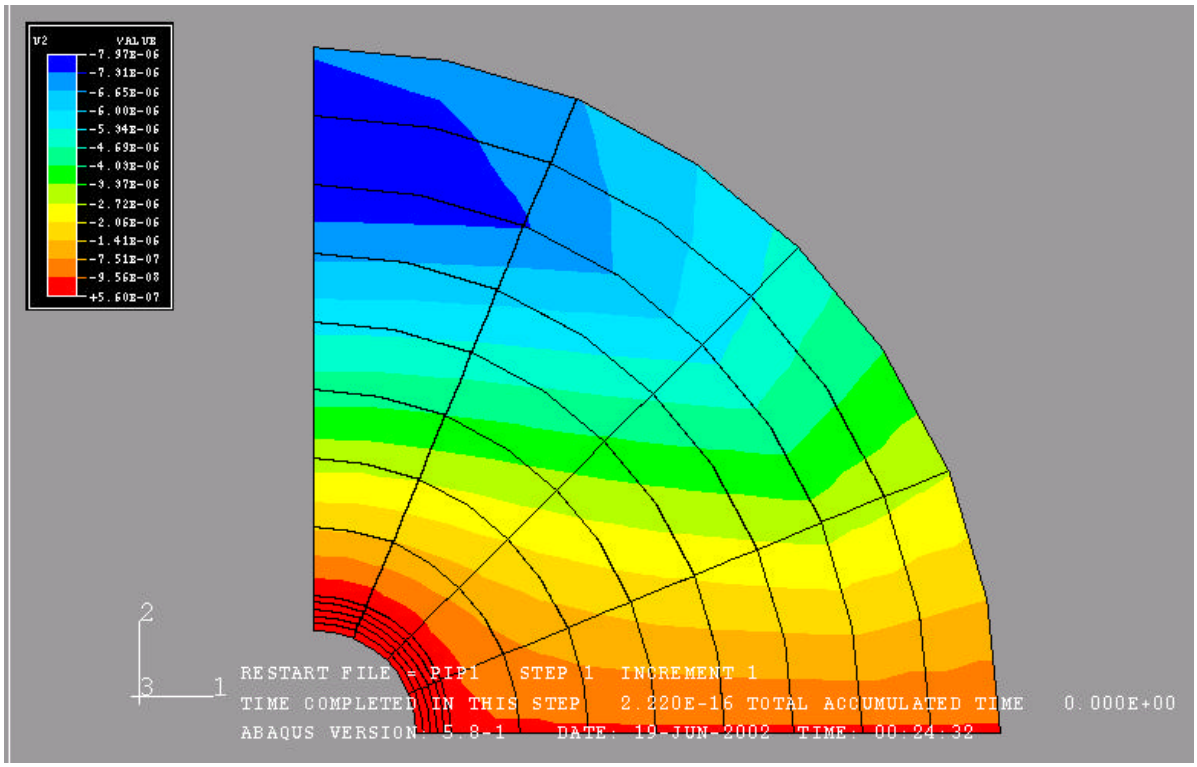

Fig.11a First principal stress profile (Cement Thickness = 3.5")

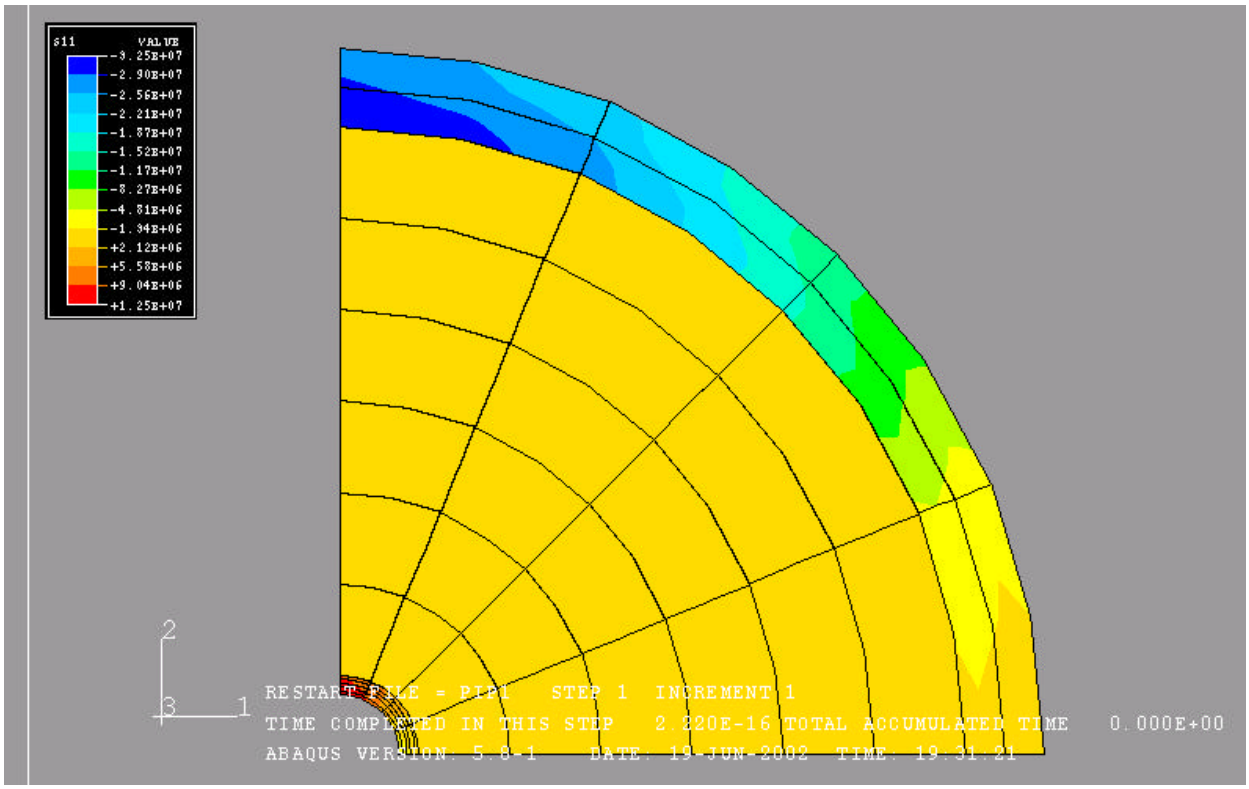

Fig.11b Second principal stress profile (Cement Thickness = 3.5")

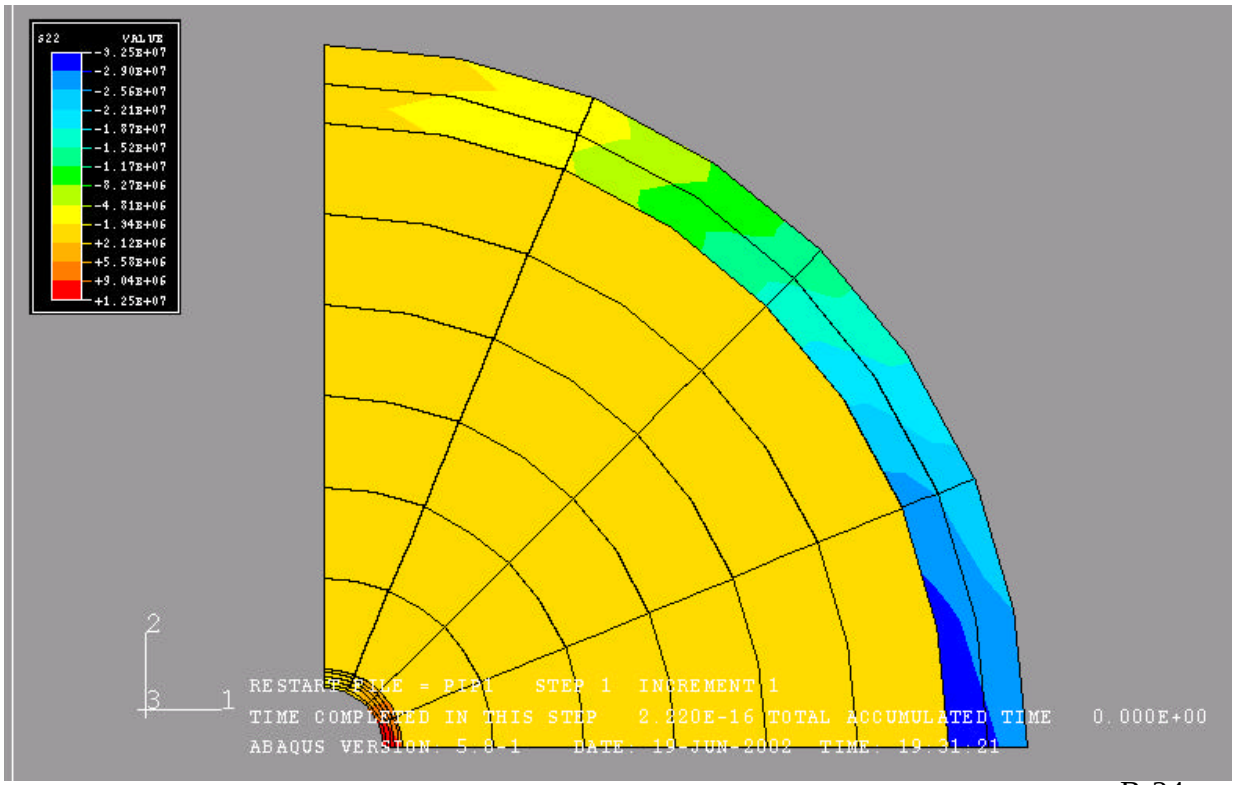

Fig.11c Horizontal displacement field (Cement Thickness = 3.5")

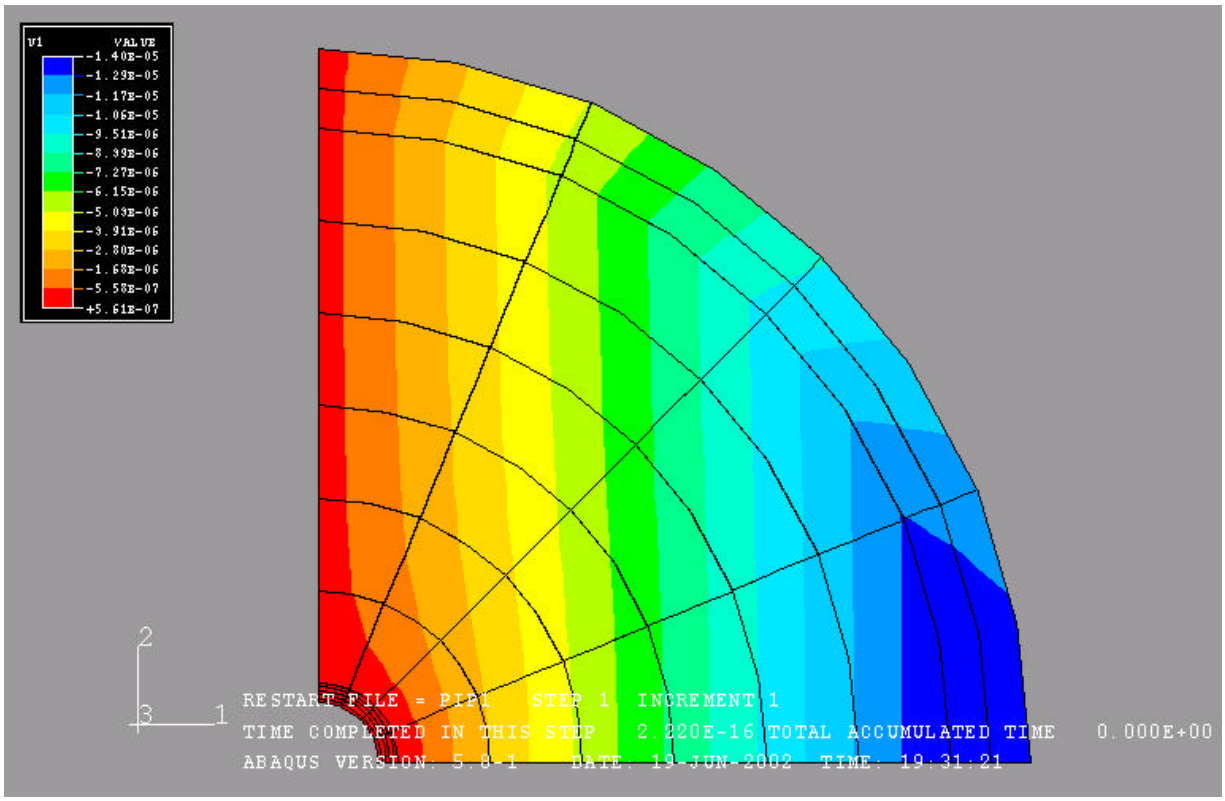

Fig.11d Vertical displacement field (Cement Thickness = 3.5")

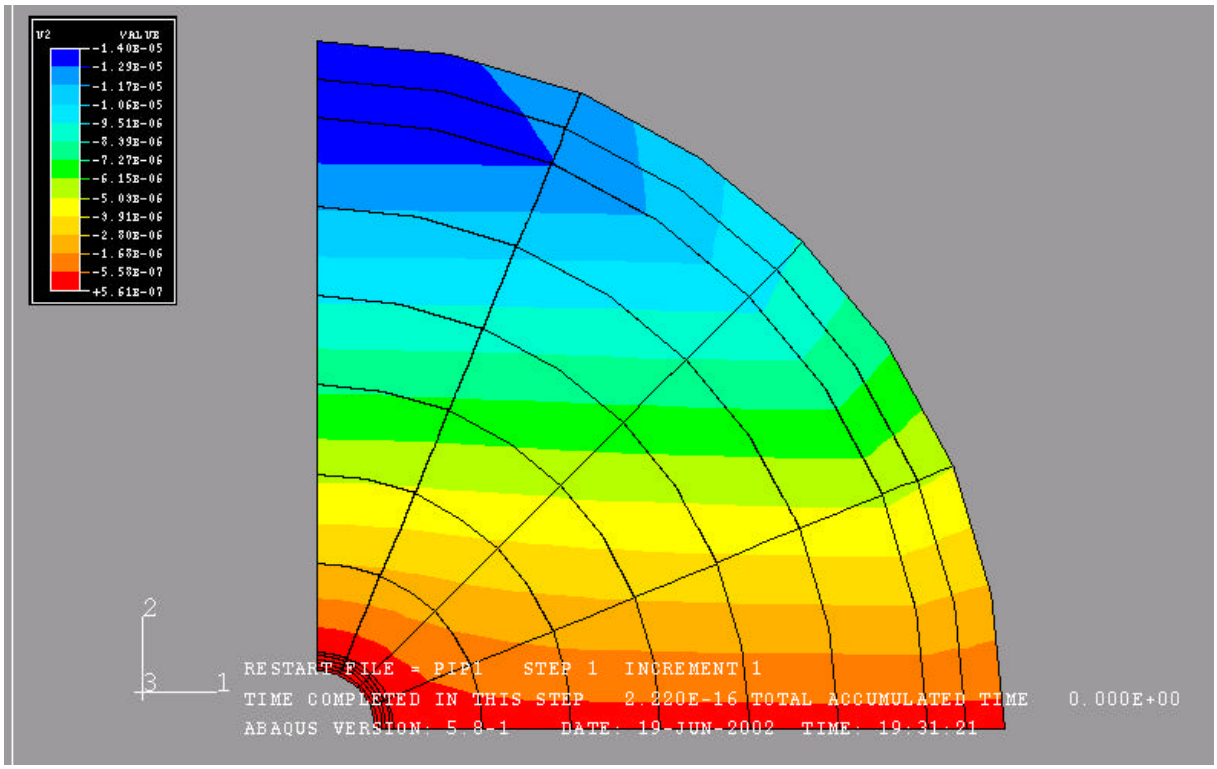

Fig.12a First principal stress profile (Cement Thickness = 5.5")

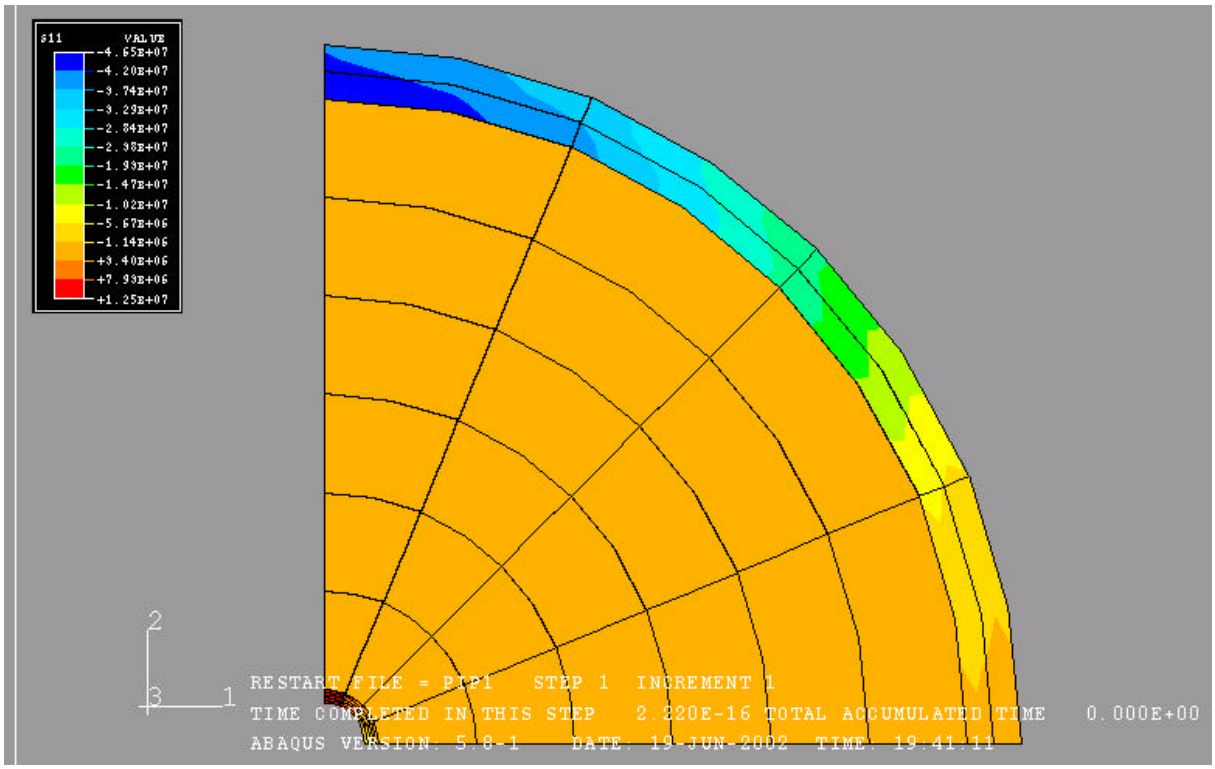

Fig.12b Second principal stress profile (Cement Thickness = 5.5")

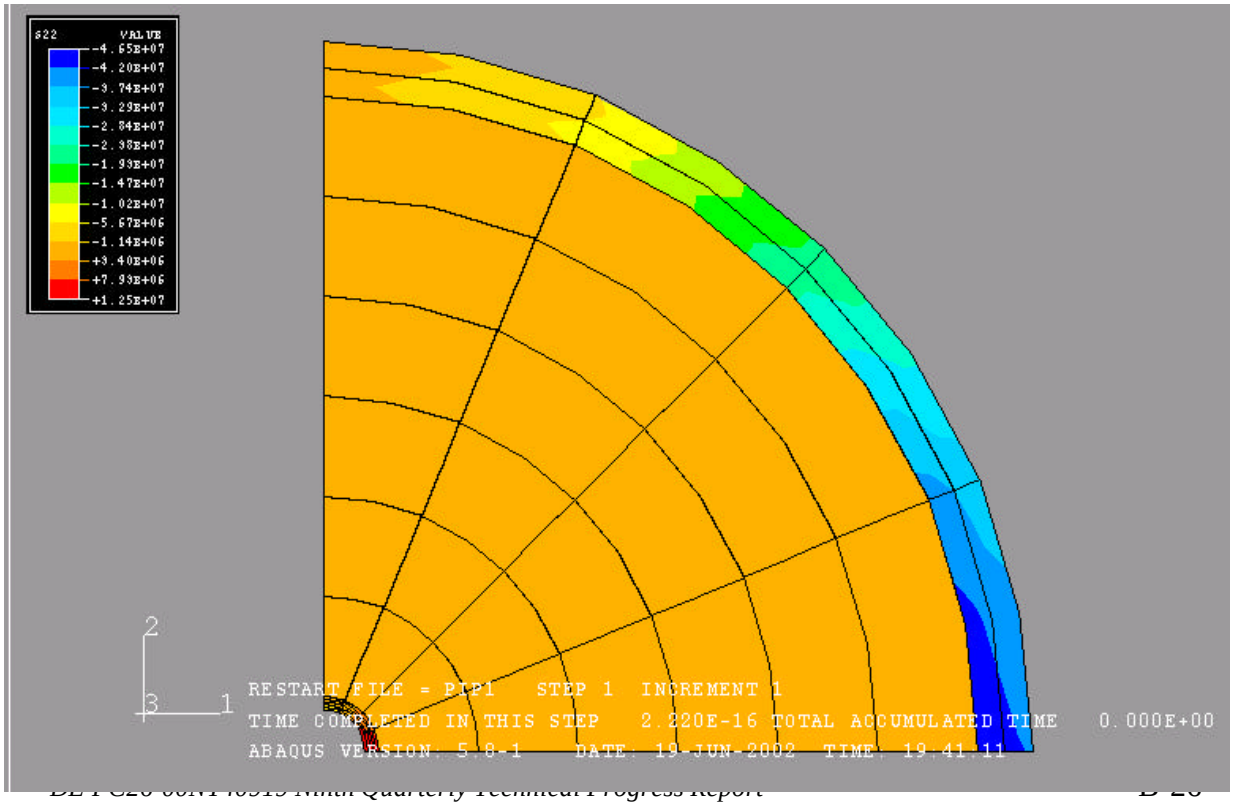

Fig.12c Horizontal displacement field (Cement Thickness = 5.5")

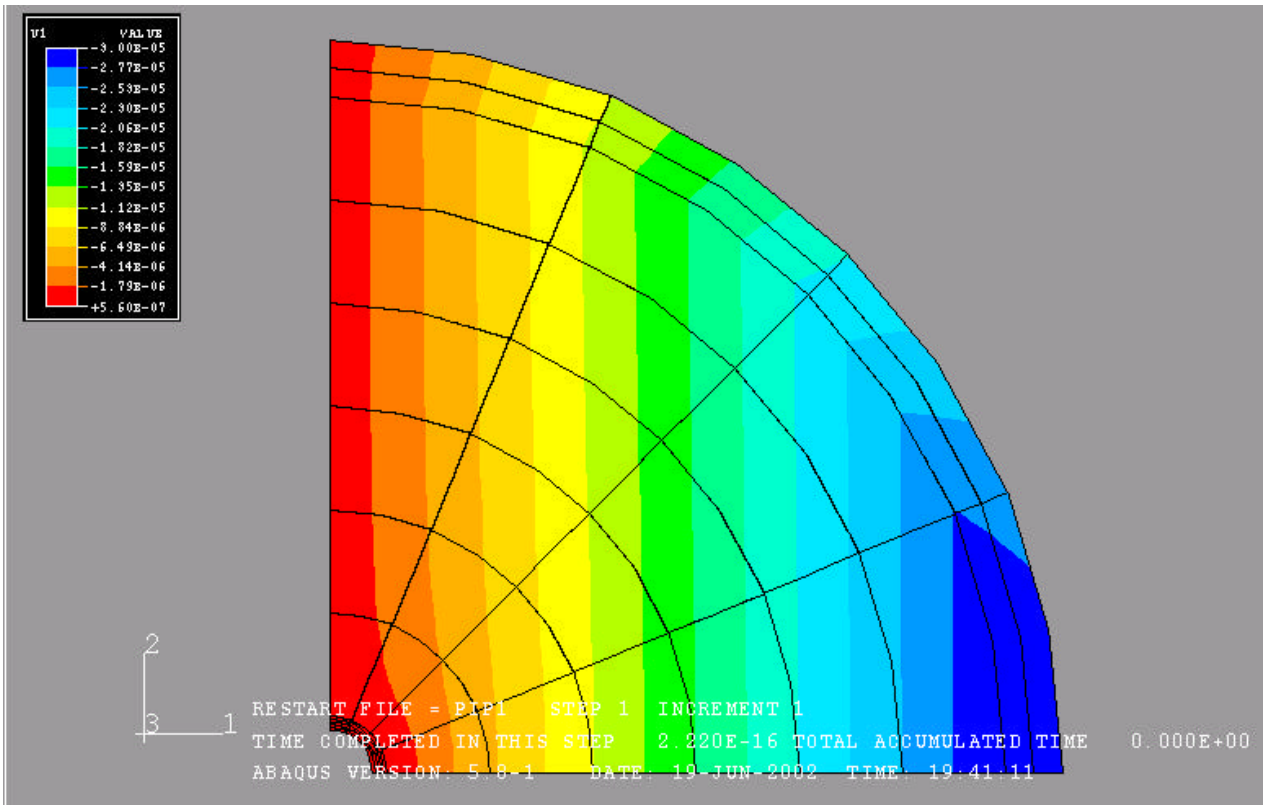

Fig.12d Vertical displacement field (Cement Thickness = 5.5")

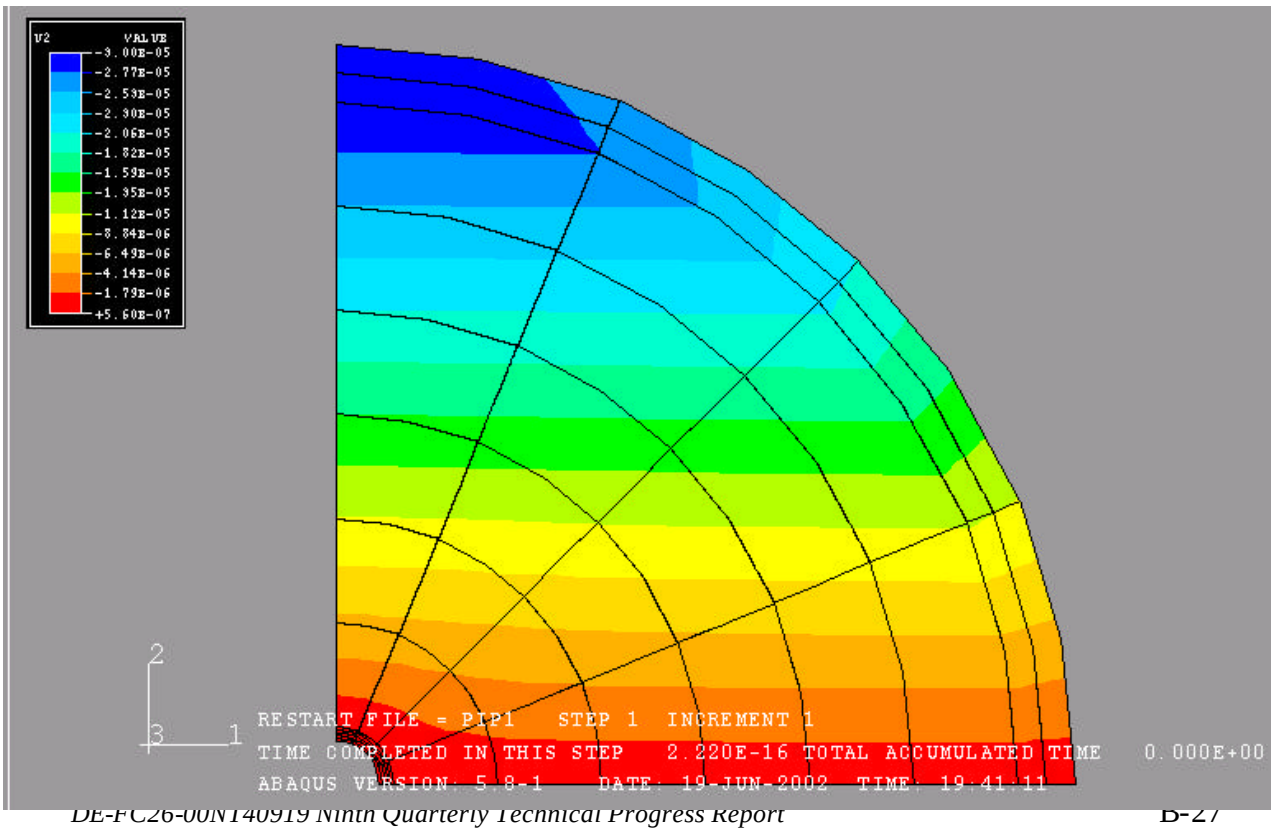

Fig.13a First principal stress profile (Cement Thickness = 7.5")

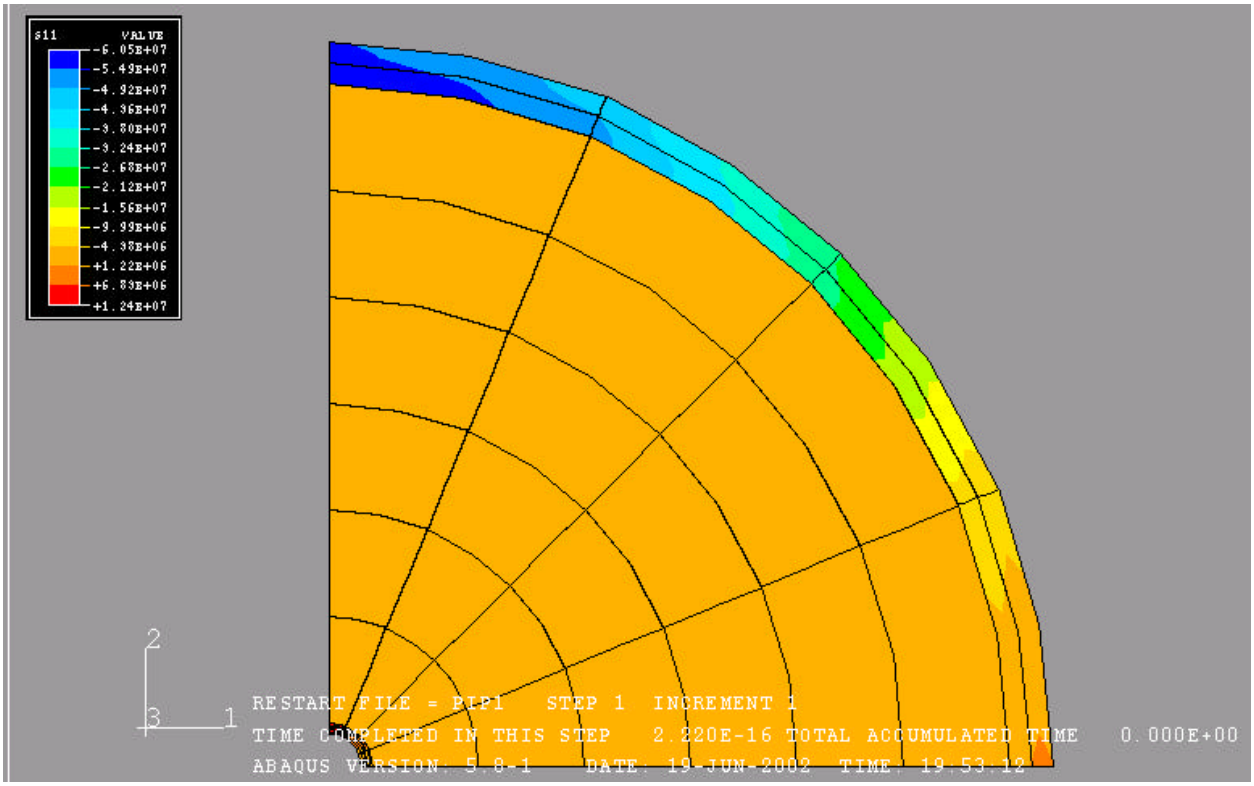

Fig.13b Second principal stress profile (Cement Thickness = 7.5")

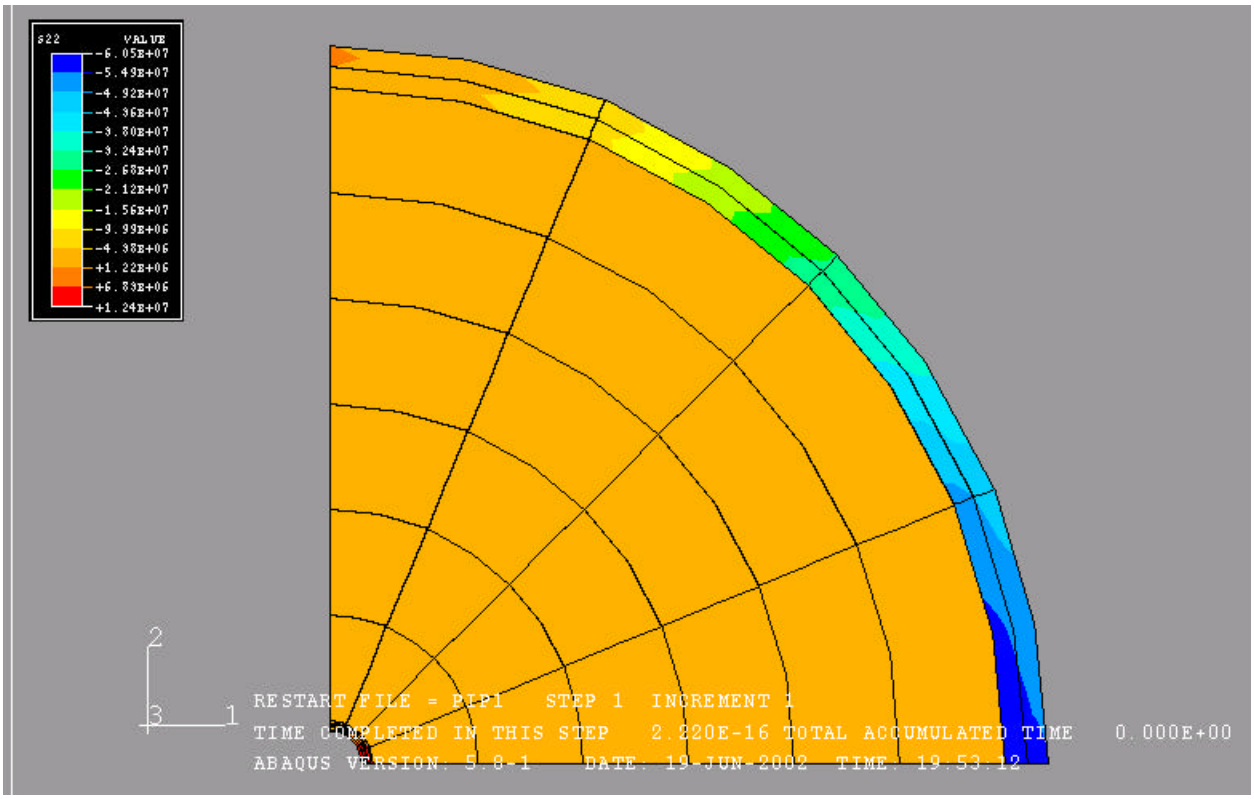
S22
VALUE
-6.05E+07
-5.49E+07
-4.92E+07
-4.36E+07
-3.80E+07
-3.24E+07
-2.68E+07
-2.12E+07
-1.56E+07
-9.99E+06
-4.38E+06
+1.22E+06
+6.83E+06
+1.24E+07
2
3
1
RESTART FILE = RIP1 STEP 1 INCREMENT 1
TIME COMPLETED IN THIS STEP 2.220E-16 TOTAL ACCUMULATED TIME 0.000E+00
ABAQUS VERSION: 5.8-1 DATE: 19-JUN-2002 TIME: 19:53:12

Fig.13c Horizontal displacement field (Cement Thickness = 7.5")

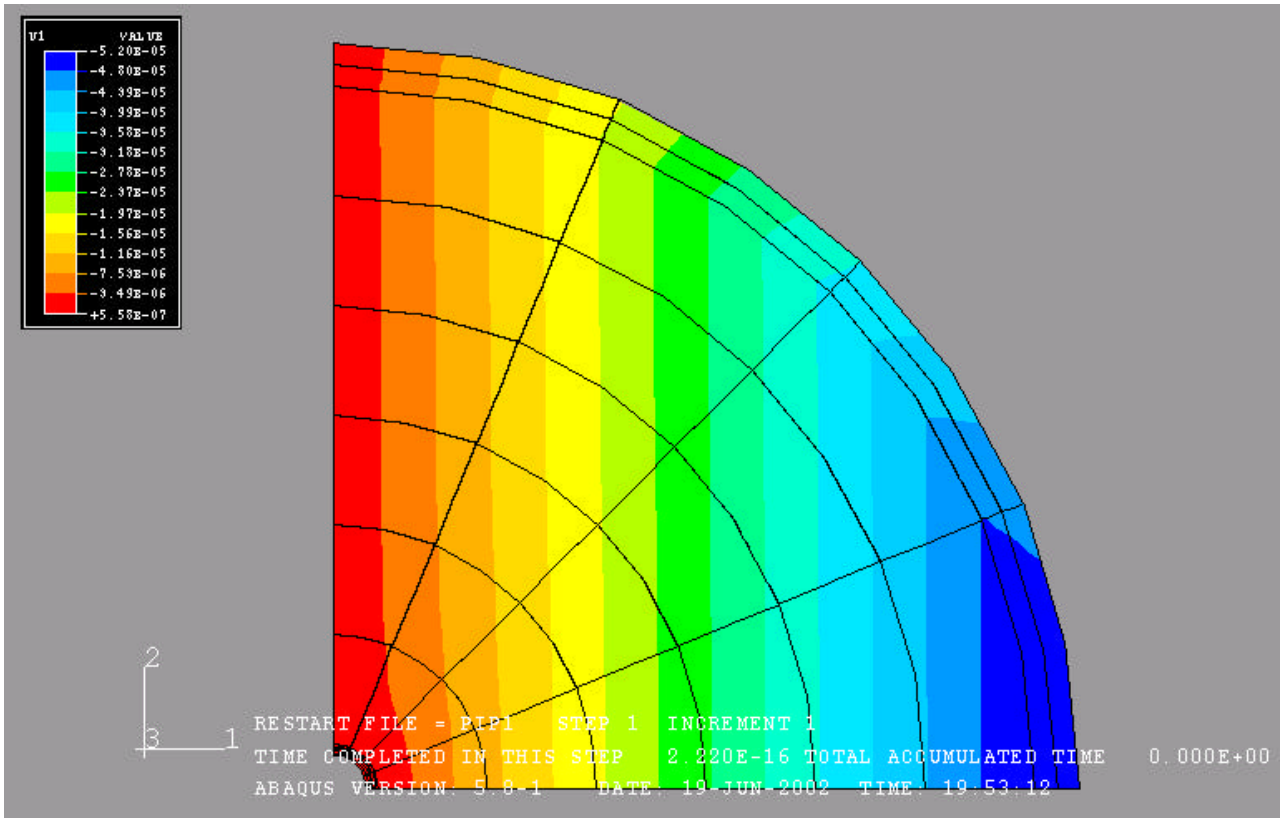

Fig.13d Vertical displacement field (Cement Thickness = 7.5")

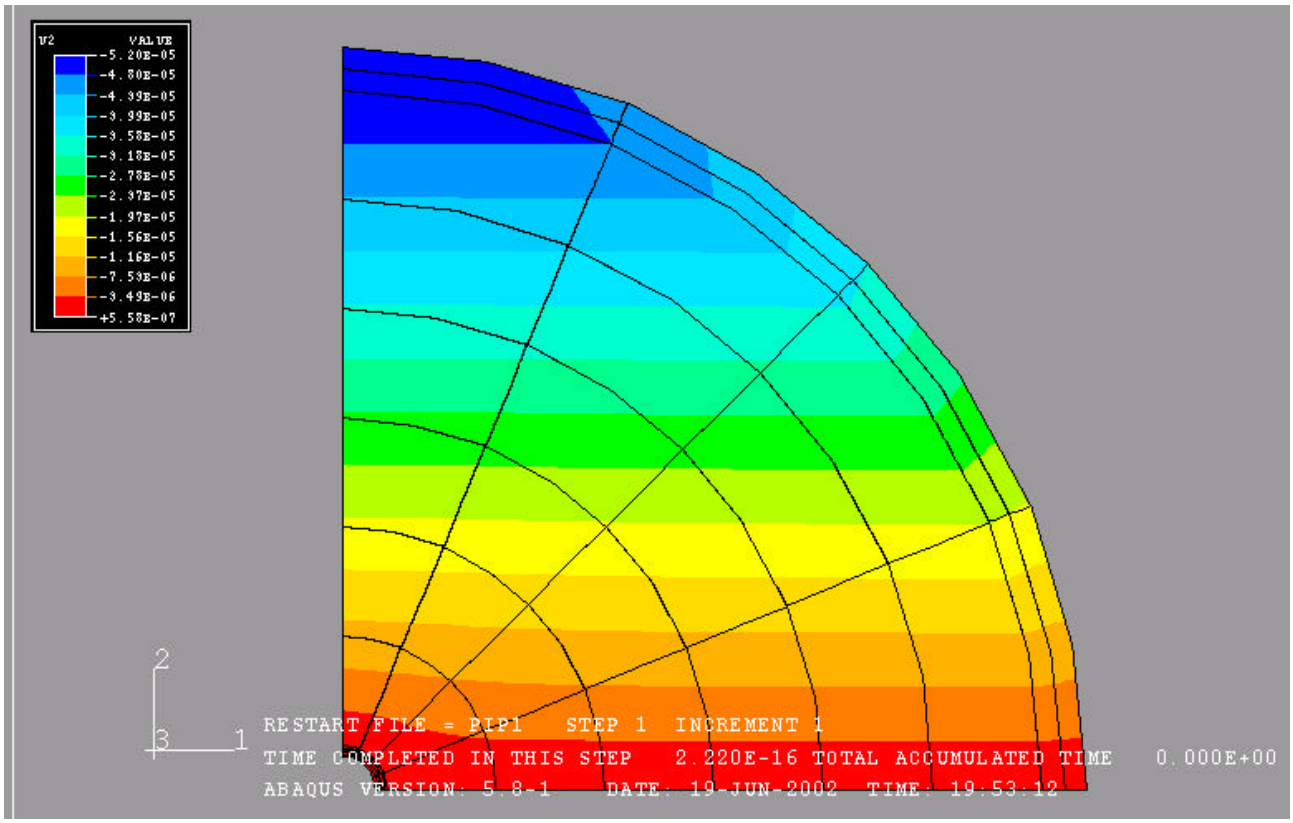

Fig.14a First principal stress profile (Young's Modulus = 1000 psi)

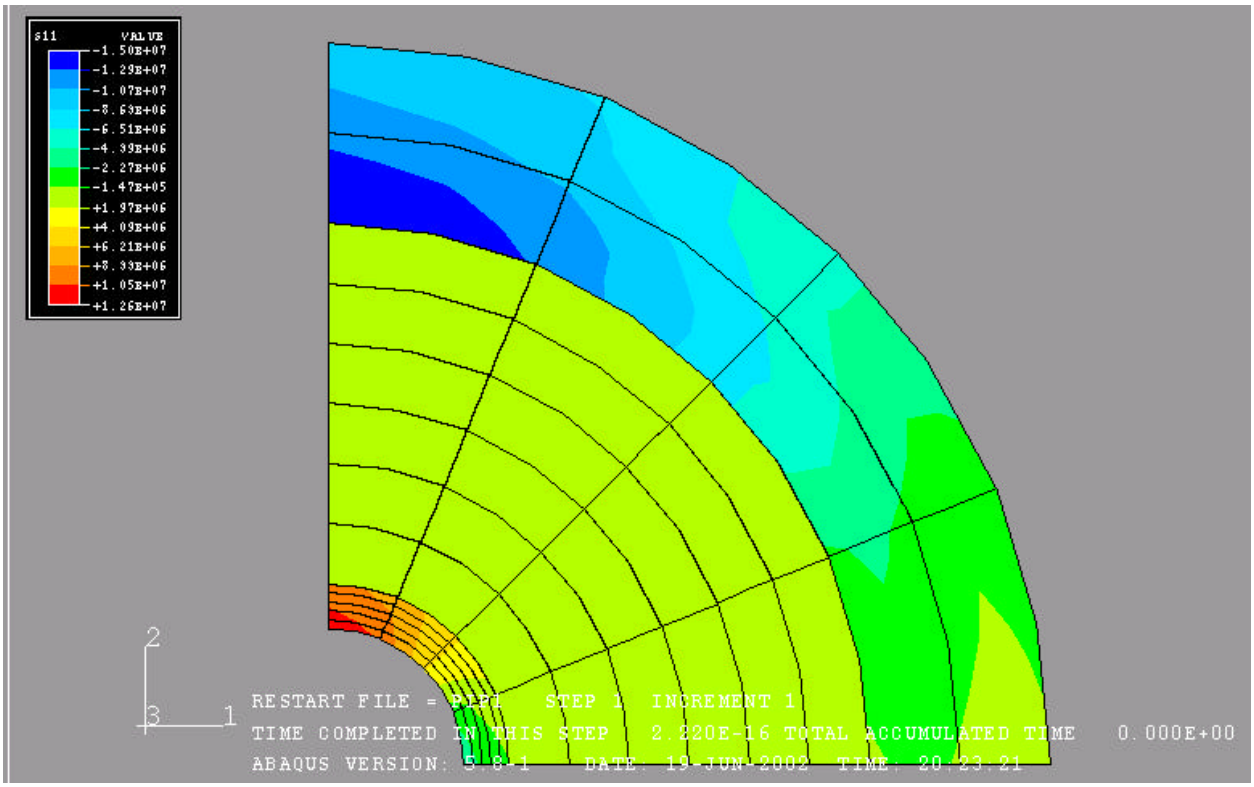

Fig.14b Second principal stress profile (Young's Modulus = 1000 psi)

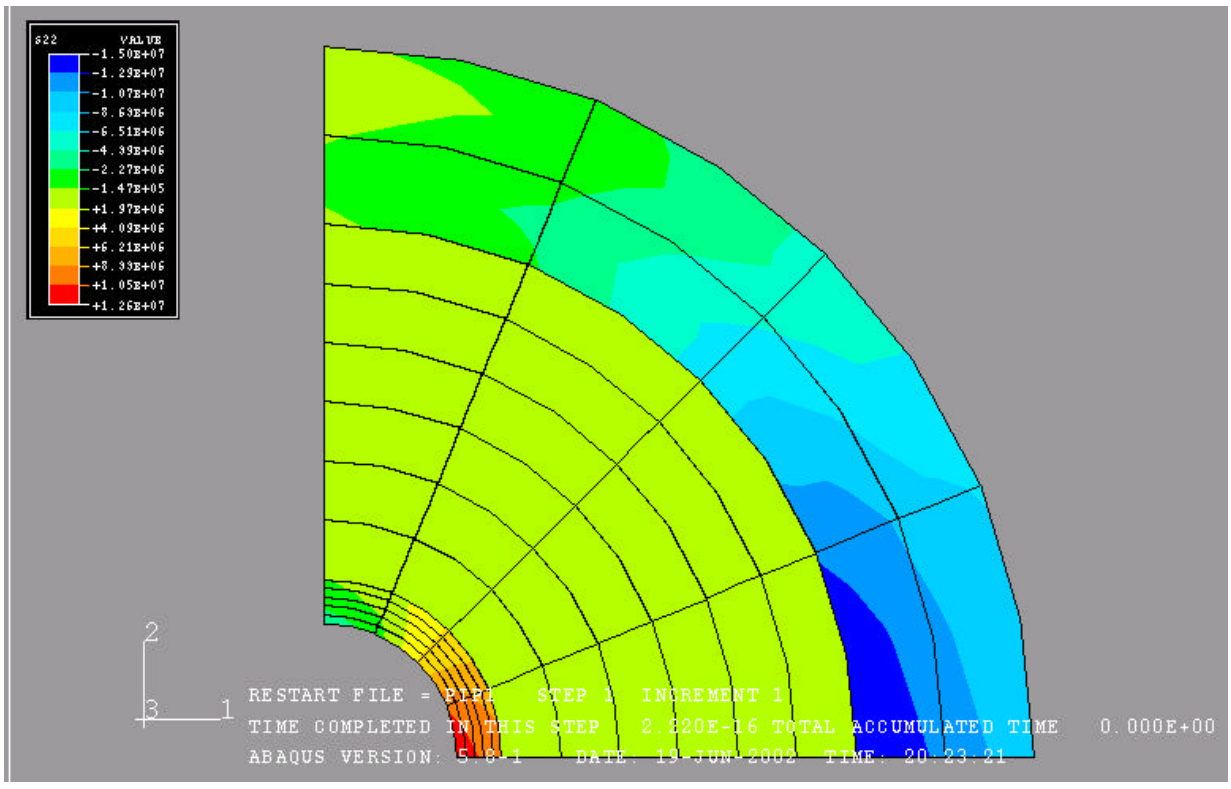

Fig.14c Horizontal displacement field (Young's Modulus = 1000 psi)

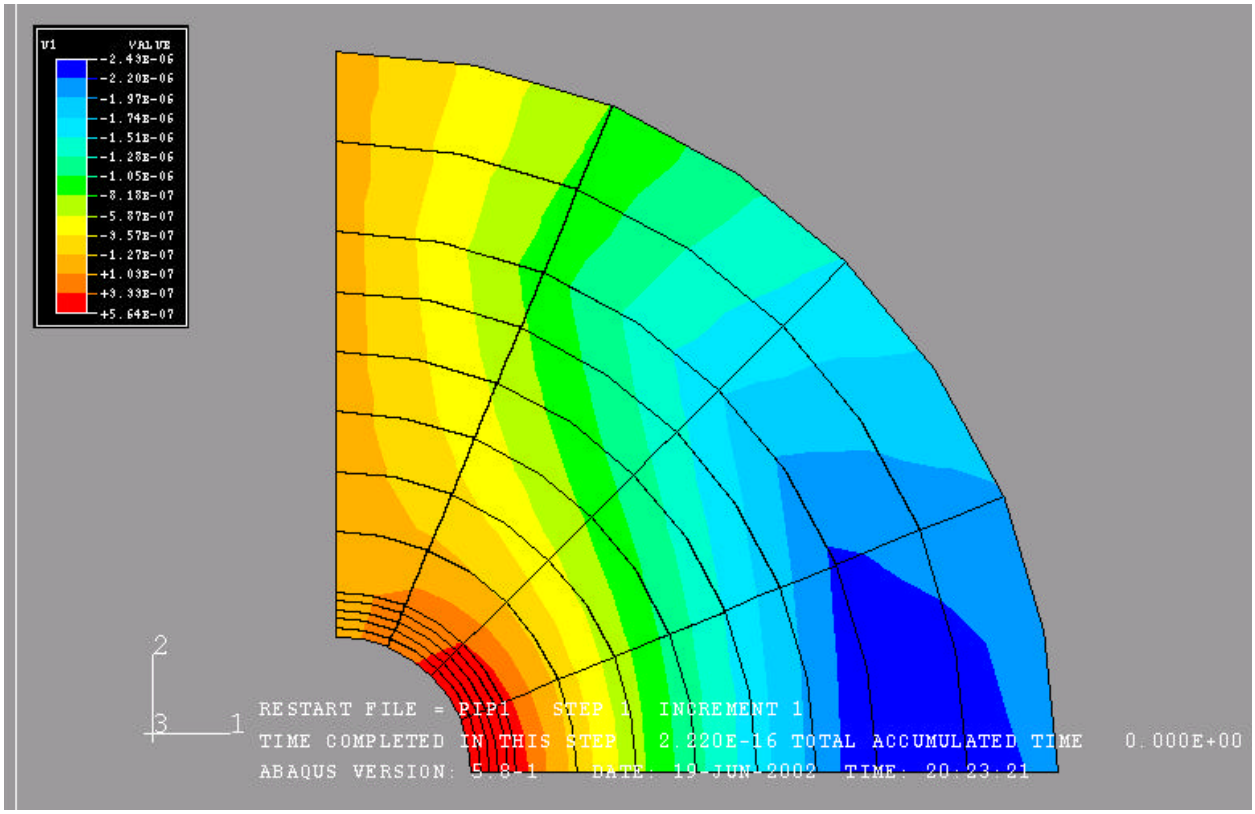

Fig.14d Vertical displacement field (Young's Modulus = 1000 psi)

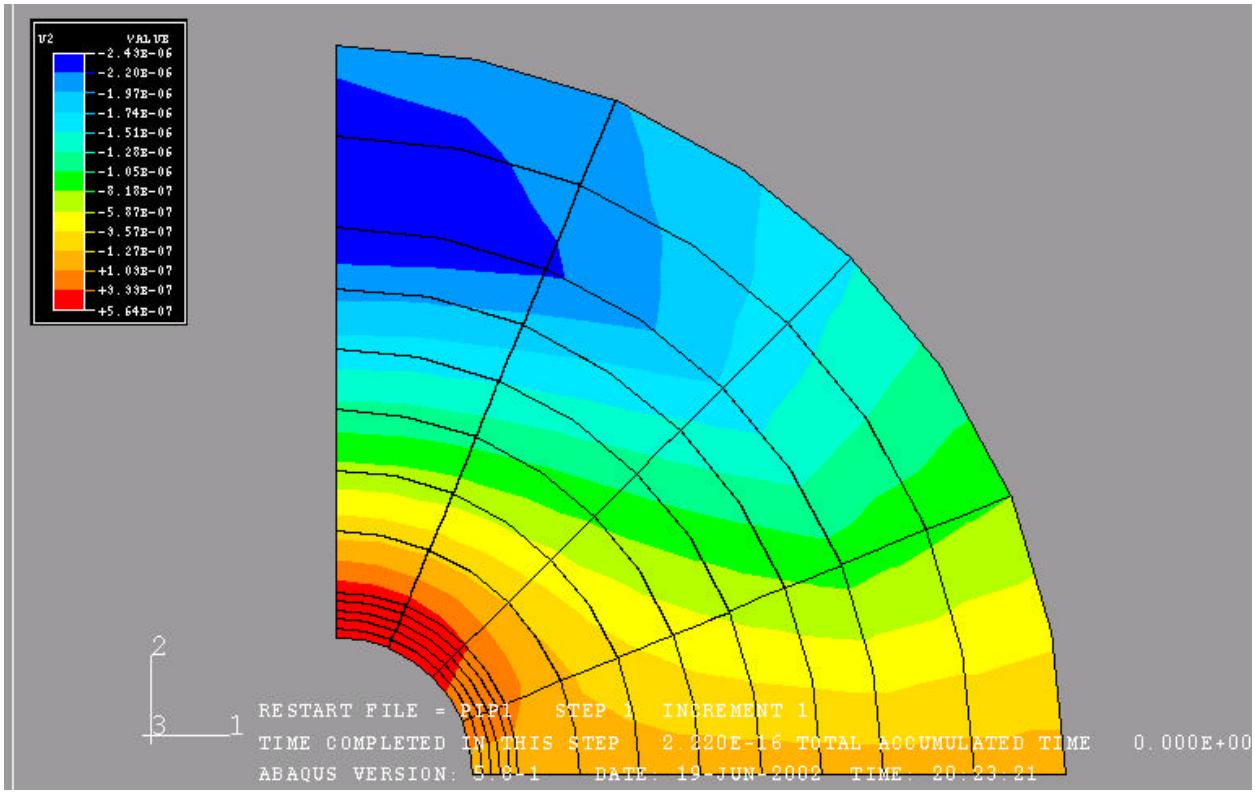

Fig.15a First principal stress profile (Young's Modulus = 3000 psi)

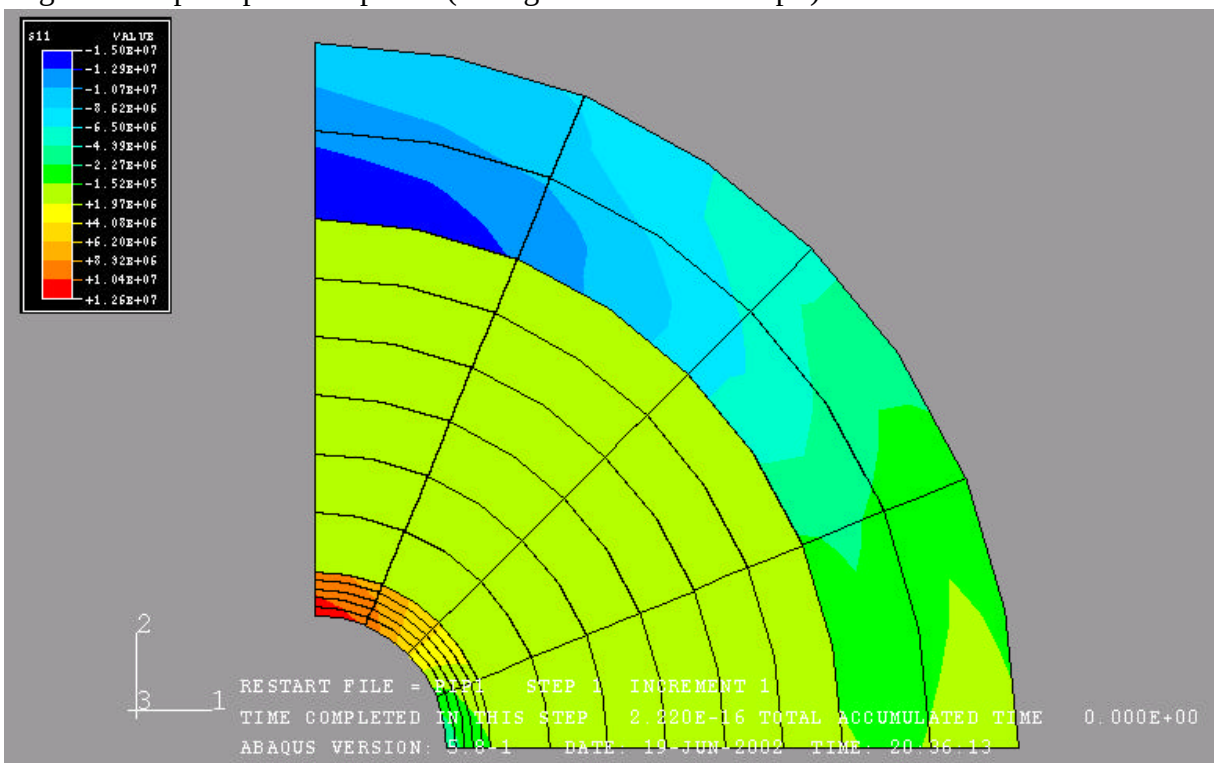

Fig.15b Second principal stress profile (Young's Modulus = 3000 psi)

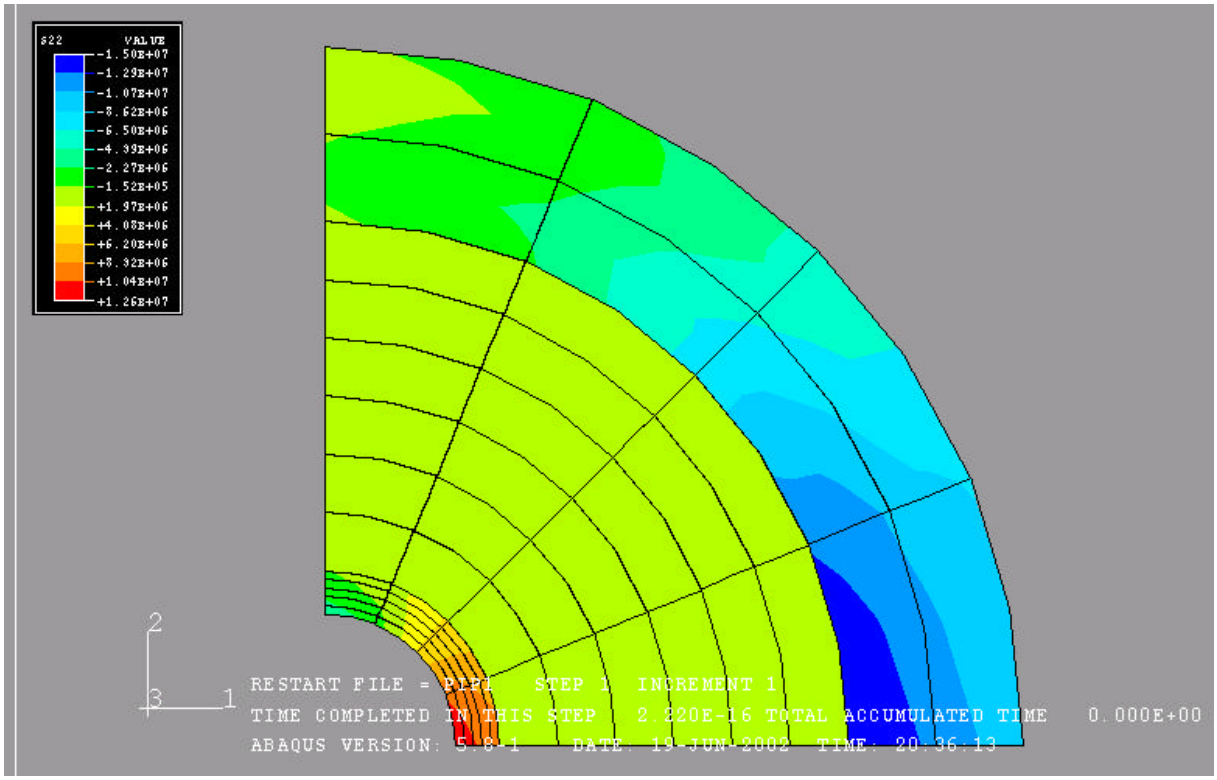

Fig.15c Horizontal displacement field (Young's Modulus = 3000 psi)

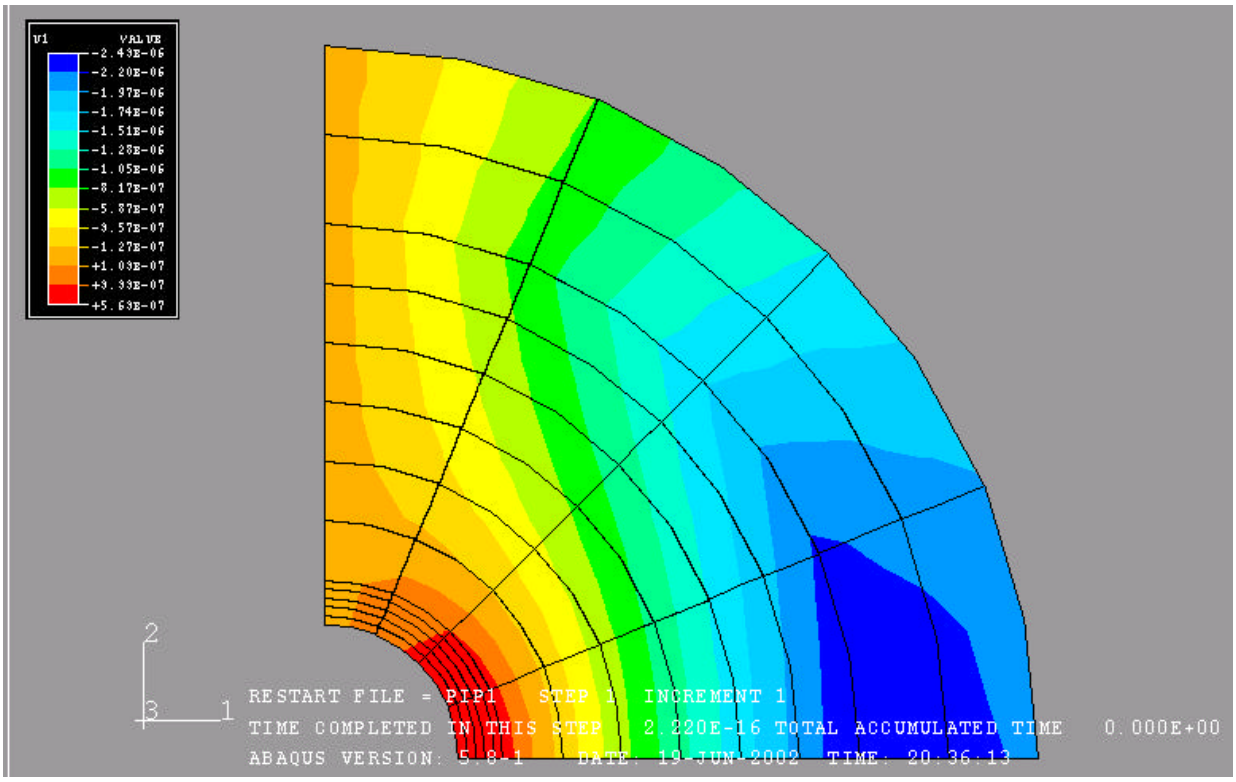

Fig.15d Vertical displacement field (Young's Modulus = 3000 psi)

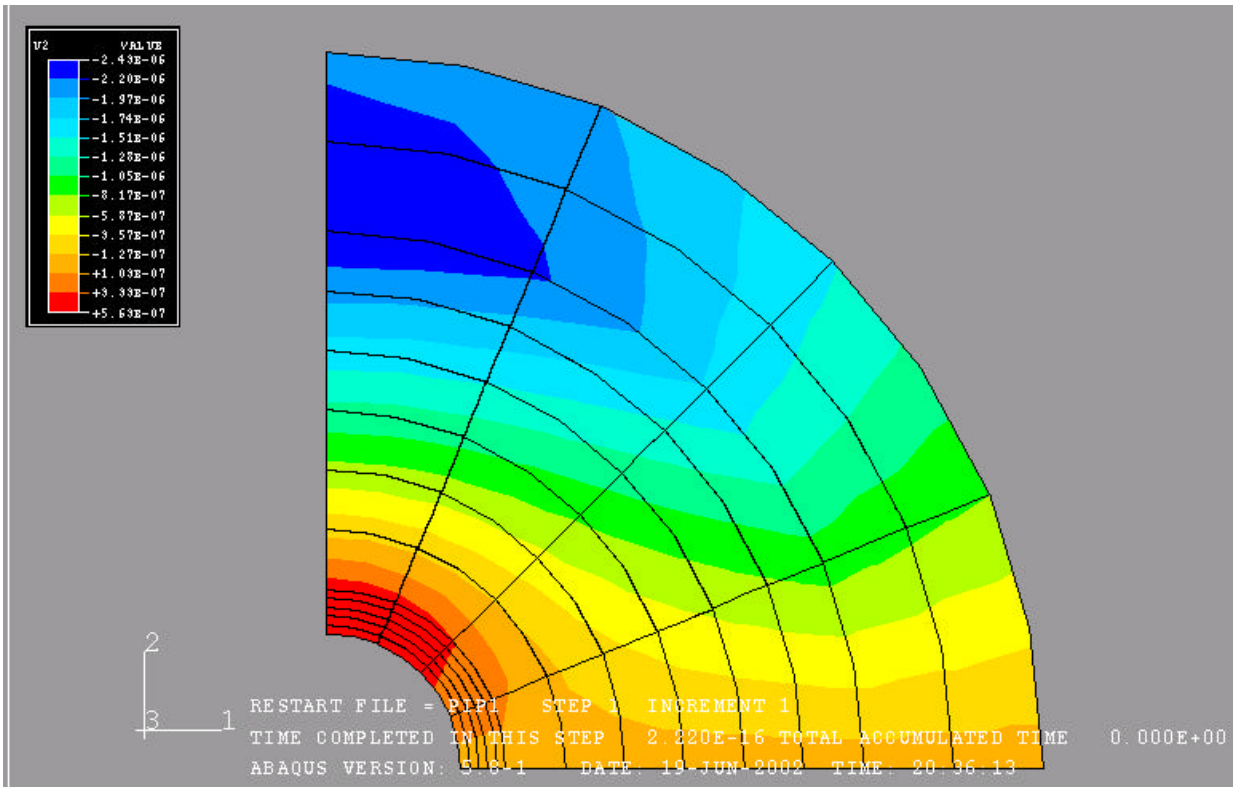

Fig.16a First principal stress profile (Young's Modulus = 5000 psi)

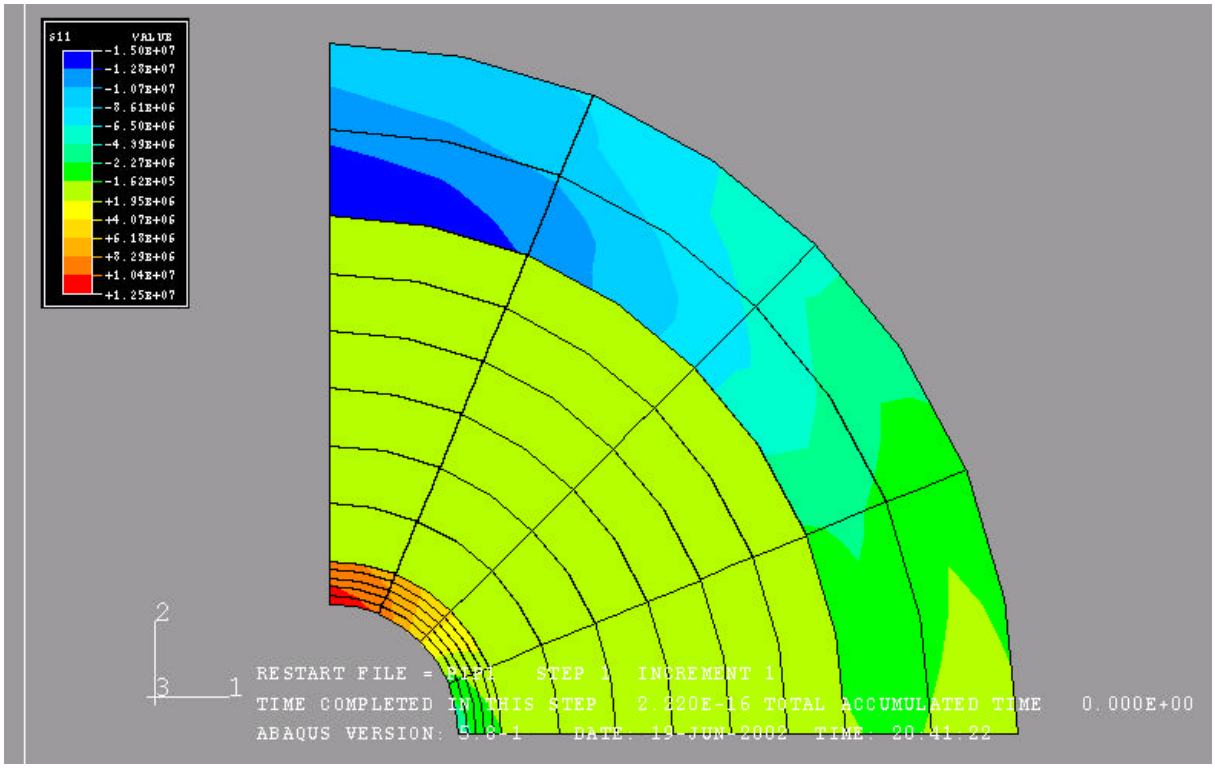

Fig.16b Second principal stress profile (Young's Modulus = 5000 psi)

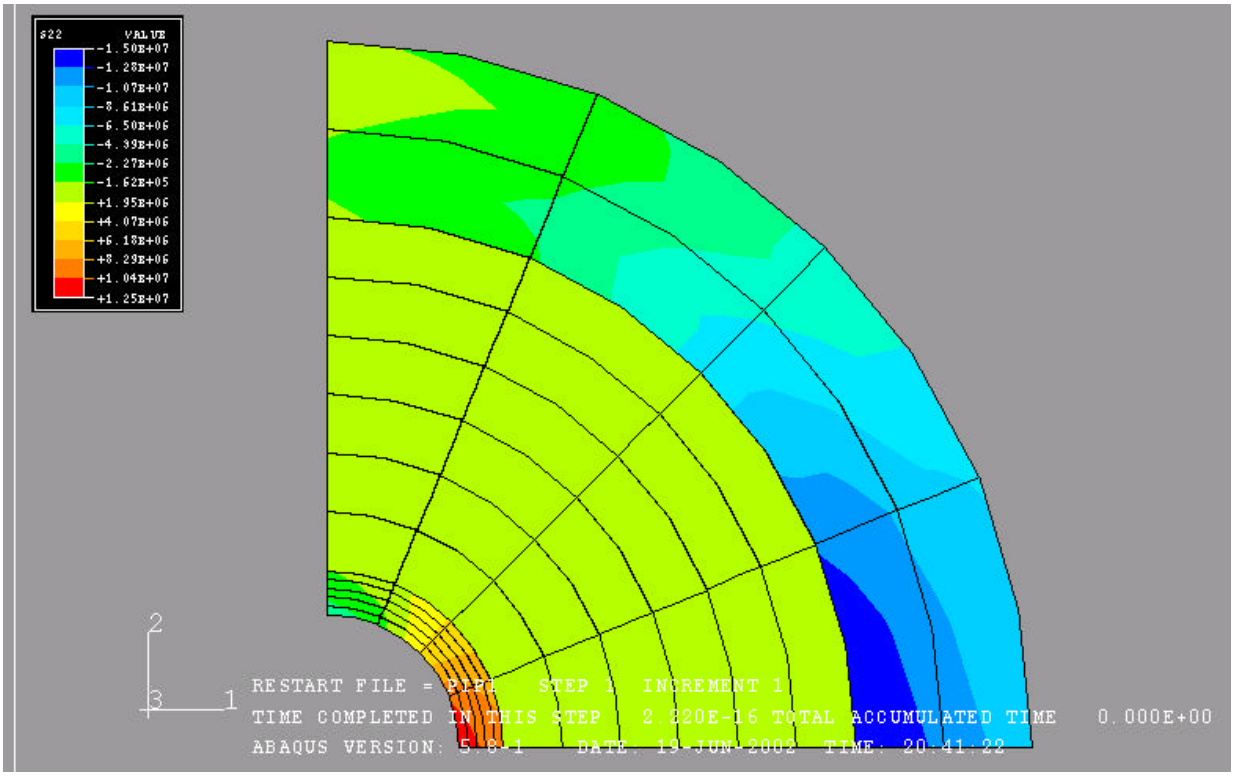

Fig.16c Horizontal displacement field (Young's Modulus = 5000 psi)

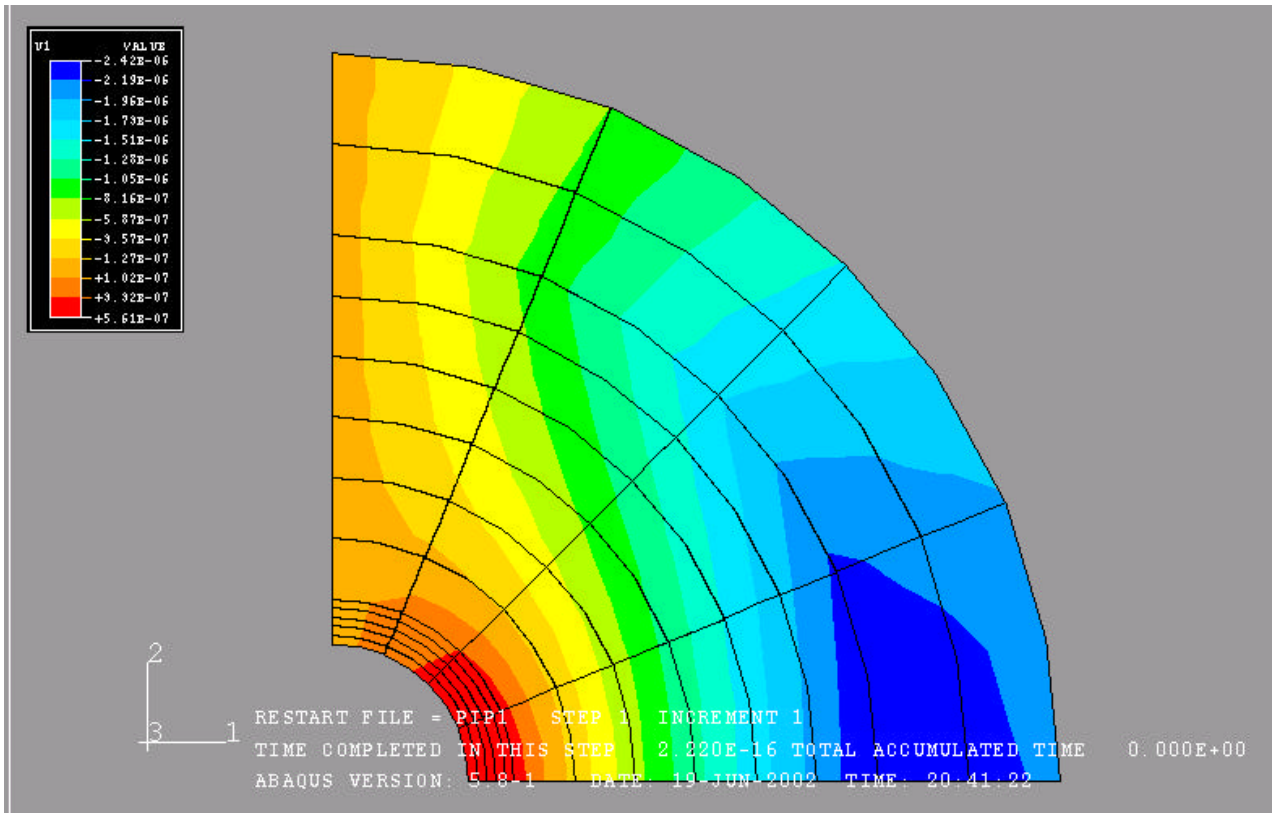

Fig.16d Vertical displacement field (Young's Modulus = 5000 psi)

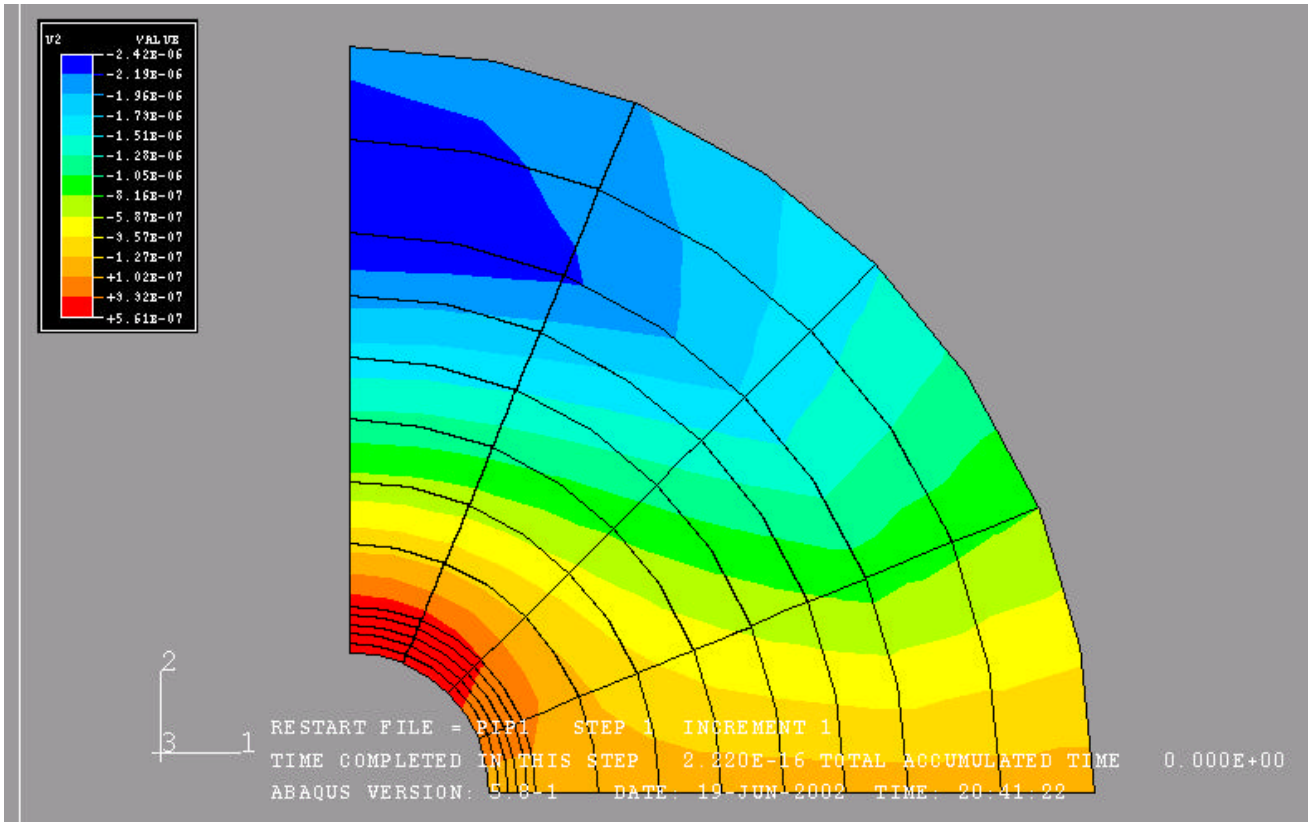

Fig.17a First principal stress profile (Poisson Ratio = 0.15)

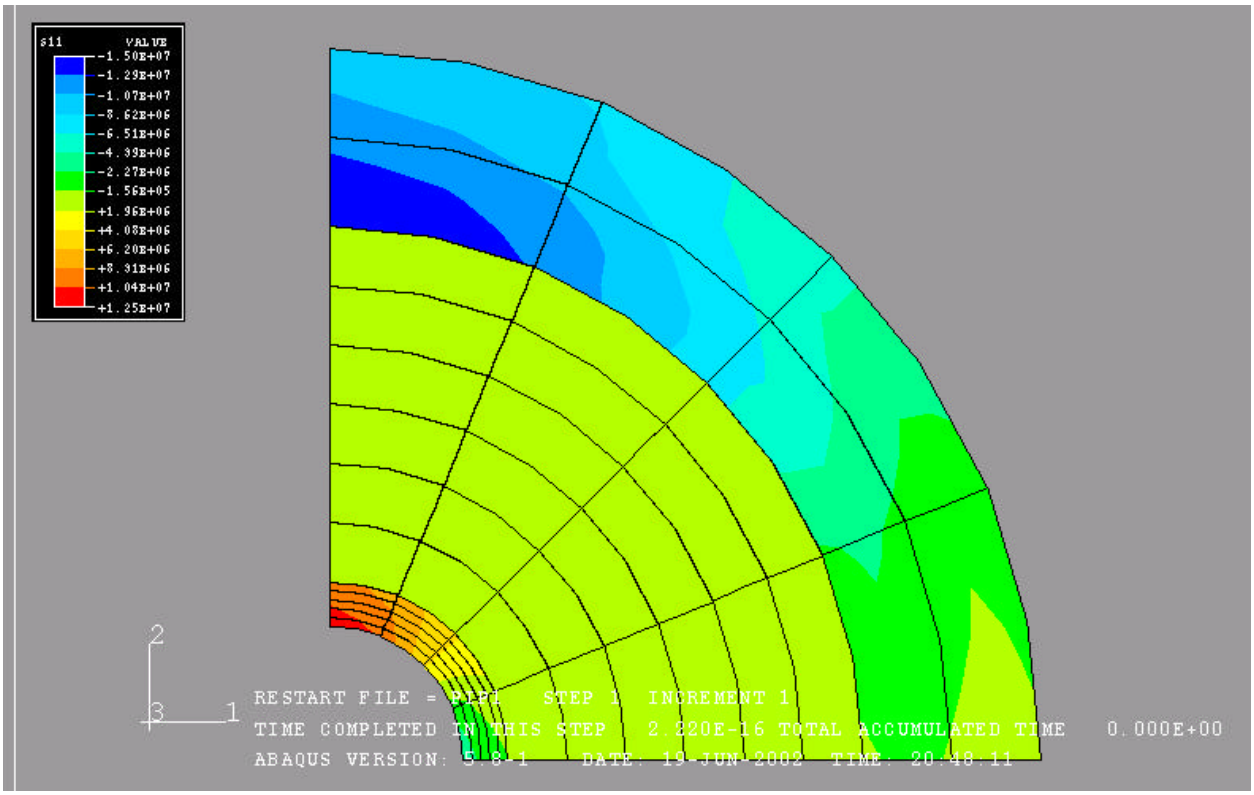

Fig.17b Second principal stress profile (Poisson Ratio = 0.15)

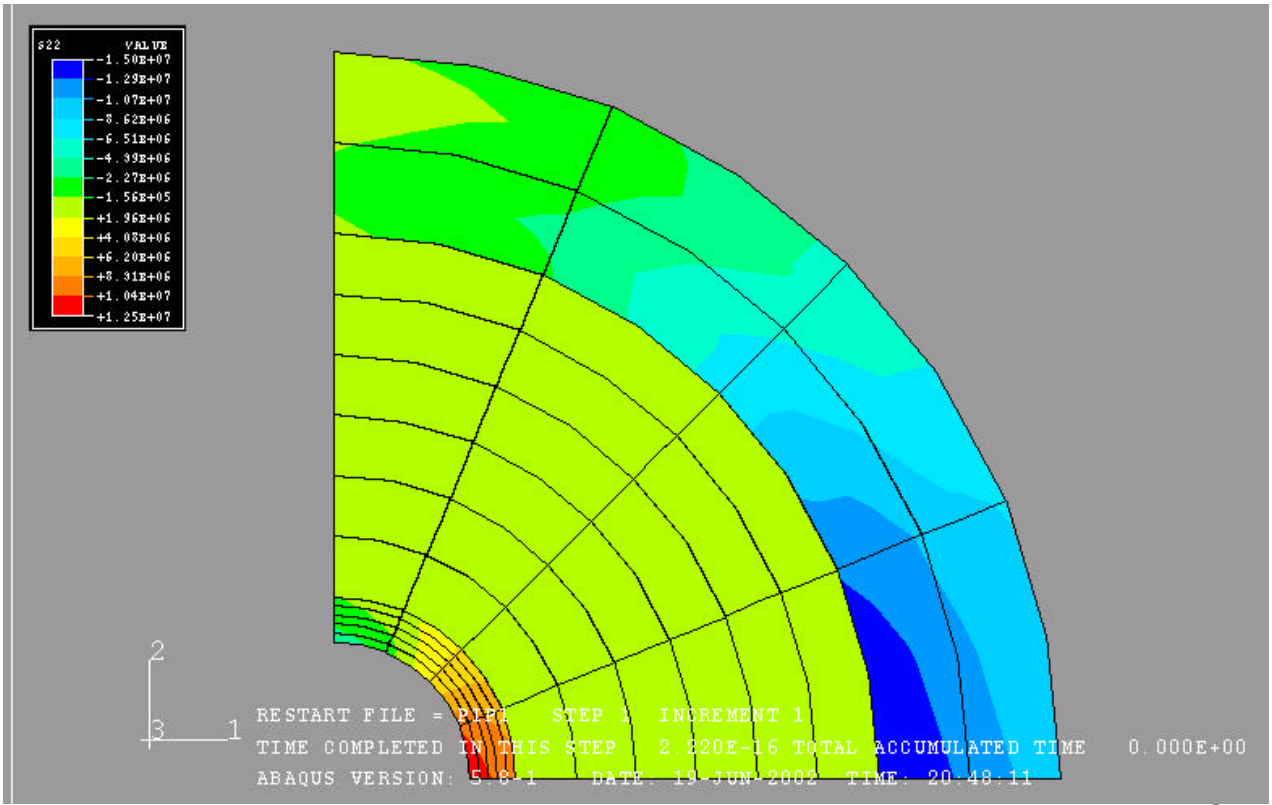

Fig.17c Horizontal displacement field (Poisson Ratio = 0.15)

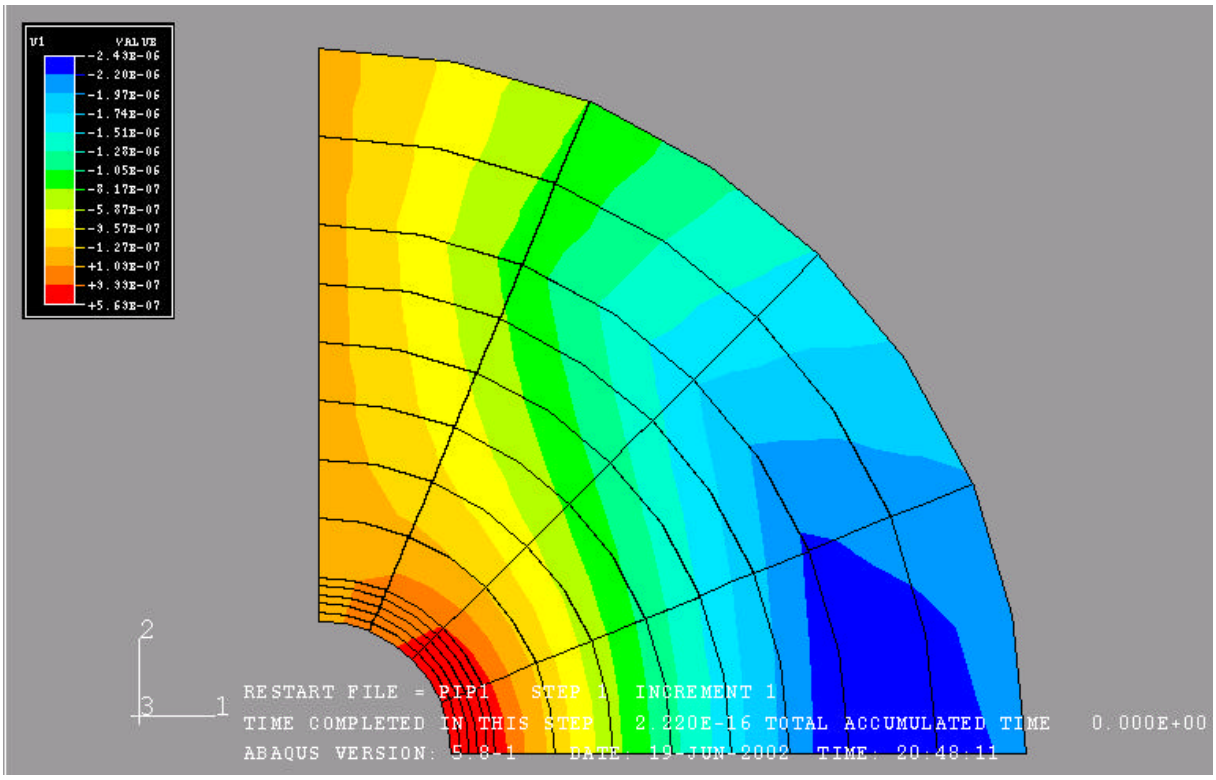

Fig.17d Vertical displacement field (Poisson Ratio = 0.15)

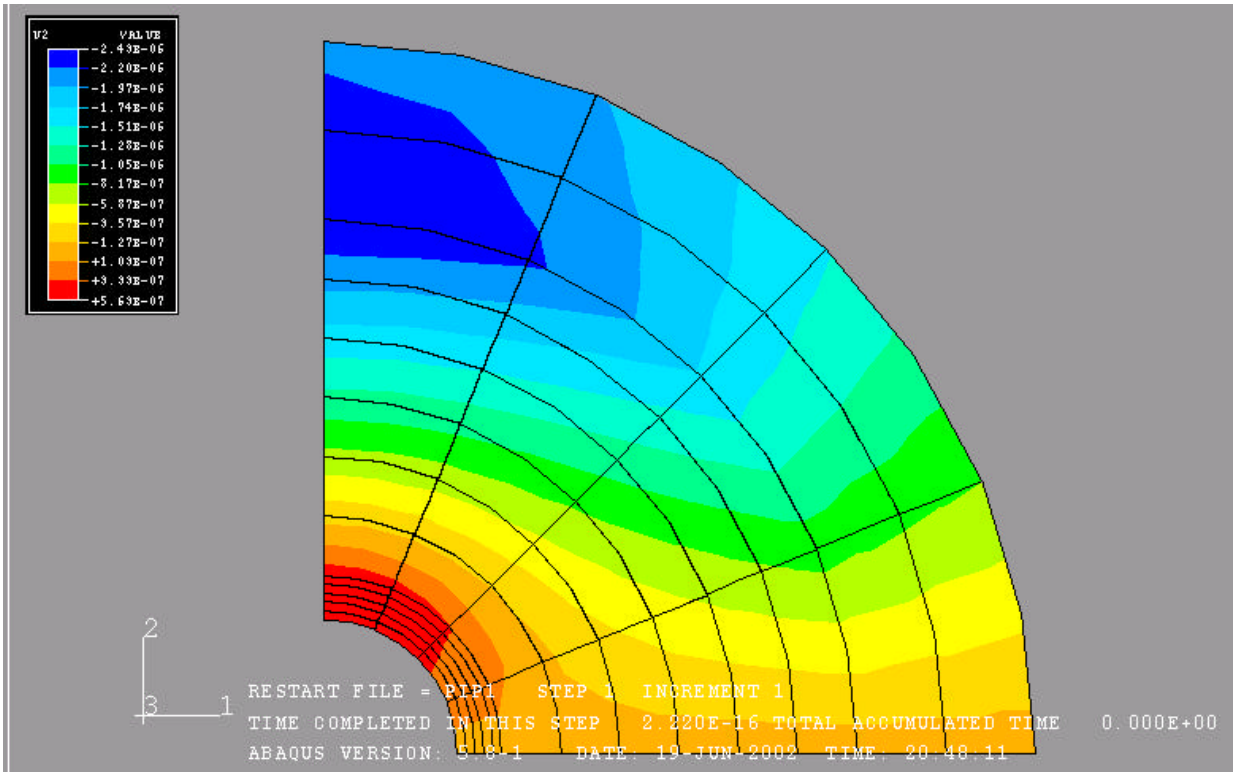

Fig.18a First principal stress profile (Poisson Ratio = 0.25)

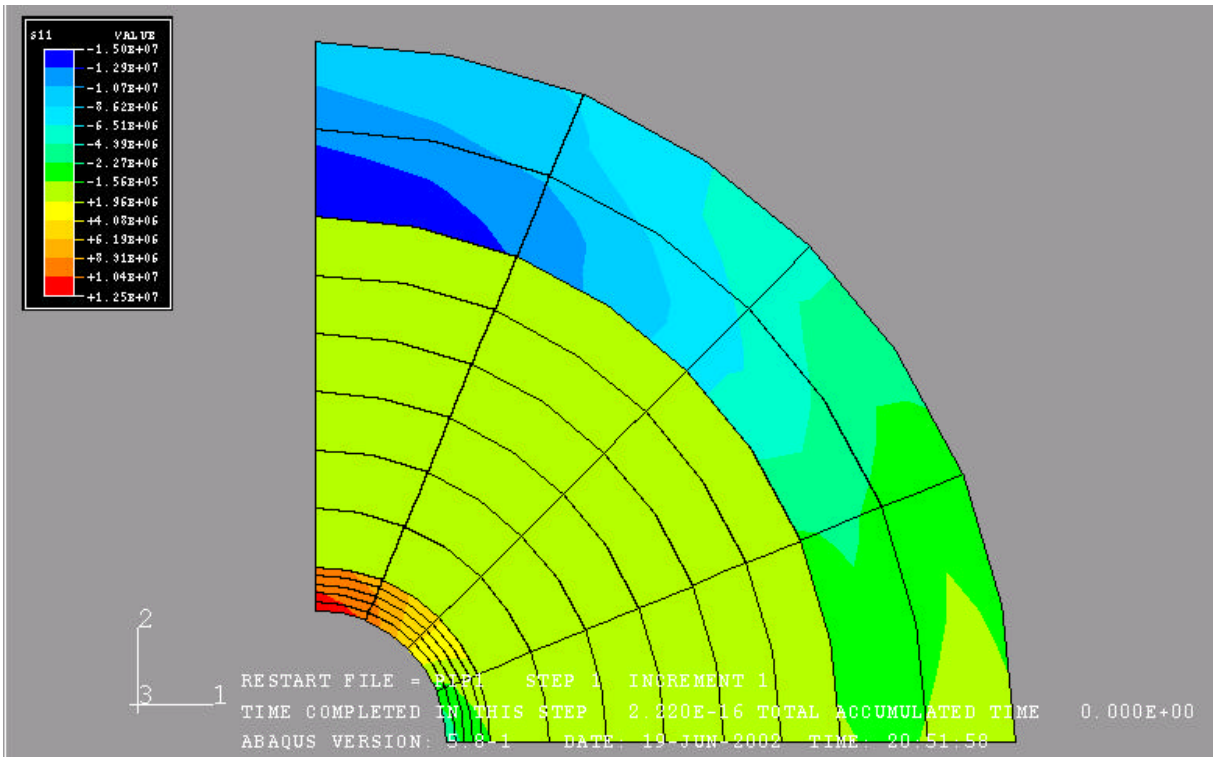

Fig.18b Second principal stress profile (Poisson Ratio = 0.25)

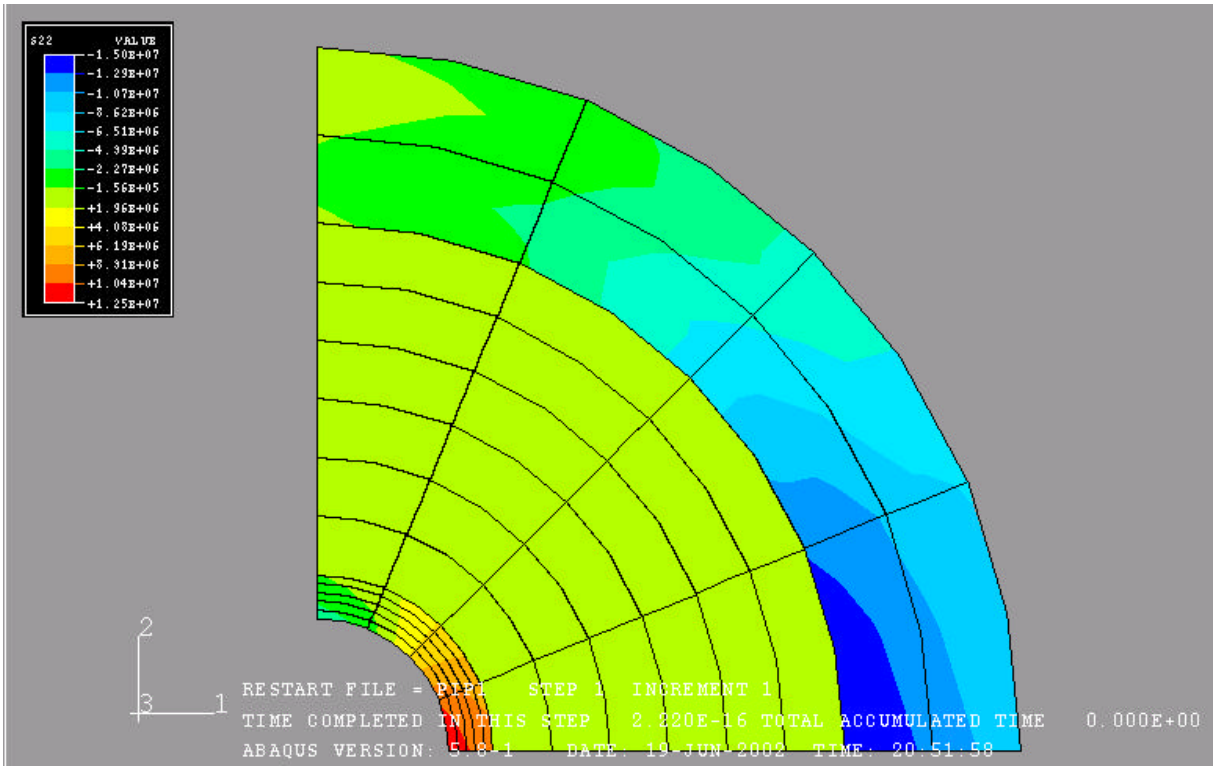

Fig.18c Horizontal displacement field (Poisson Ratio = 0.25)

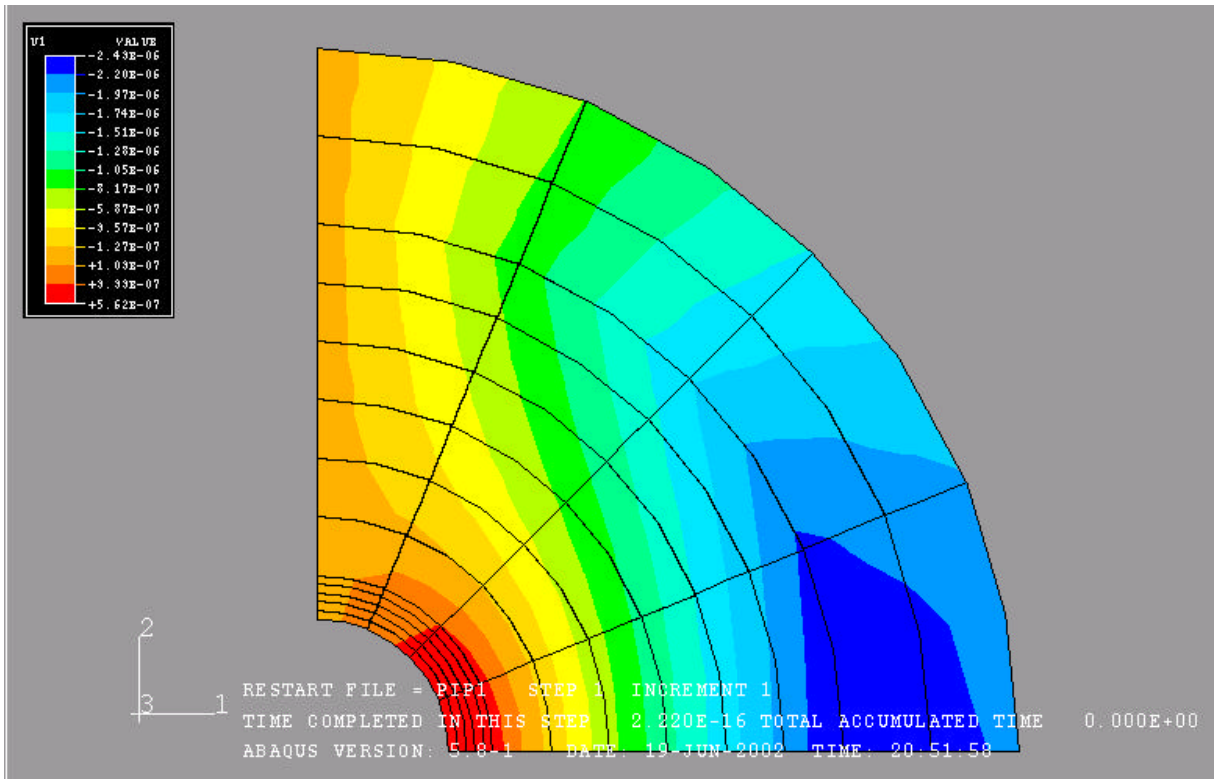

Fig.18d Vertical displacement field (Poisson Ratio = 0.25)

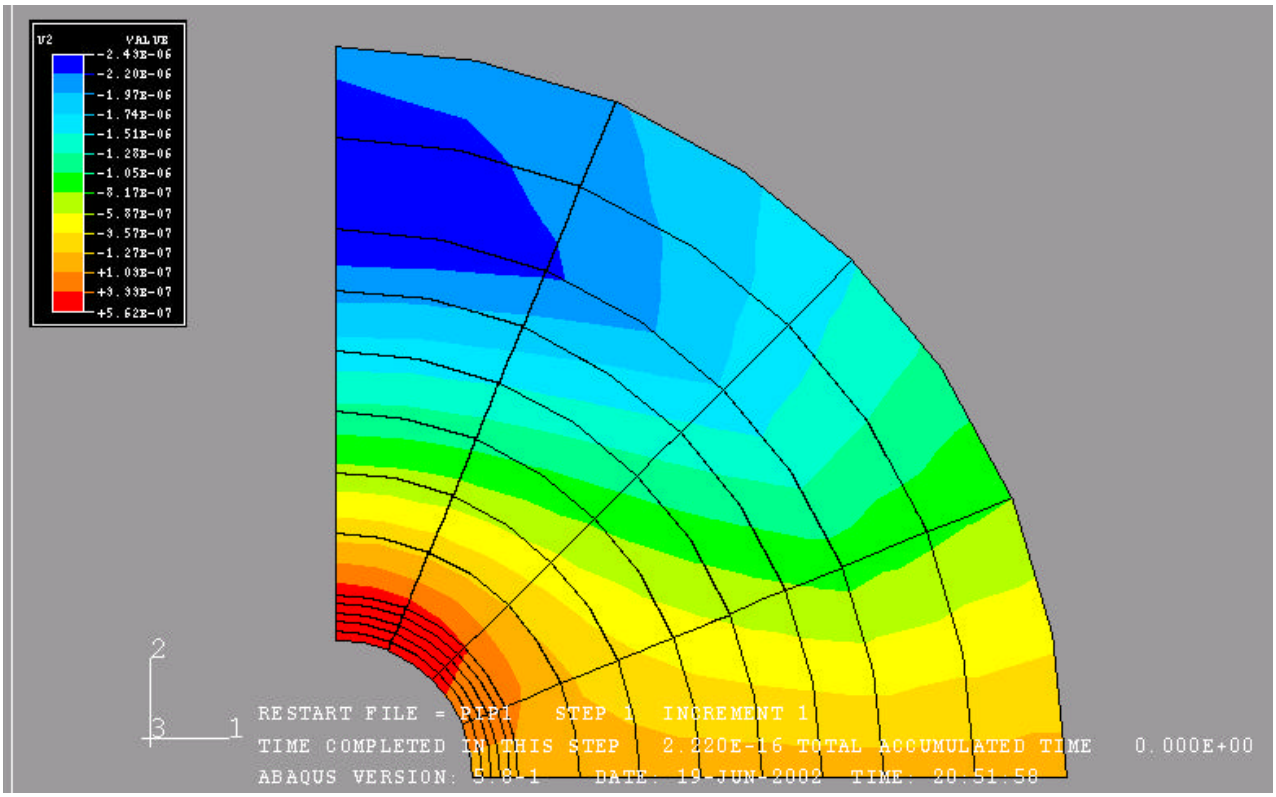
V2
VALUE
-2.43E-06
-2.20E-06
-1.97E-06
-1.74E-06
-1.51E-06
-1.28E-06
-1.05E-06
-8.17E-07
-5.87E-07
-3.57E-07
-1.27E-07
+1.03E-07
+3.33E-07
+5.62E-07
2
3
1
RESTART FILE = PIP1 STEP 1 INCREMENT 1
TIME COMPLETED IN THIS STEP 2.220E-16 TOTAL ACCUMULATED TIME 0.000E+00
ABAQUS VERSION: 5.8-1 DATE: 19-JUN-2002 TIME: 20:51:58

Fig.19a First principal stress profile (Poisson Ratio = 0.45)

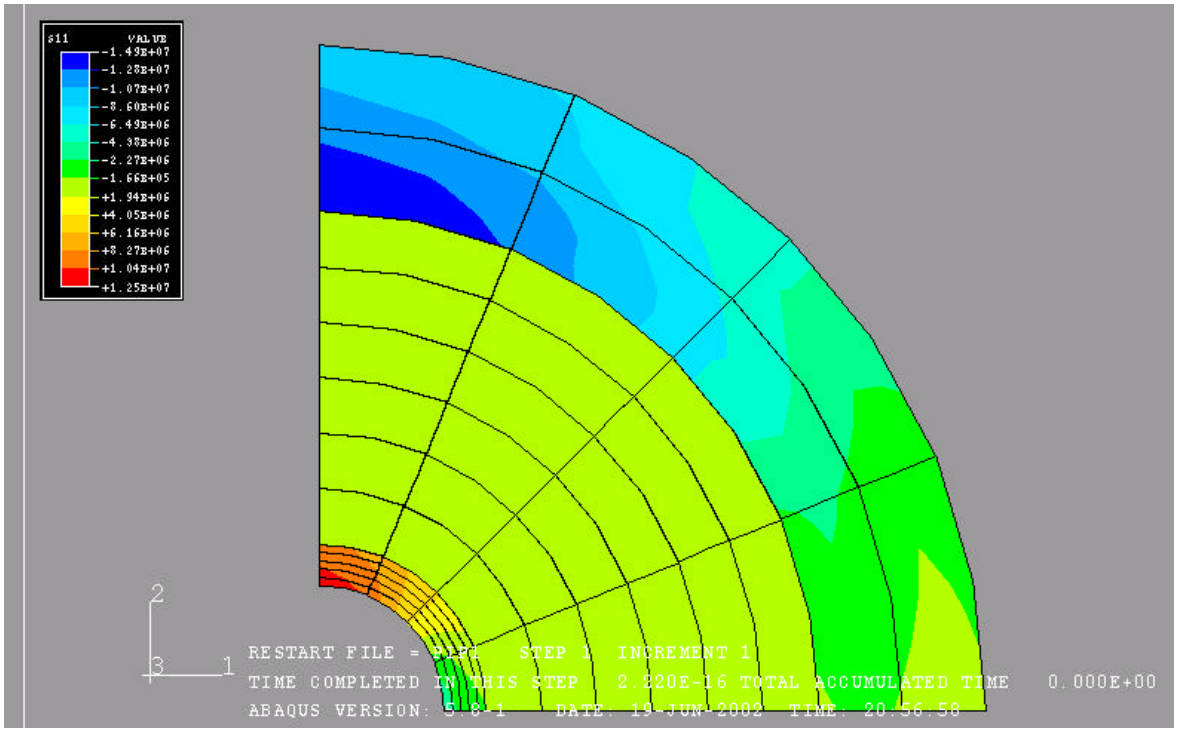

Fig.19b Second principal stress profile (Poisson Ratio = 0.45)

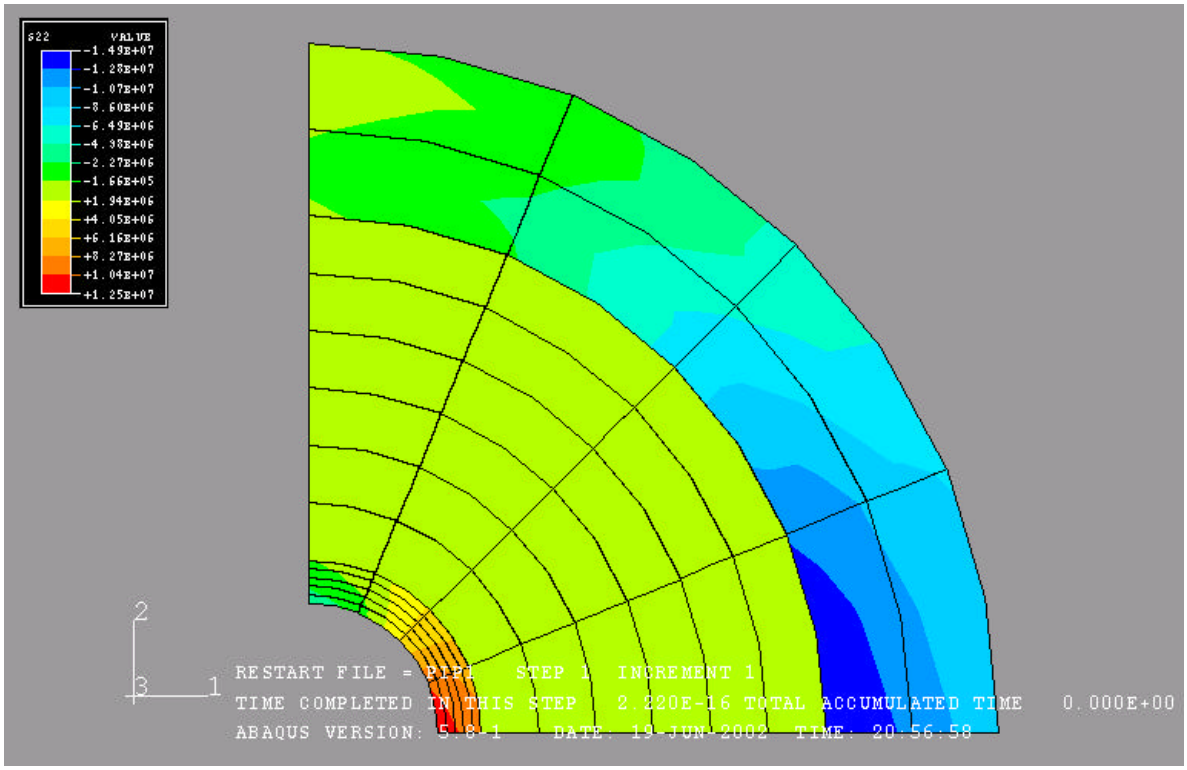

Fig.19c Horizontal displacement field (Poisson Ratio = 0.45)

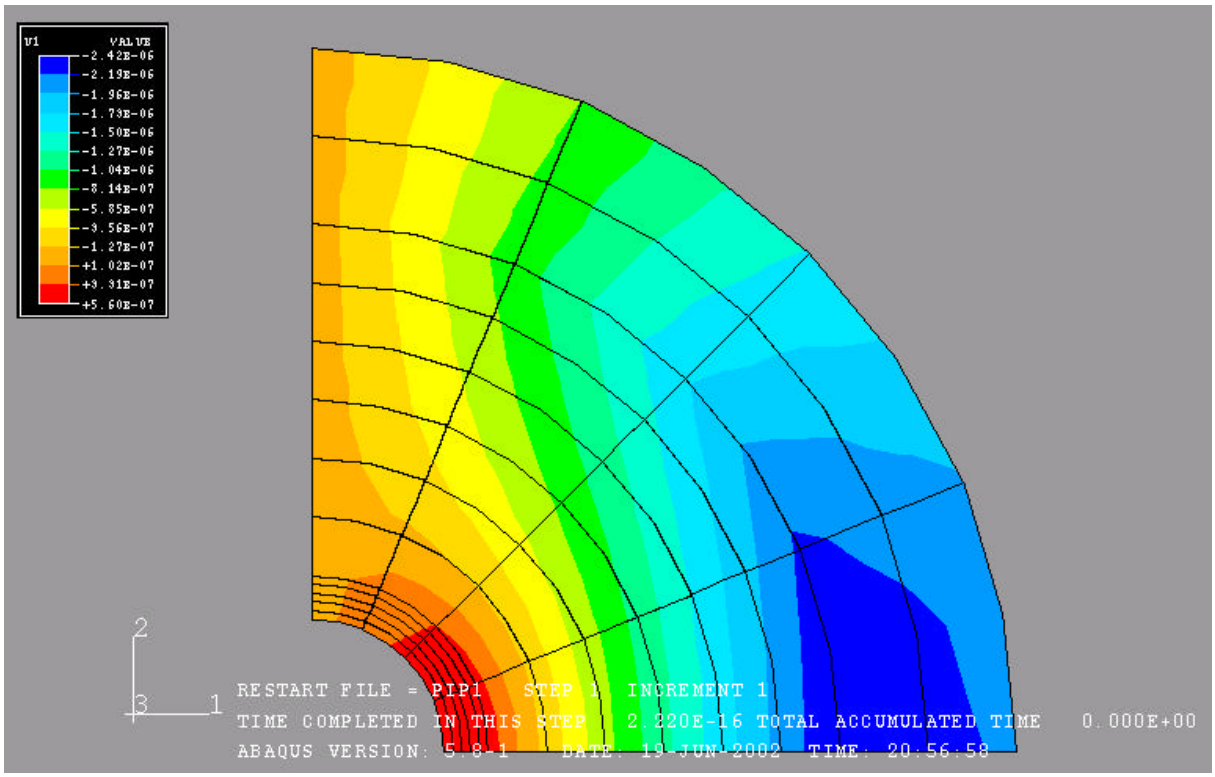

Fig.19d Vertical displacement field (Poisson Ratio = 0.45)

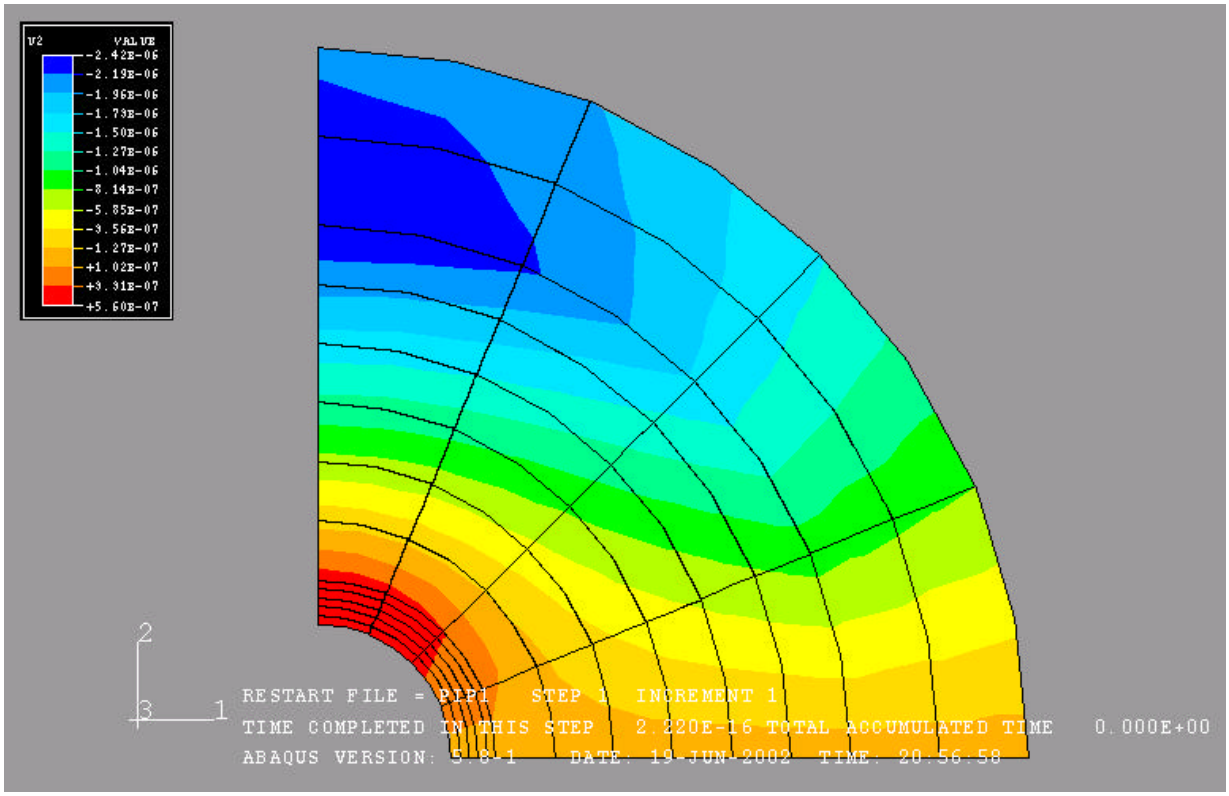

Fig.20a First principal stress profile (T_{in} = 80 F)

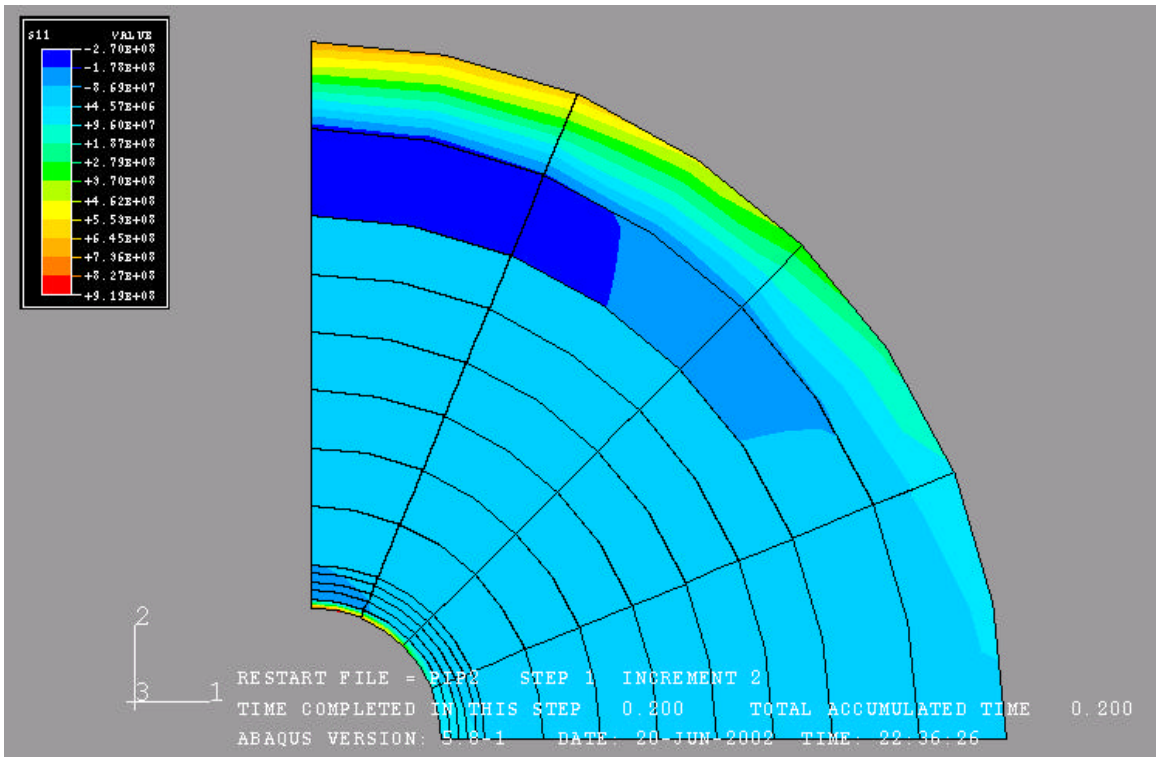

Fig.20b Temperature profile (T_{in} = 80 F)

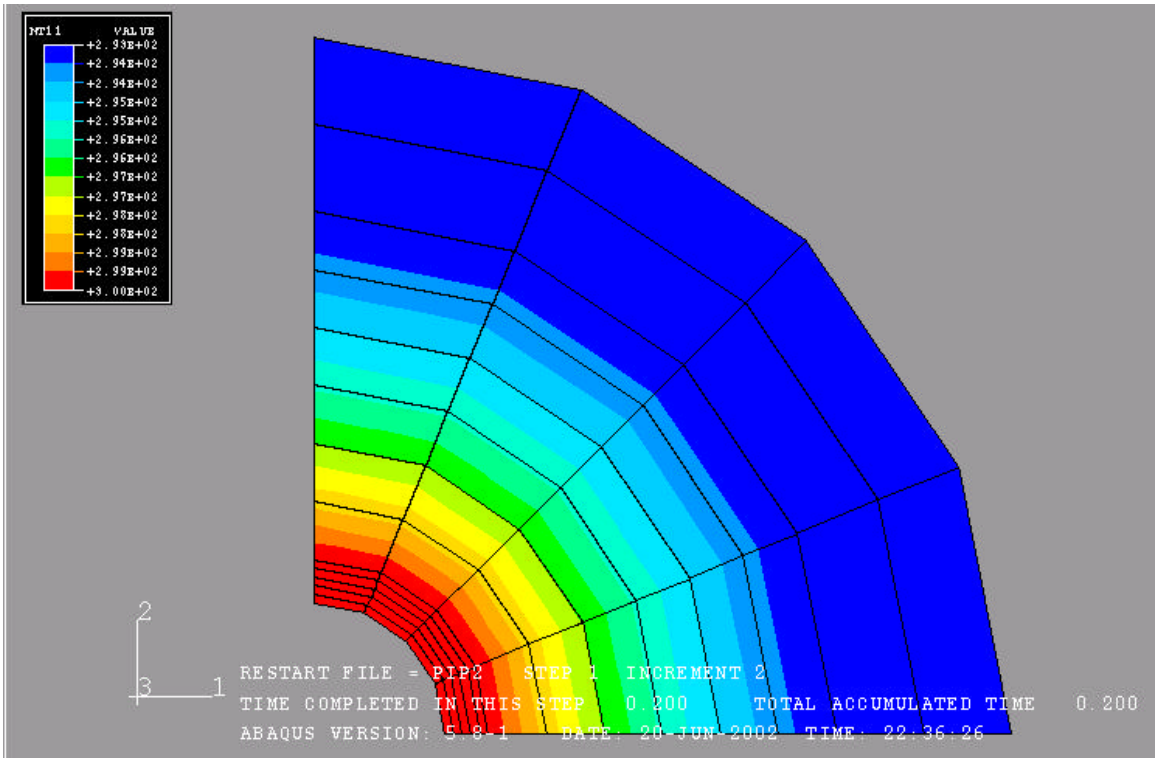

Fig.20c Horizontal displacement field (T_{in} = 80 F)

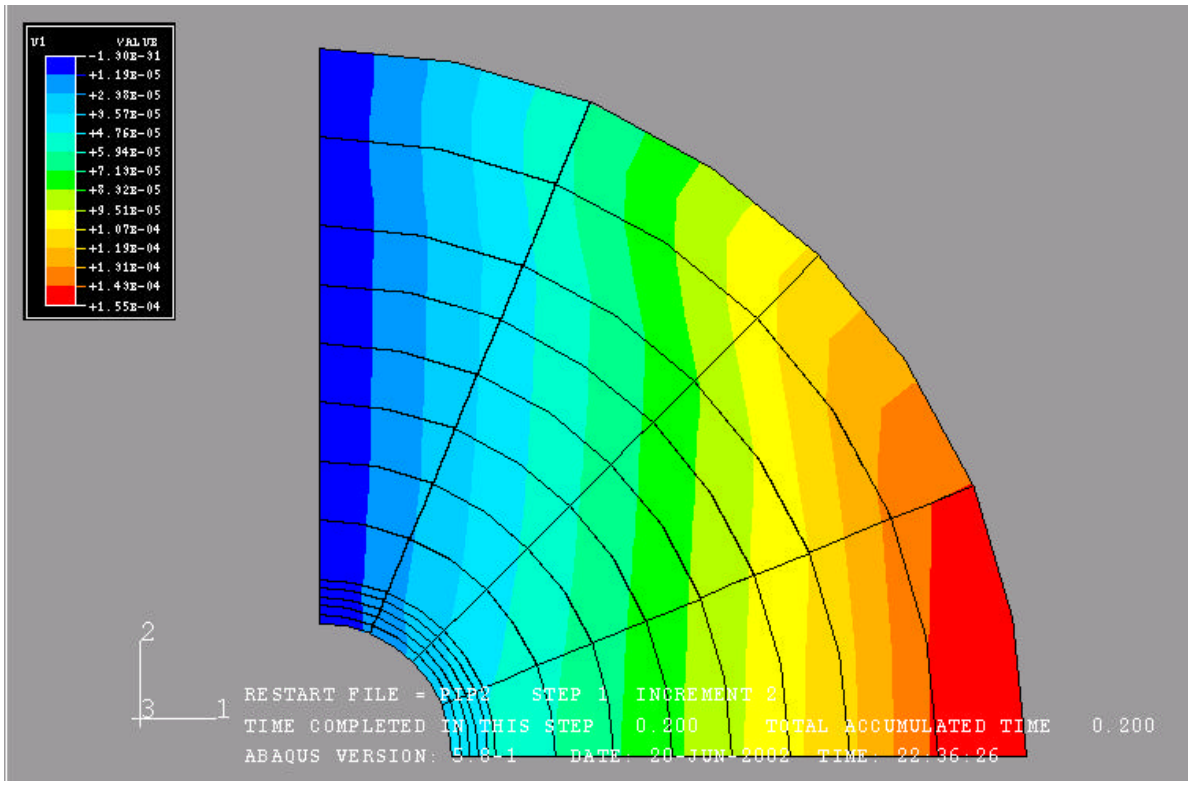

Fig.20d Vertical displacement field (T_{in} = 80 F)

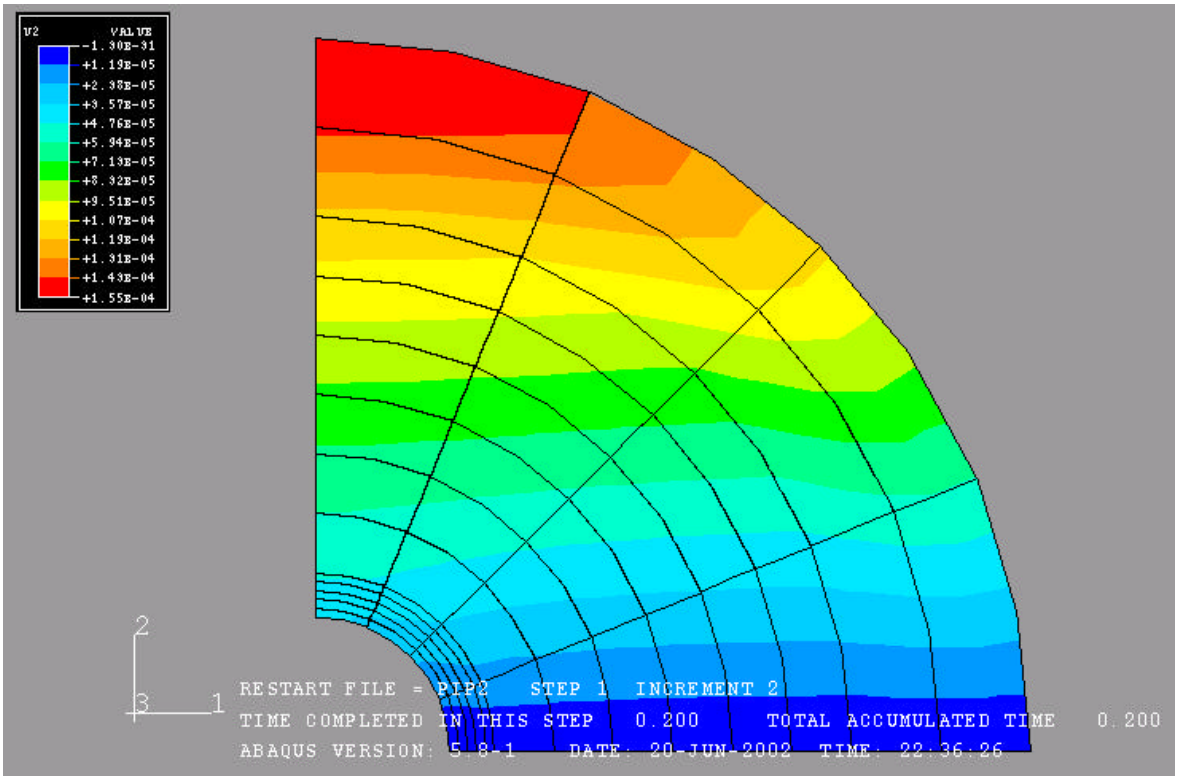

Fig.21a First principal stress profile (T_{in} = 110 F)

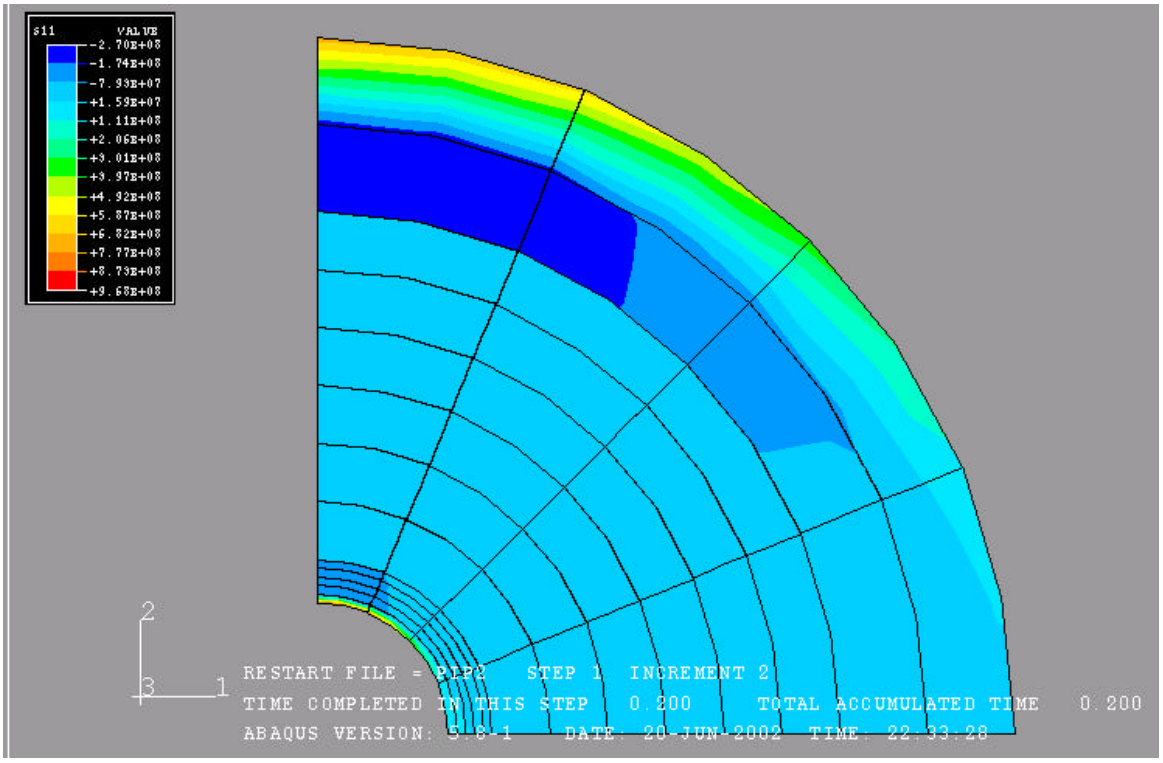

Fig.21b Temperature profile (T_{in} = 110 F)

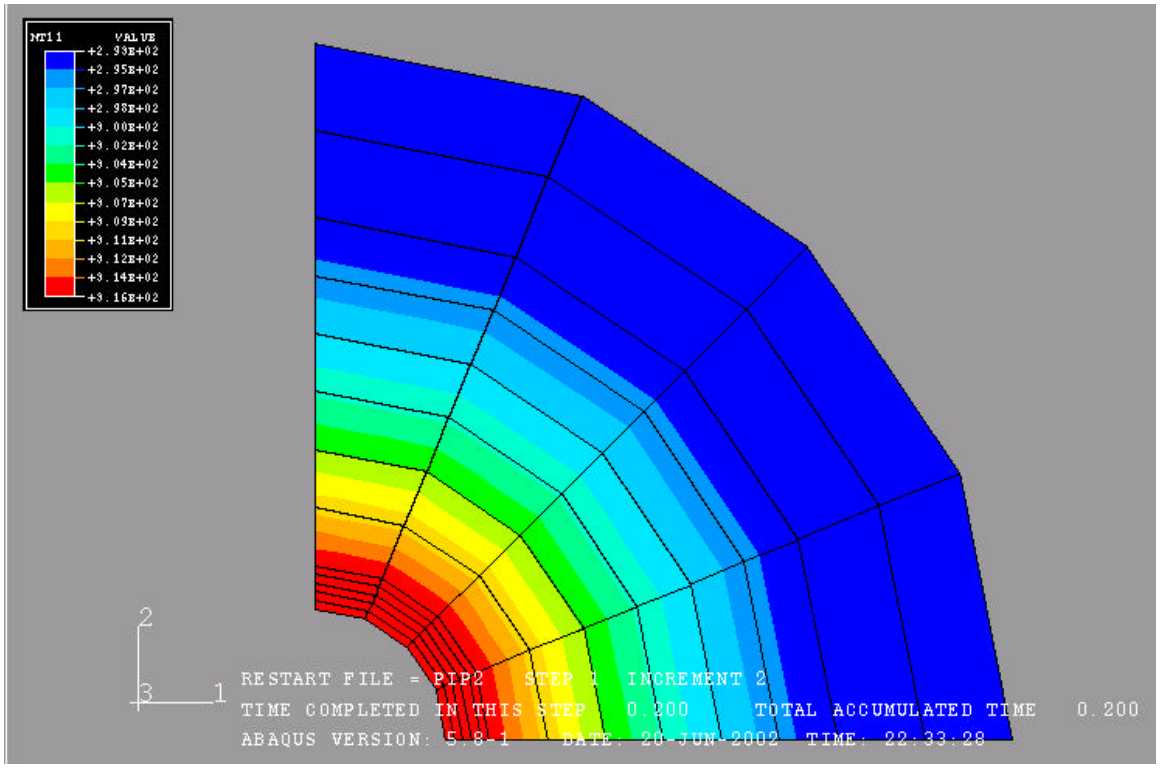

Fig.21c Horizontal displacement field (T_{in} = 110 F)

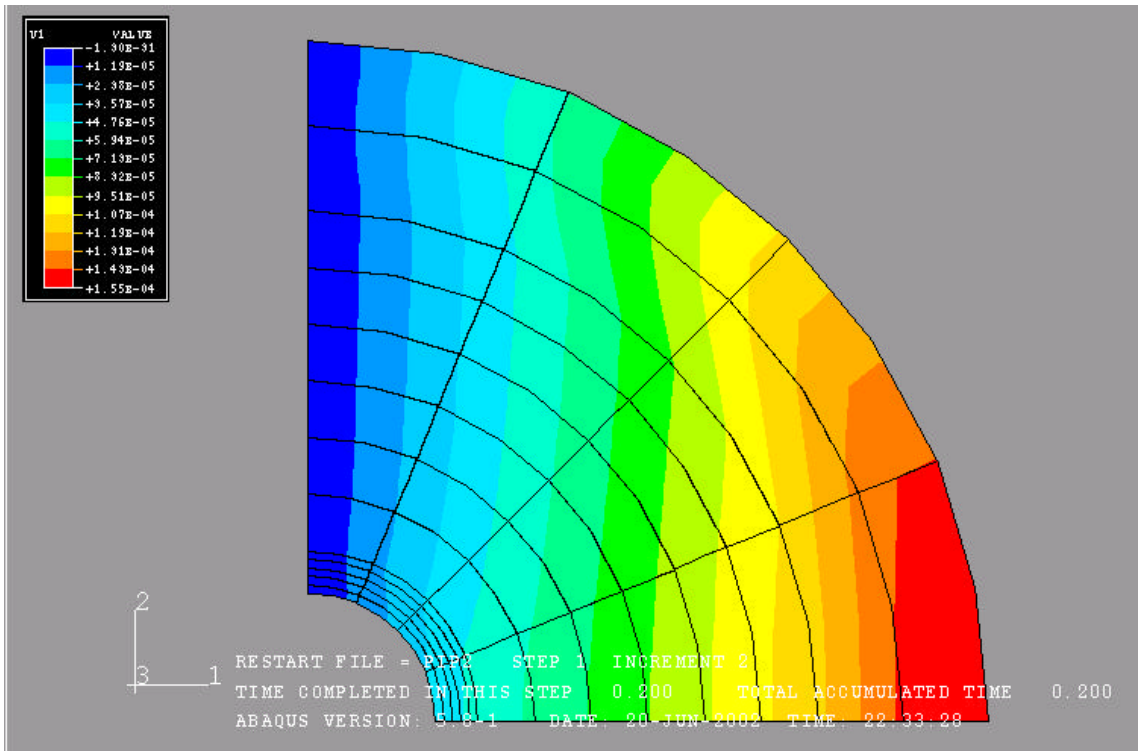

Fig.21d Vertical displacement field (T_{in} = 110 F)

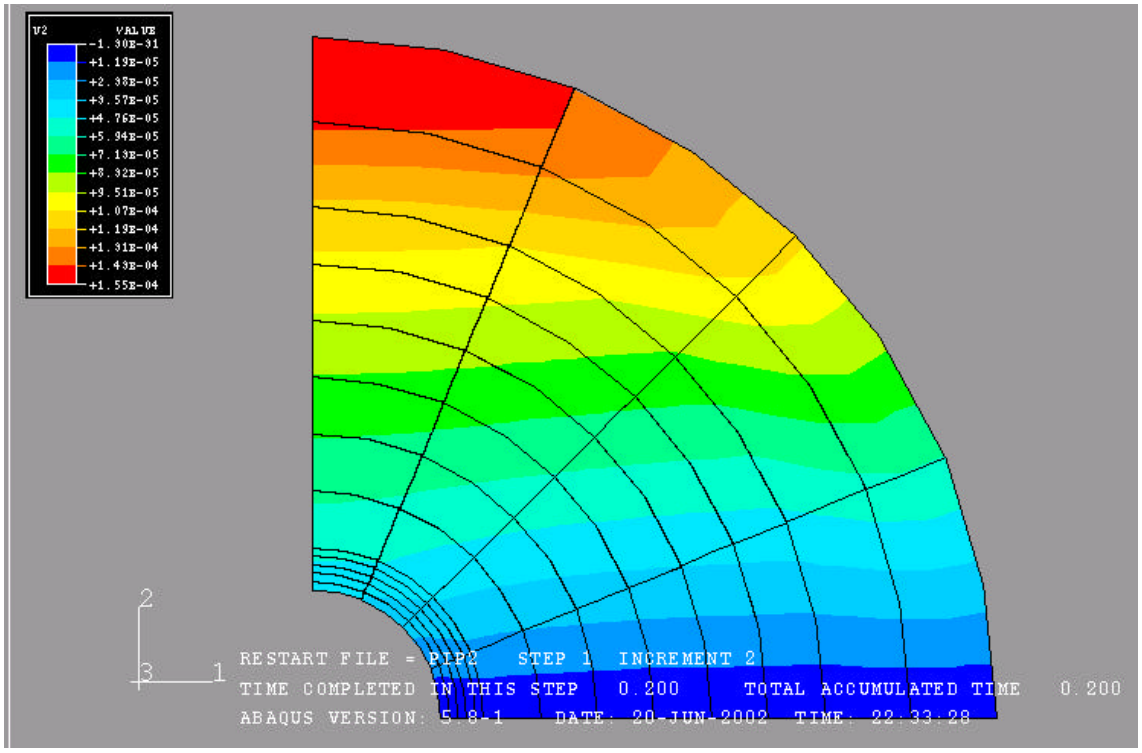

Fig.22a First principal stress profile (T_{in} = 150 F)

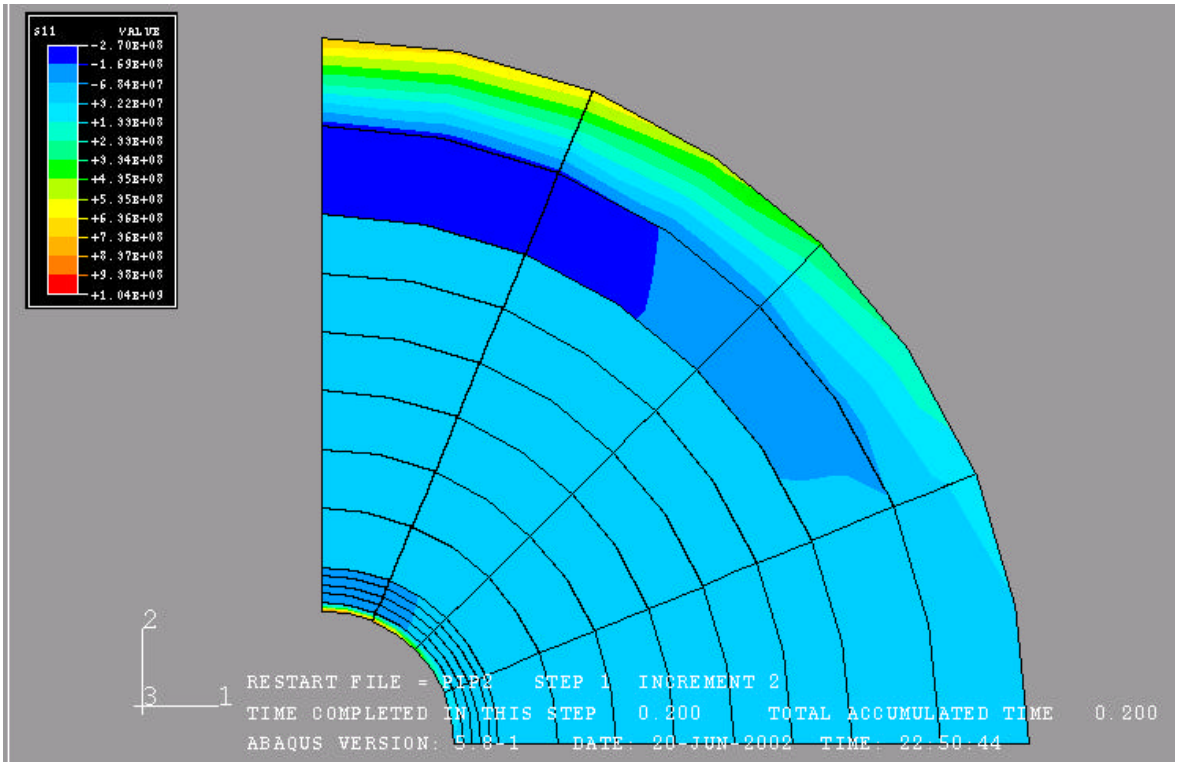

Fig.22b Temperature profile (T_{in} = 150 F)

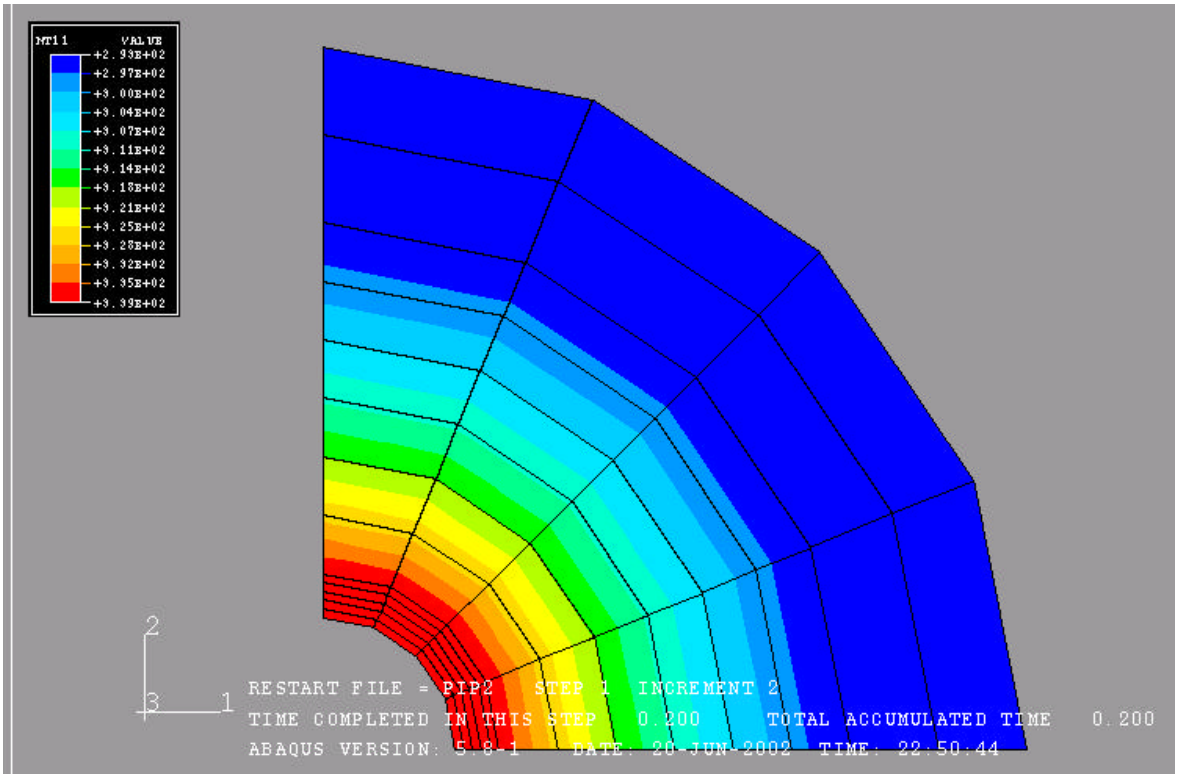

Fig.22c Horizontal displacement field (T_{in} = 150 F)

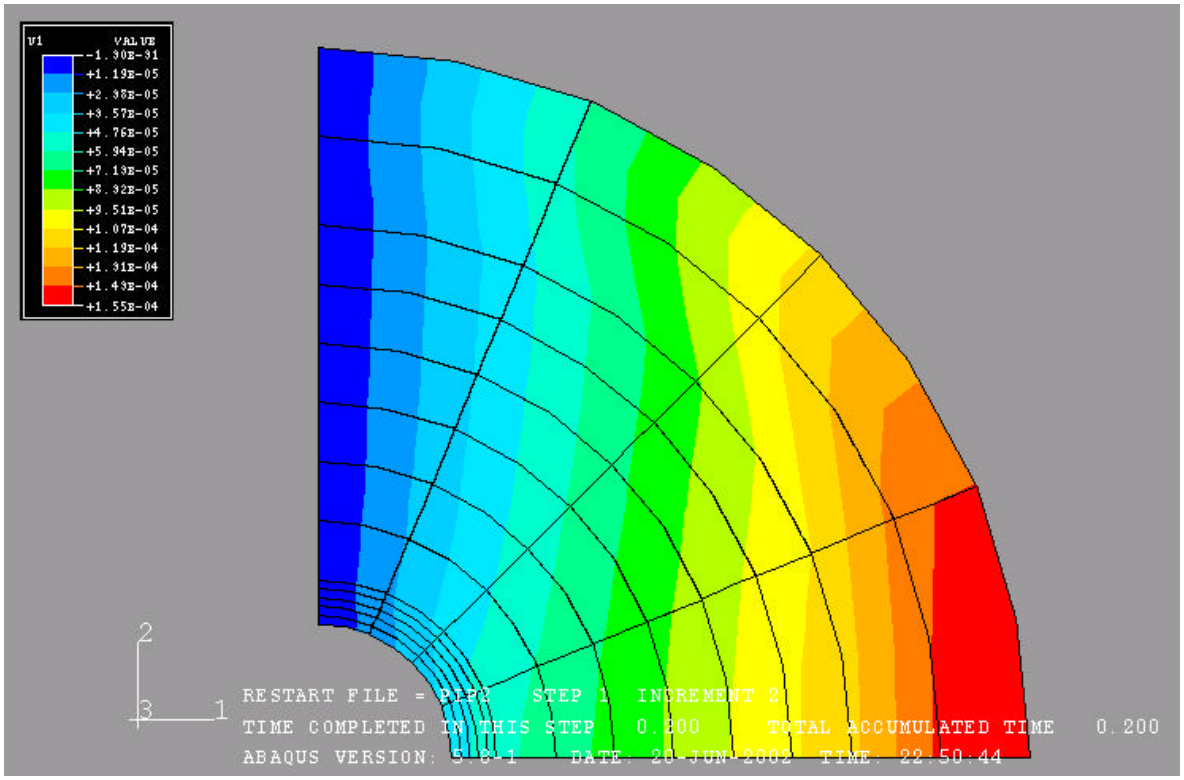

Fig.22d Vertical displacement field (T_{in} = 150 F)

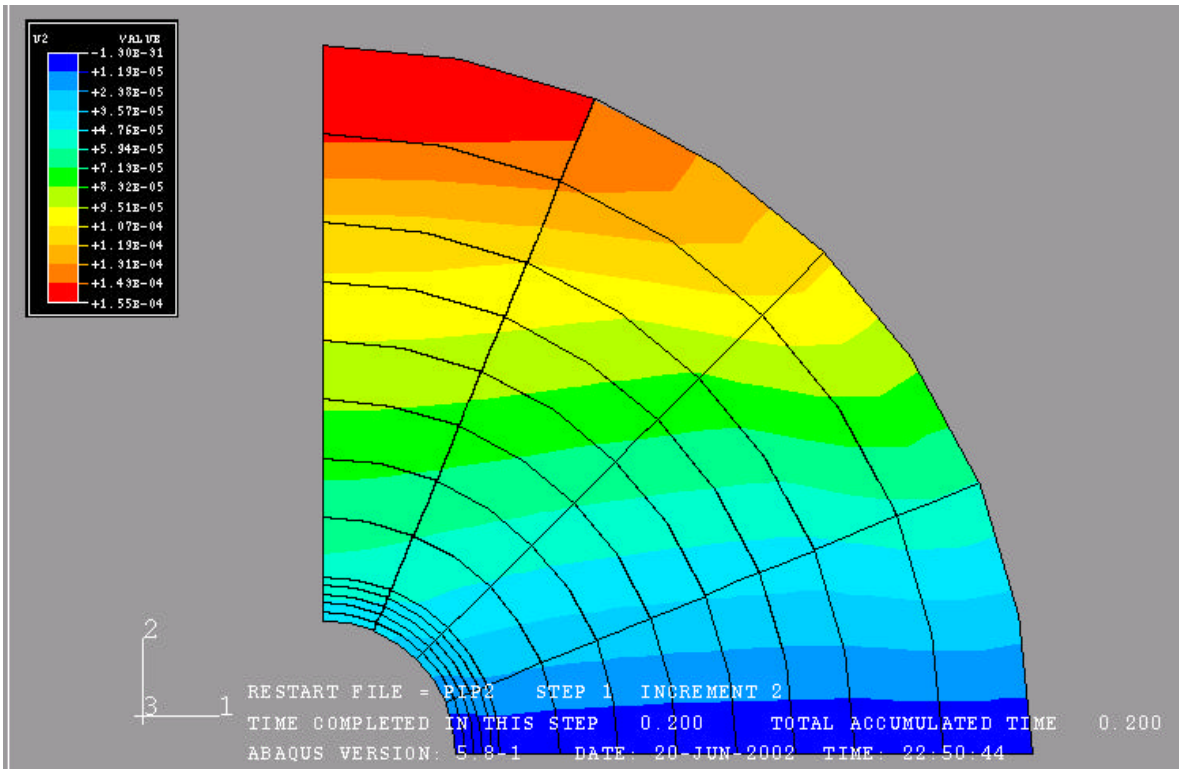

Fig.23a First principal stress profile (T_{in} = 180 F)

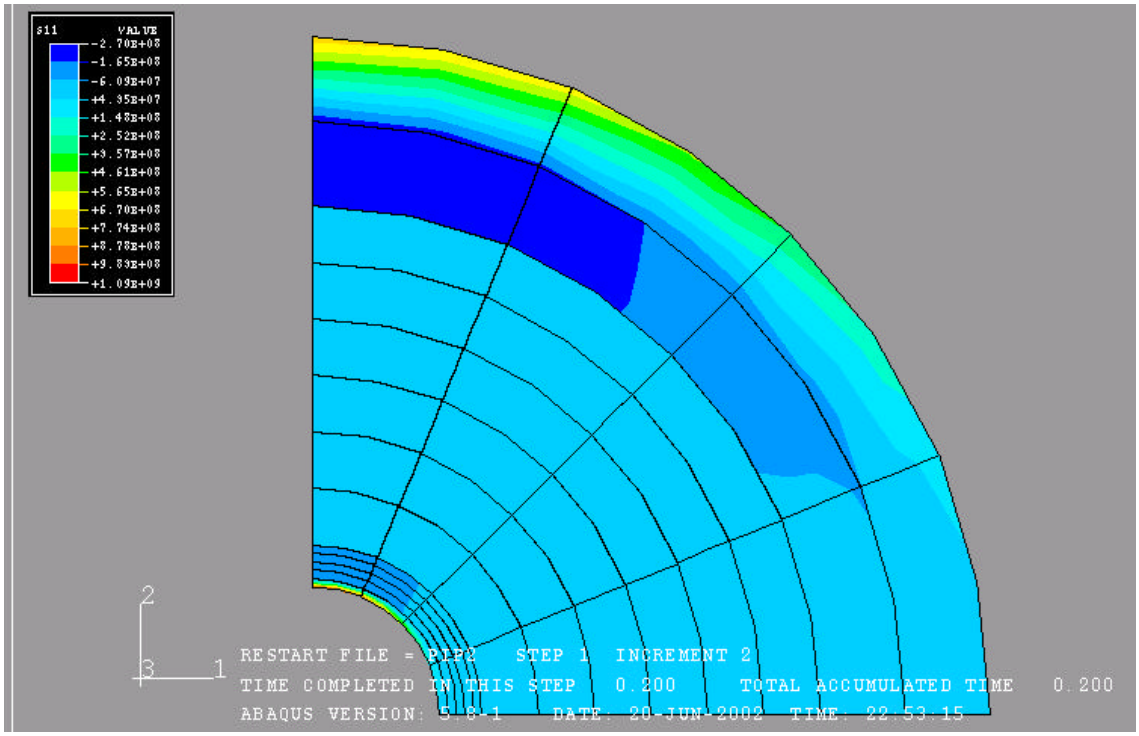

Fig.23b Temperature profile (T_{in} = 180 F)

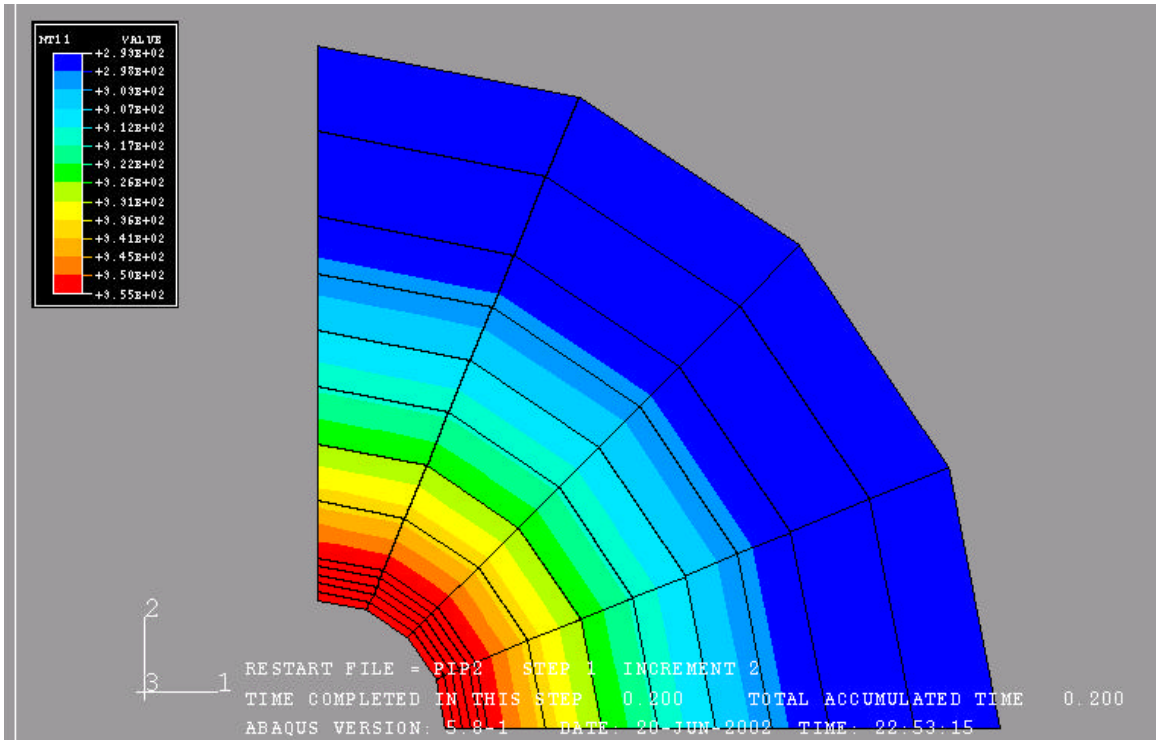

Fig.23c Horizontal displacement field (T_{in} =180 F)

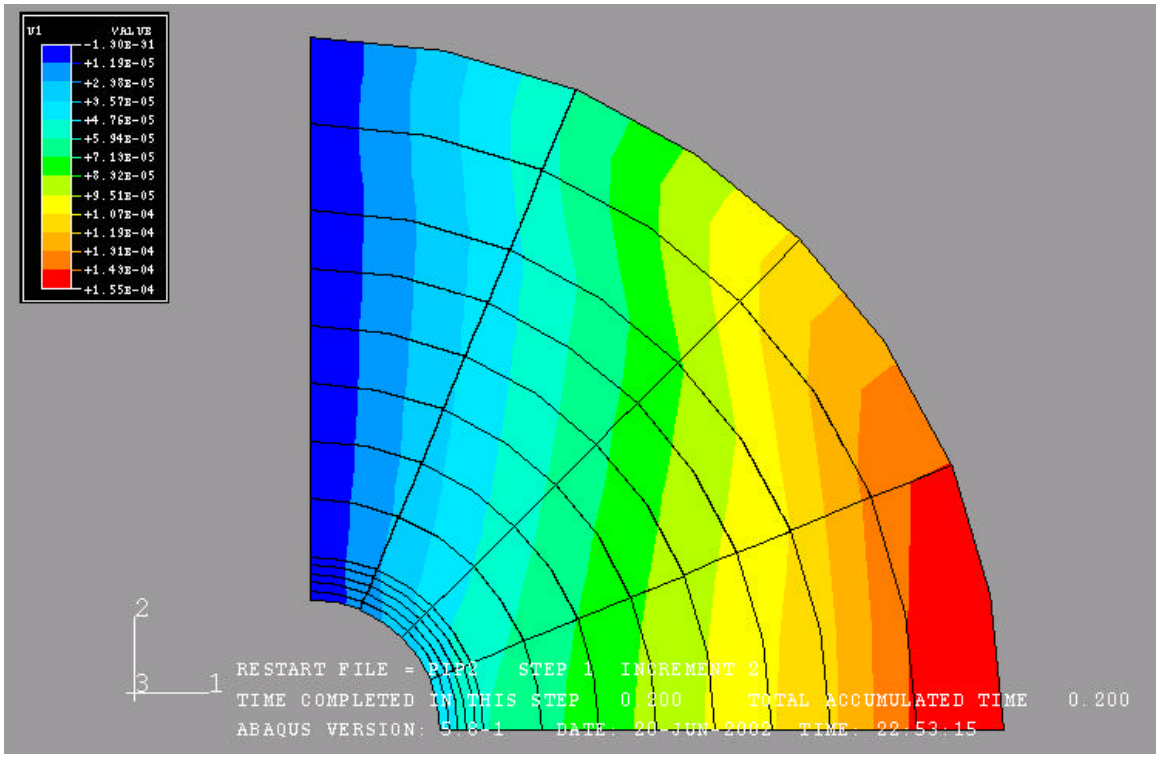

Fig.23d Vertical displacement field (T_{in} = 180 F)

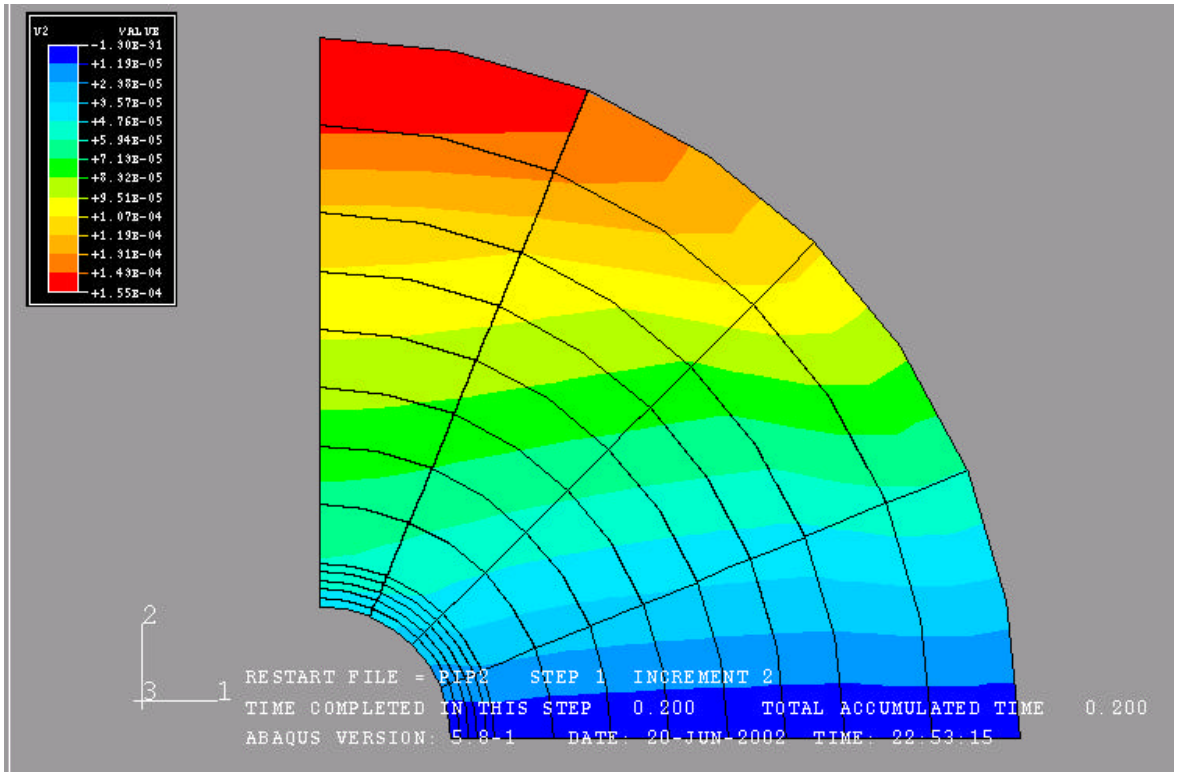

Fig.24a First principal stress profile (Casing Pressure = 500 psi)

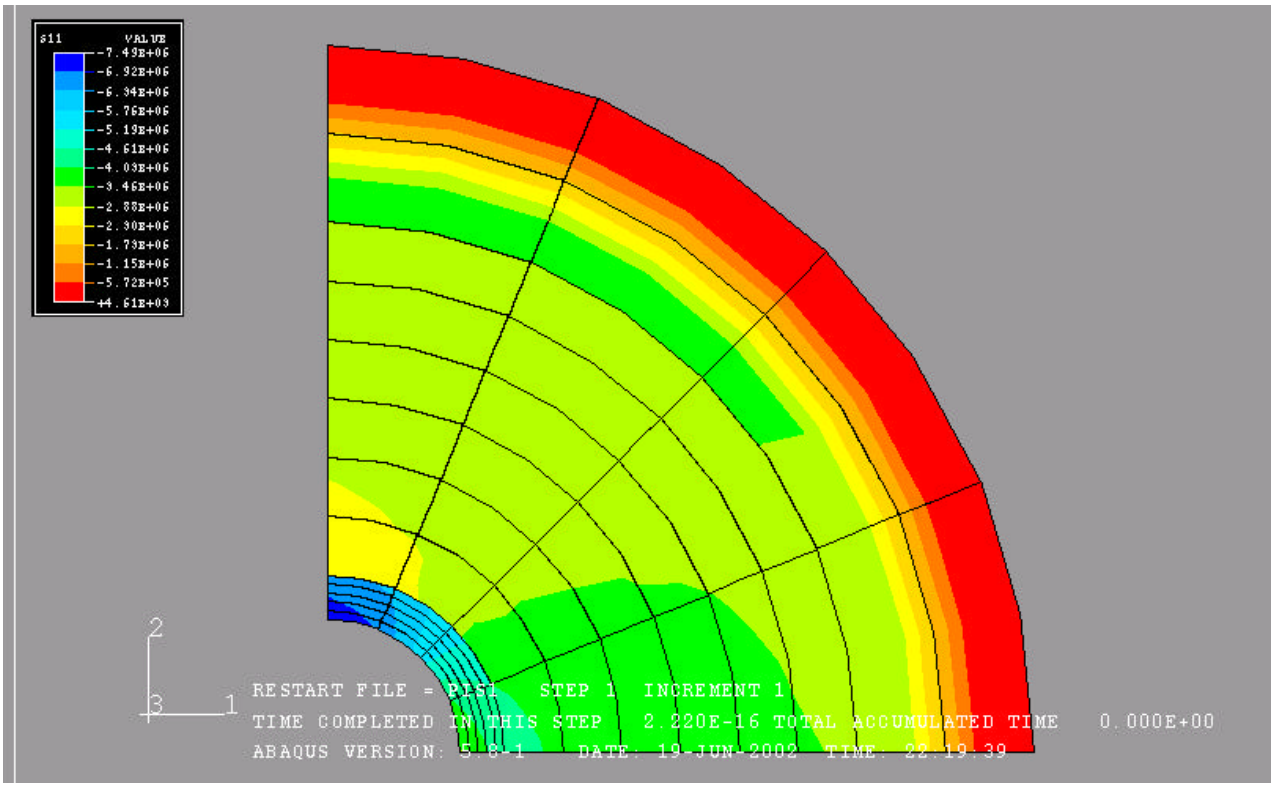

Fig.24b Second principal stress profile (Casing Pressure = 500 psi)

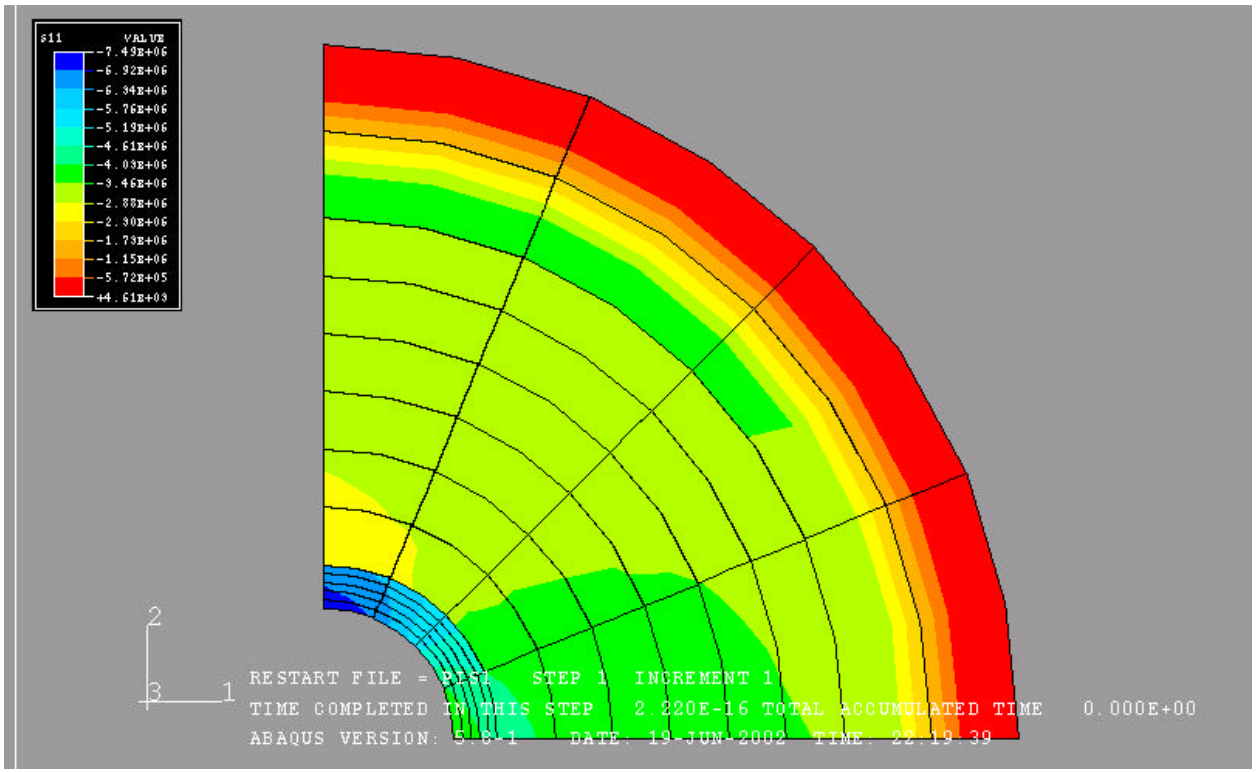
S11
VALUE
-7.49E+06
-6.92E+06
-6.34E+06
-5.76E+06
-5.19E+06
-4.61E+06
-4.03E+06
-3.46E+06
-2.88E+06
-2.30E+06
-1.73E+06
-1.15E+06
-5.72E+05
+4.61E+03
2
3
1
RESTART FILE = PLS1 STEP 1 INCREMENT 1
TIME COMPLETED IN THIS STEP 2.220E-16 TOTAL ACCUMULATED TIME 0.000E+00
ABAQUS VERSION: 5.8-1 DATE: 19-JUN-2002 TIME: 22:19:39

Fig.24c Horizontal displacement field (Casing Pressure = 500 psi)

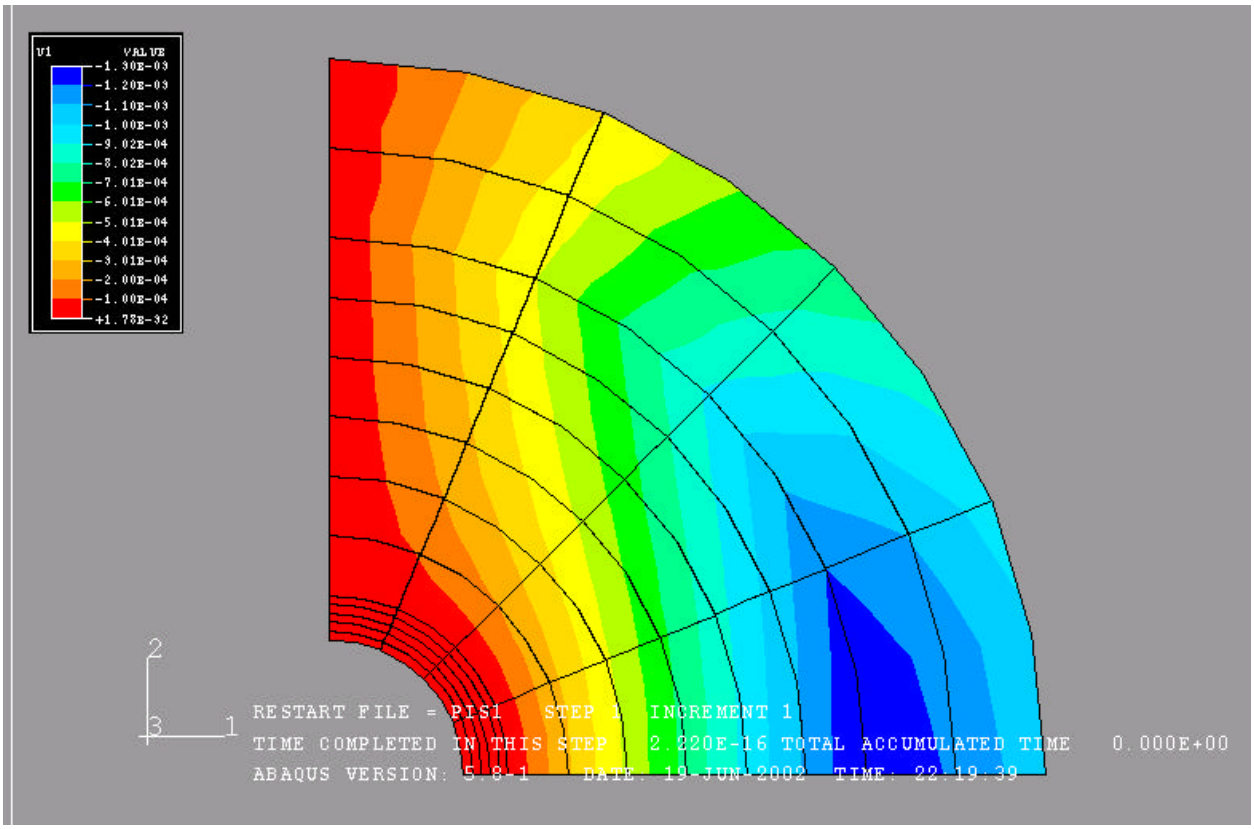

Fig.24d Vertical displacement field (Casing Pressure = 500 psi)

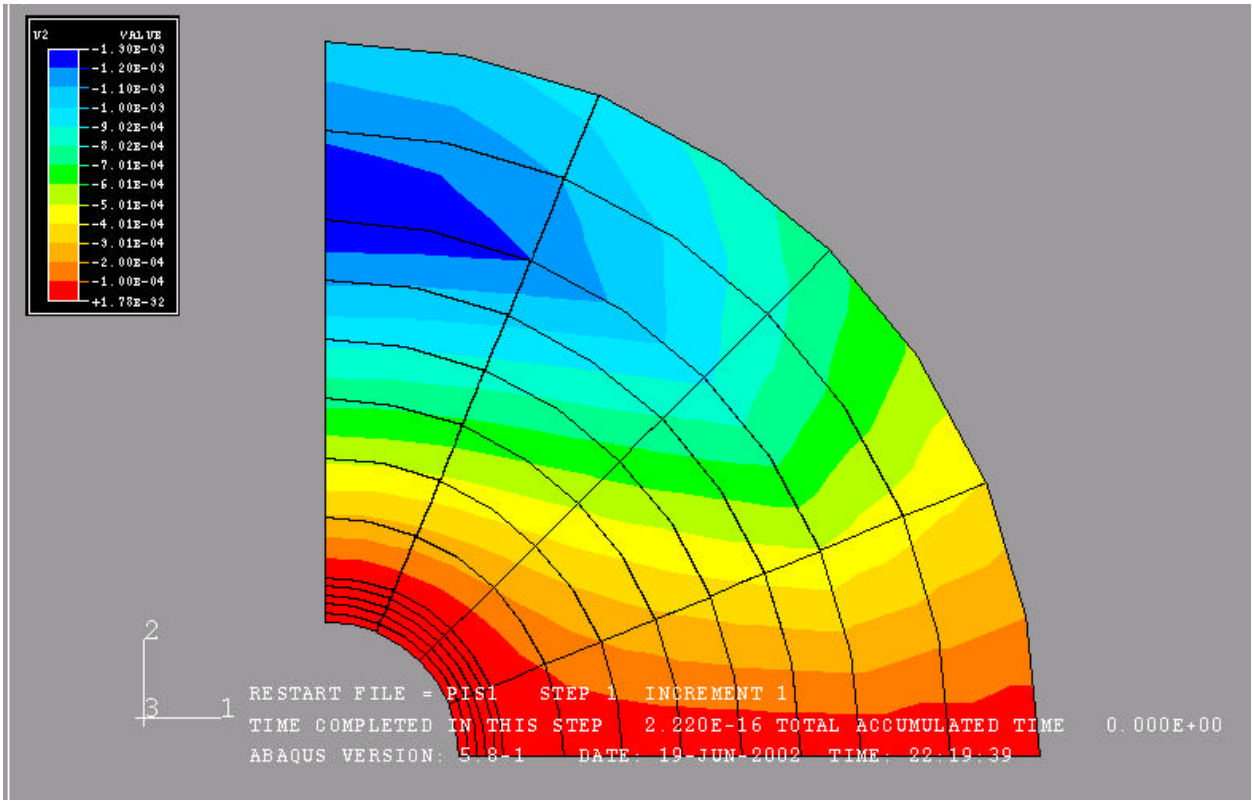

Fig.25a First principal stress profile (Casing Pressure = 1000 psi)

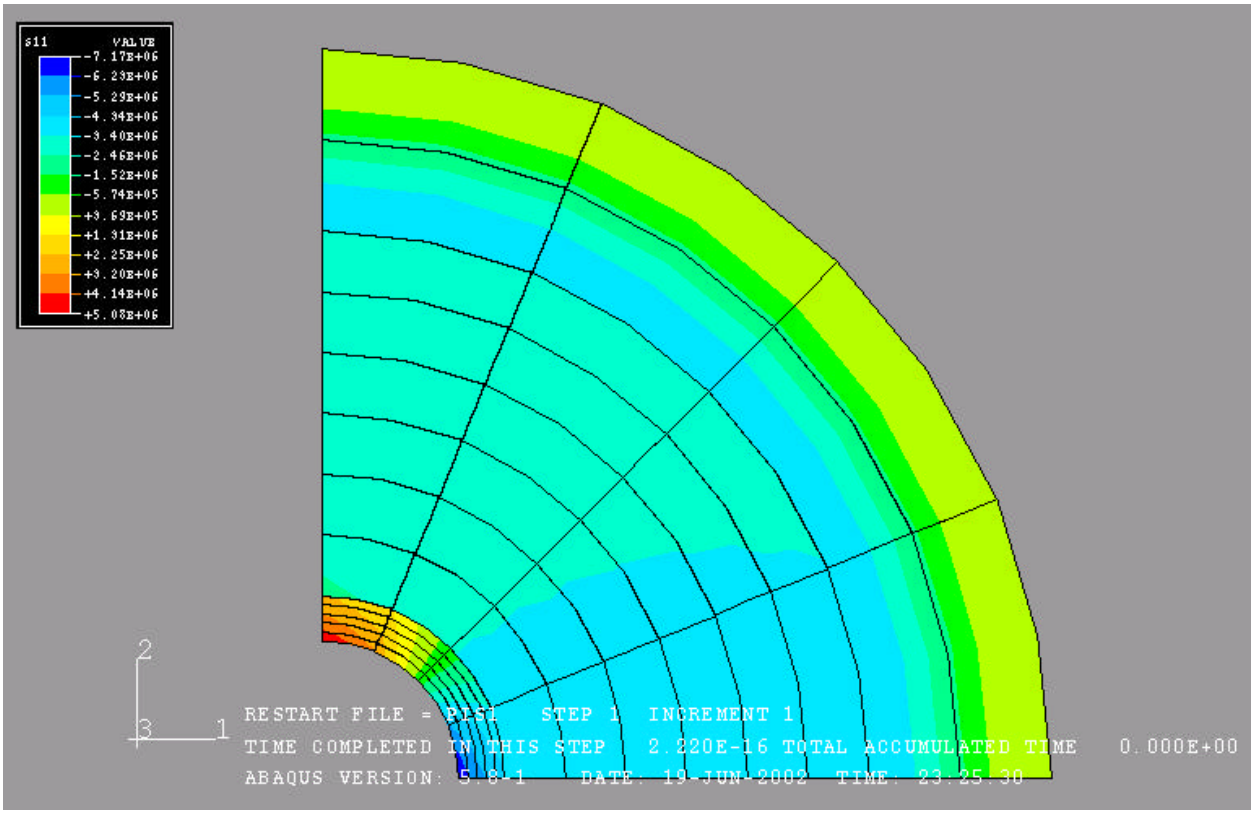

Fig.25b Second principal stress profile (Casing Pressure = 1000 psi)

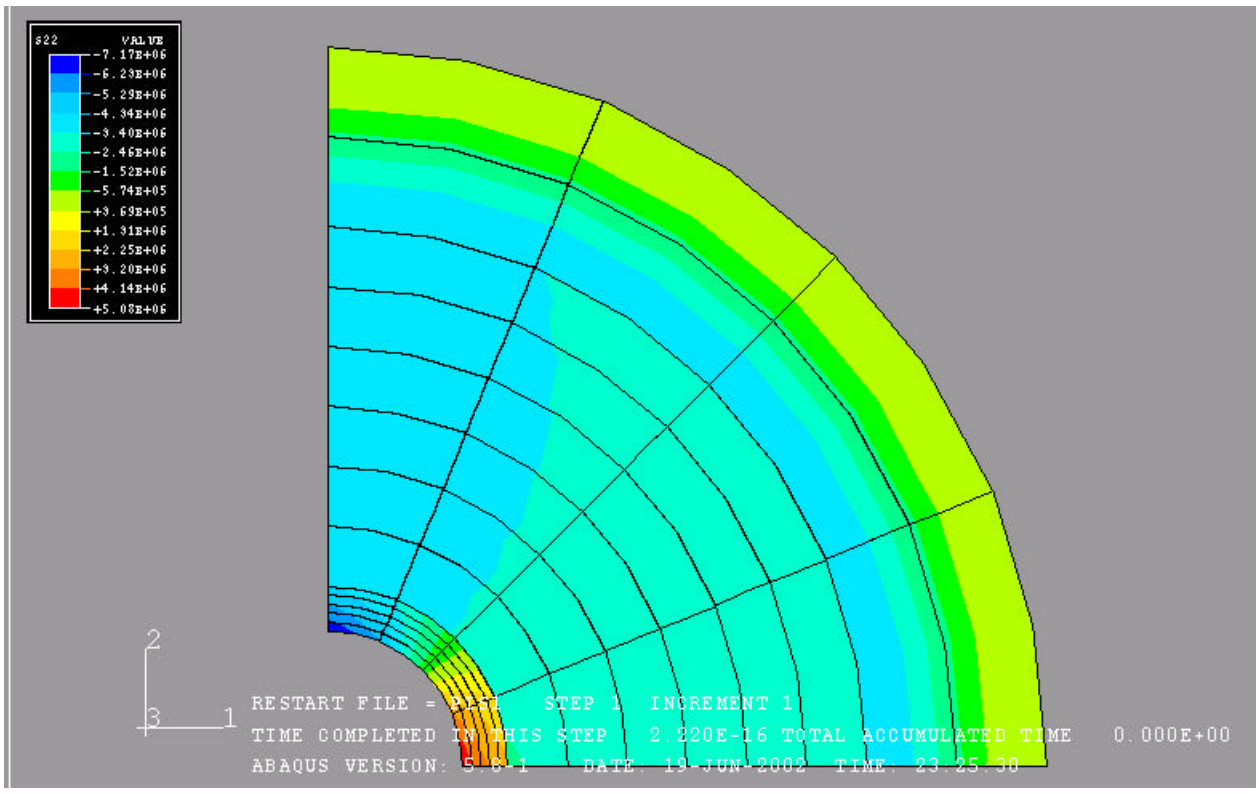

Fig.25c Horizontal displacement field (Casing Pressure = 1000 psi)

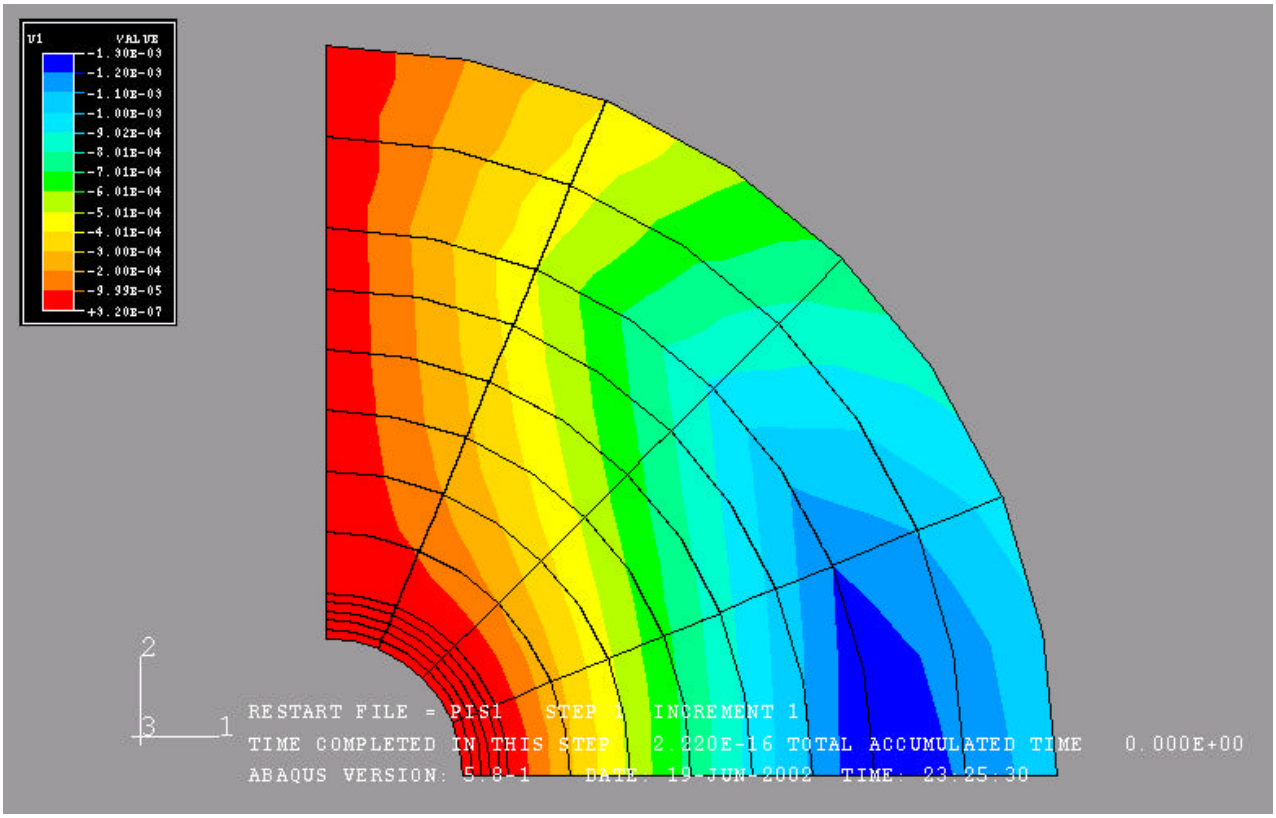

Fig.25d Vertical displacement field (Casing Pressure = 1000 psi)

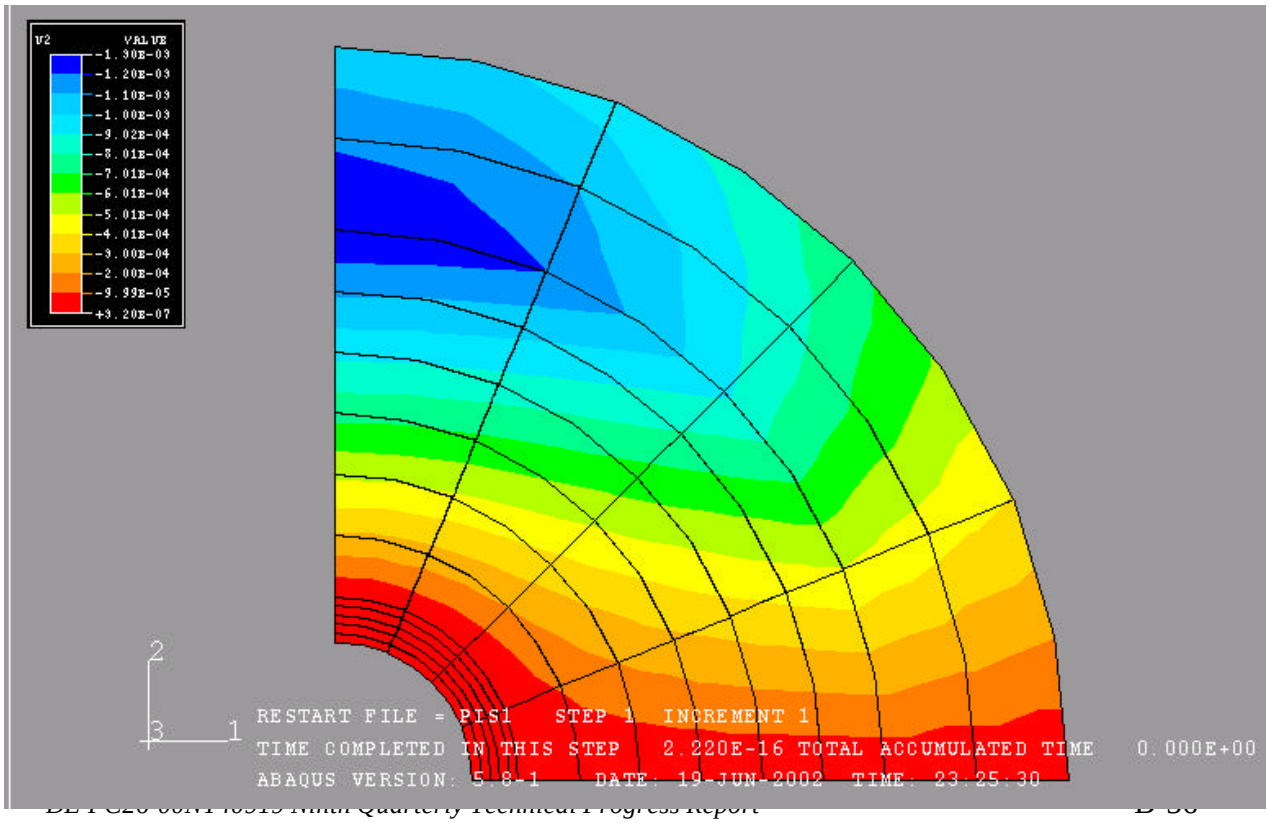

Fig.26a First principal stress profile (Casing Pressure = 5000 psi)

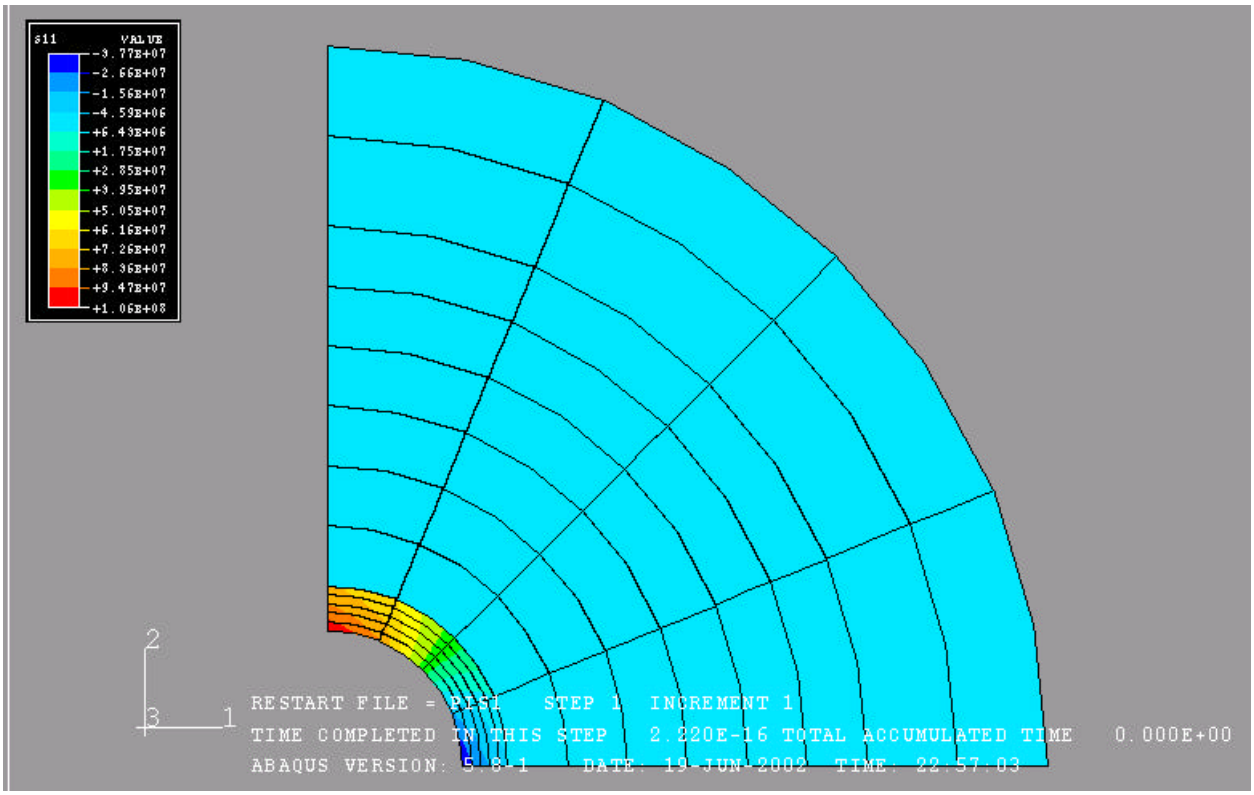

Fig.26b Second principal stress profile (Casing Pressure = 5000 psi)

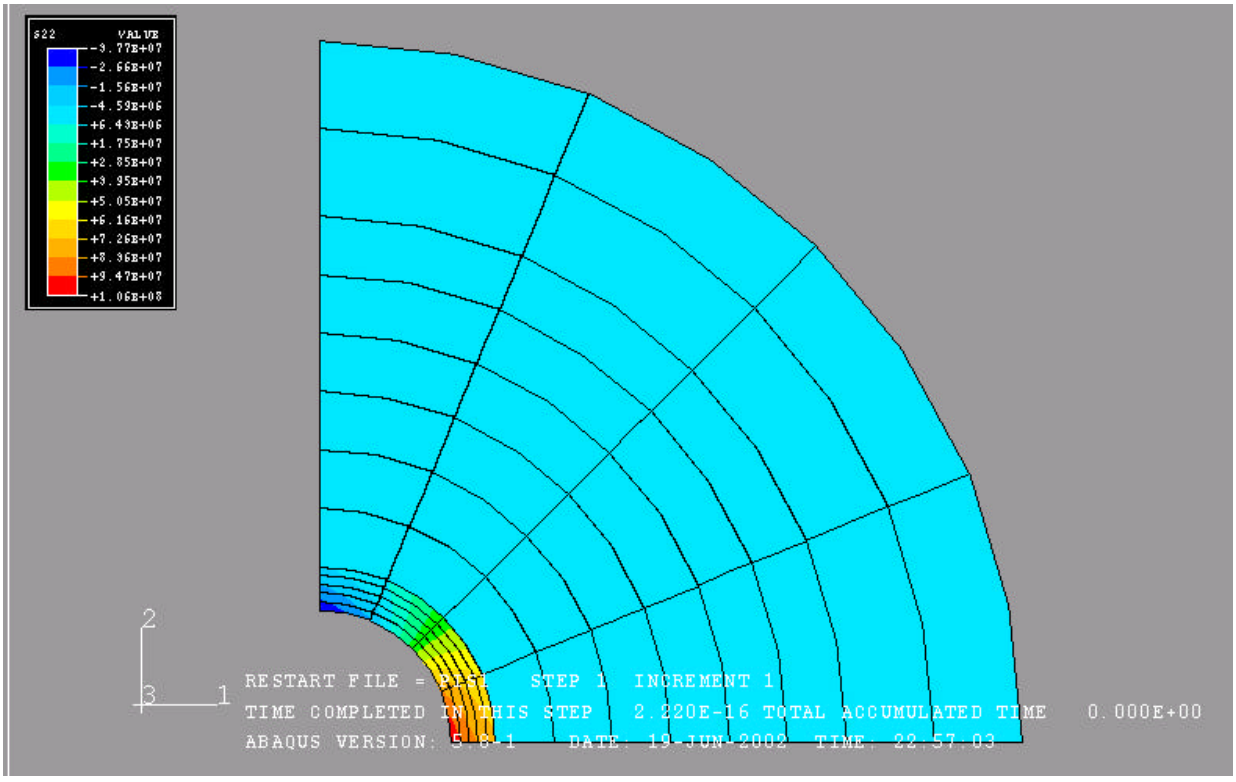

Fig.26c Horizontal displacement field (Casing Pressure = 5000 psi)

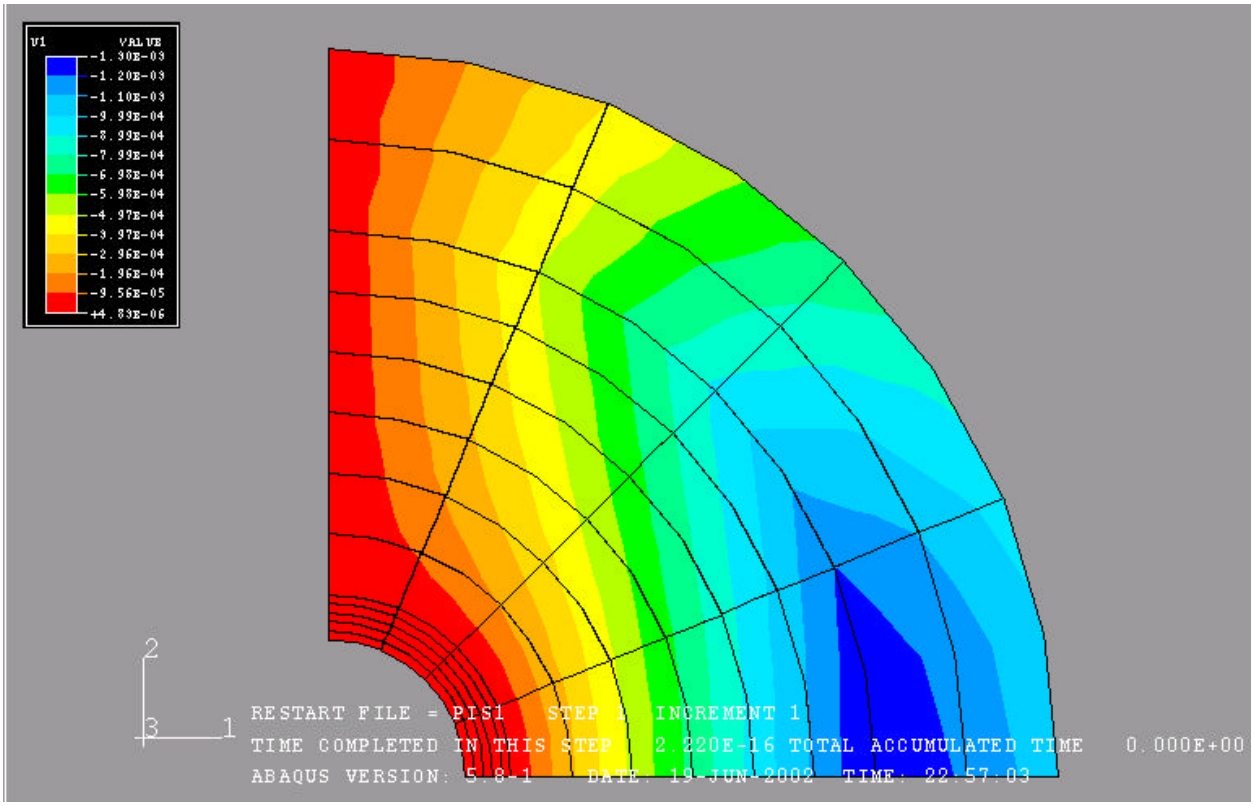

Fig.26d Vertical displacement field (Casing Pressure = 5000 psi)

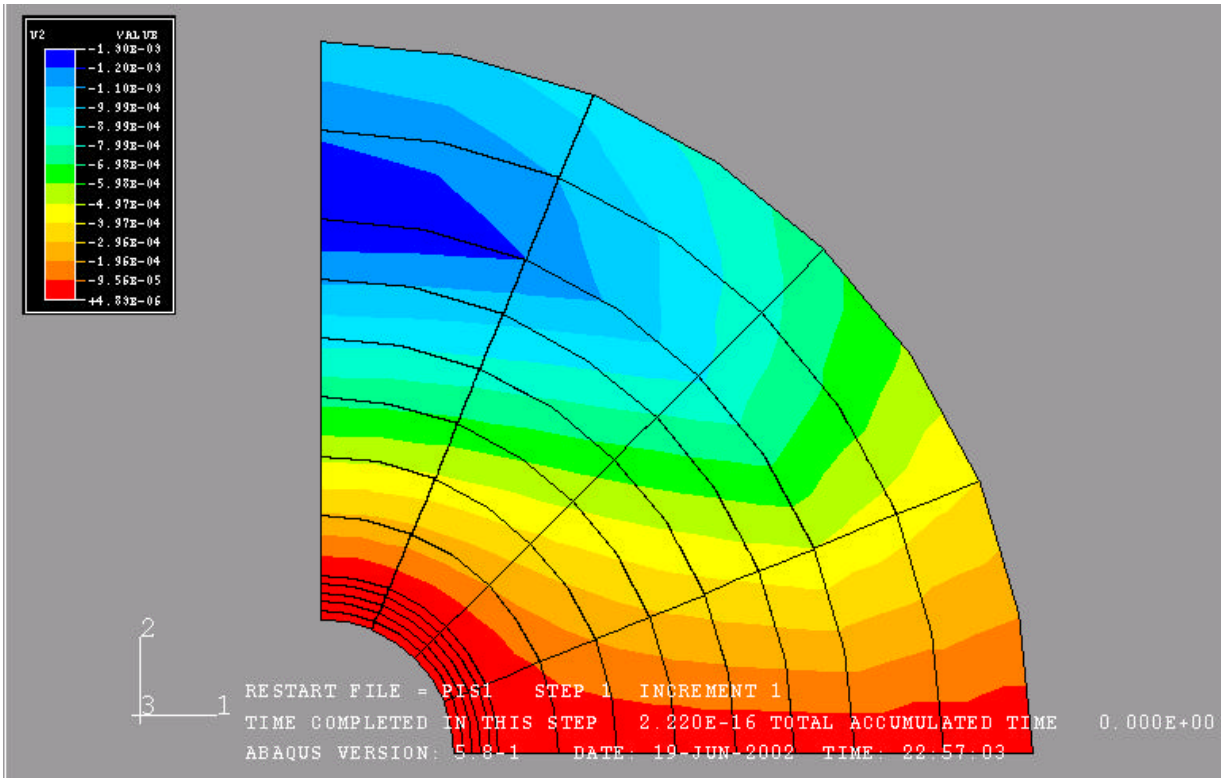

MMS Project

Long-Term Integrity of Deepwater Cement Systems Under Stress/Compaction Conditions

Report 3

Issued November 27, 2002

CEMENTING SOLUTIONS, INC.

Table of Contents

Objectives

The overall objective of this research project is to determine the properties that affect cement's capability to a produce fluid-tight seal in an annulus and to develop correlations between cement properties and sealing performance under downhole conditions. The testing reported previously in progress reports 1 and 2 has helped to refine and confirm the test procedures that will be used for the remainder of the project.

Research conducted during this project period focused on continued measurement and correlation of cement mechanical properties, mechanical bond integrity of a cemented annulus, and mathematical simulation of stresses induced in a cemented annulus. Mechanical property testing included measurement of tensile strength and Young's Modulus measurements under various confining loads. Mechanical integrity testing included shear bond and annular seal testing on specimens cured under various cyclic curing schedules. Mathematical simulation of casing and cement stress and strain induced by thermal and pressure cycling was also performed during this project period.

Conventional Performance Testing

Composition

The compositions tested in this project are detailed in **Table 1** below.

Table 1—Cement Compositions for Testing

Comp. No.	Description	Cement	Additives	Water Requirement (gal/sk)	Density (lb/gal)	Yield (ft^3/sk)
1	Neat slurry	TXI Type 1	—	5.23	15.6	1.18
2	Neat slurry with fibers					
3	Foam slurry	TXI Type 1	0.03 gal/sk Witcolate 0.01 gal/sk Aromox C-12 1% CaCl	5.2	12.0	1.19
4	Bead slurry	TXI Type 1	13.19% K-46 beads	6.69	12.0	1.81
5	Latex slurry	TXI Type 1	1.0 gal/sk LT-D500	4.2	15.63	1.17
6	Latex fiber slurry	TXI Type 1	1.0 gal/sk LT-D500 3.5% carbon milled fibers 0.50% Melkrete	4.09	15.63	1.20
7	Class H with silica	Class H	35% coarse silica 0.6% retarding fluid loss additive	5.38	16.4	1.40
8	Class H with silica and fibers	Class H	35% coarse silica 0.6% retarding fluid loss additive 3.2% milled fibers	5.38	16.4	1.43

Compressive Strength Testing

A summary of the compressive strength tests conducted was included in Report 2, and will not be repeated in this report. Please see Report 2 for a detailed description of these tests.

Report 2 discussed concerns about a possible discrepancy in compressive strength data provided by Westport and CSI. Compressive strength testing of representative compositions was conducted at Westport Laboratory to check the accuracy of CSI's test procedure. The results presented in **Table 2**, which represent the averages of three samples tested, indicate that data from the outside laboratory tracks closely with that of CSI.

Table 2—Comparison of Compressive Strengths

Location	Compressive Strength (psi) at 45°F	Compressive Strength (psi) at 80°F
Westport	1400	2015
CSI	1455	1920

Rock Properties Testing

Young's Modulus Testing

Composition 1 samples were cured in an unconfined condition (removed from mold after 24 hours and allowed to cure the remainder of the time outside of the mold) and tested at confining pressures of 0; 1,500; and 5,000 psi. The results are presented in **Table 3**.

Similar tests were conducted for Compositions 3 and 4 at confining pressures of 0, 500, and 1,000 psi, and for Composition 5 at confining pressures of 0, 250, and 500 psi. The results are presented in **Tables 4 through 6**.

Table 3—Composition 1, Compressive Young's Modulus

Confining Pressure (psi)	Effective Strength (psi)	Young's Modulus (psi)
0	8645	16.7 E 5
1500	8160	11.1 E 5
5000	8900	9.1 E 5

Table 4—Composition 3, Compressive Young's Modulus

Confining Pressure (psi)	Effective Strength (psi)	Young's Modulus (psi)
0	2885	5.8 E 5
500	3950	6.8 E 5
1000	4510	6.1 E 5

Table 5—Composition 4, Compressive Young's Modulus

Confining Pressure (psi)	Effective Strength (psi)	Young's Modulus (psi)
0	5150	9.5 E 5
500	6000	8.1 E 5
1000	6150	1 E 5

Table 6—Composition 5, Compressive Young's Modulus

Confining Pressure (psi)	Effective Strength (psi)	Young's Modulus (psi)
0	3500	5.6 E 5
250	5250	8.9 E 5
500	6000	9.4 E 5

Figure 1—Young's modulus testing of Composition 2 (neat Type 1 with fibers)

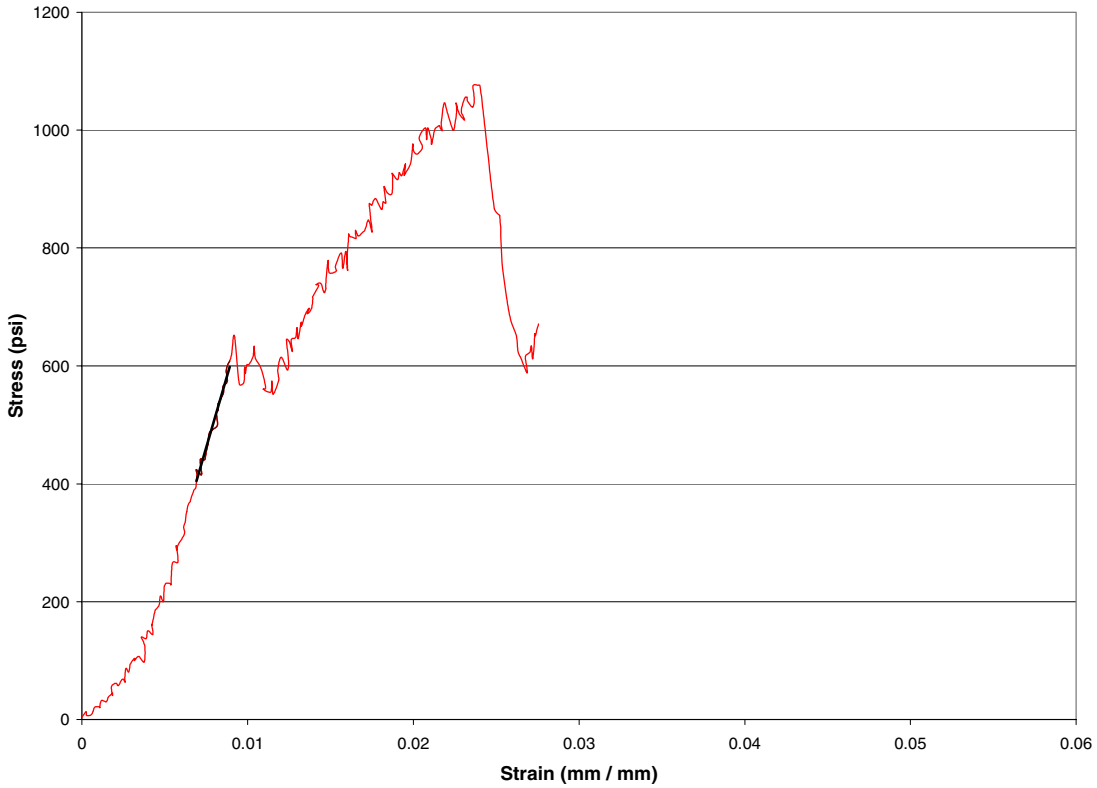

Figure 2—Young's modulus testing of Composition 5 (Type I latex without fibers)

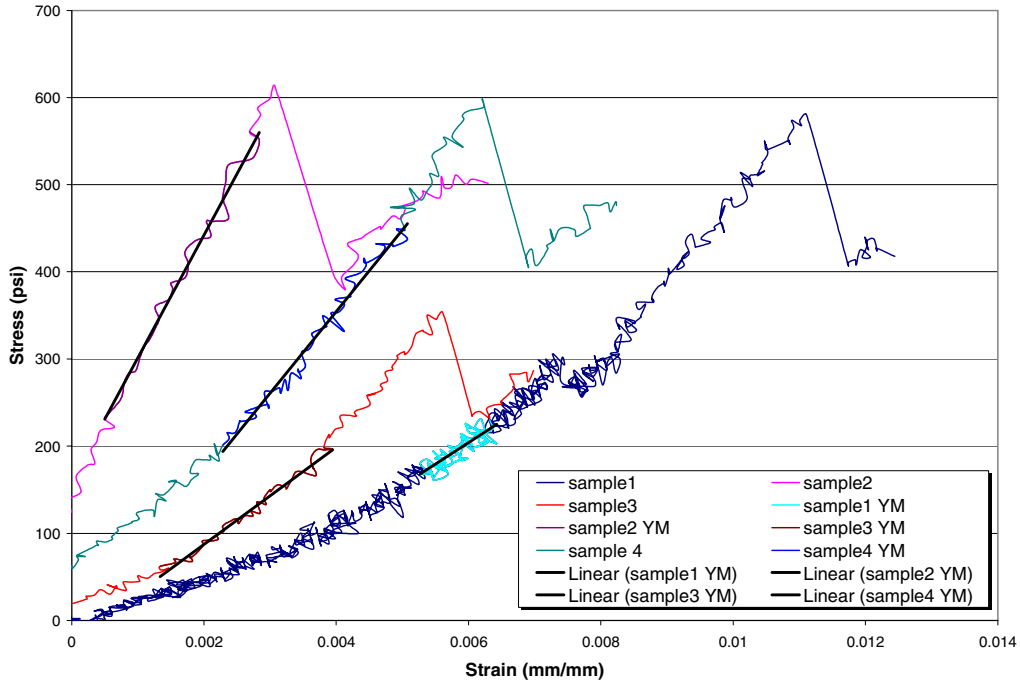

Figure 3—Young's modulus testing of Composition 6 (Type I latex with fibers)

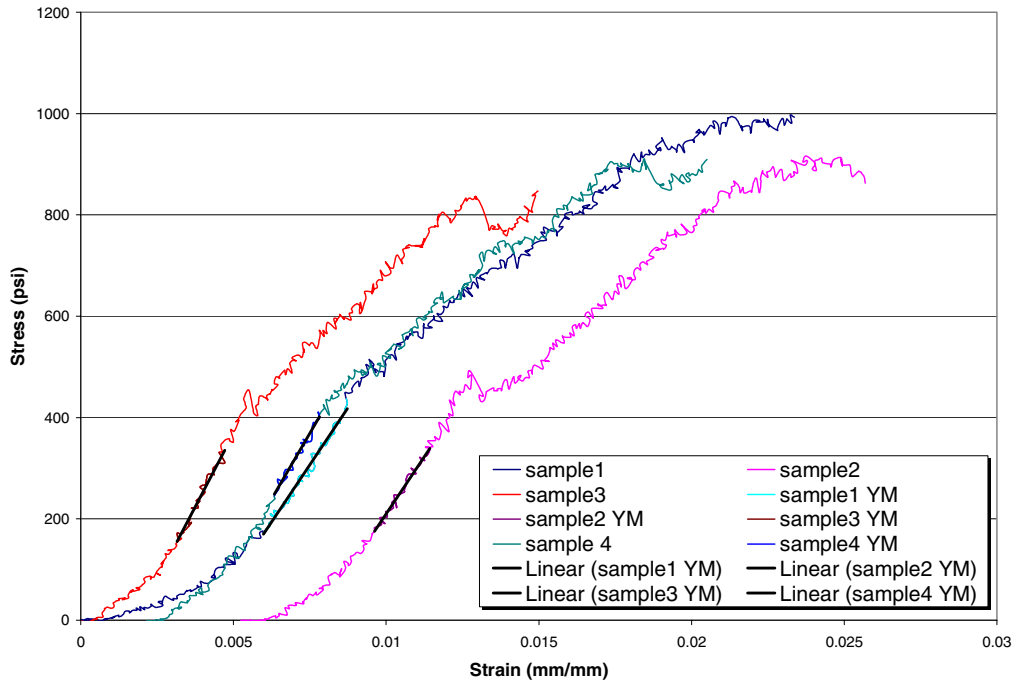

Tensile Strength Testing

The data presented in **Table 7** indicate that the tensile strength of Composition 4 was significantly higher than that of the other compositions tested.

Table 7—Tensile Strength Comparison

Slurry	Tensile Strength (psi)
Composition 1	394* / 213**
Composition 2	1071
Composition 3	253
Composition 5	539
Composition 6	902

* Sample was cured outside the mold.

** Sample was cured in the mold.

Hydrostatic Pressure Testing

The first hydrostatic pressure tests performed on a 10 lb/gal slurry (**Table 8**) were discussed in Report 2, and is being included in Report 3 for comparison purposes, as we present results obtained with a 12-lb/gal slurry (**Table 9**).

In both sets of tests, the initial sample was tested to failure. Subsequent cycle tests were performed with separate samples. The results are shown in Figures 4 through 9.

Table 8—Hydrostatic Cycles for 10-lb/gal Foam

Cycle No.	Hydrostatic (psi)	Young's Modulus (psi)
1 (initial)*	—	5.57E+05
2 (up)**	1000	3.38E+05
3 (down)**	100	6.71E+05
4 (up)**	1500	5.71E+05
5 (down)**	100	7.98E+05
6 (up)**	2000	6.68E+05
7 (down)**	100	8.49E+05***

* Initial sample taken to failure

** Tests performed on separate (not initial) samples

*** No deformation calculations performed for Cycle 7

Table 9—Hydrostatic Cycle for 12-lb/gal Foam

Cycle No.	Hydrostatic (psi)	Young's Modulus (psi)
1 (initial)*	—	8.24E+05
2 (up)**	600	1.30E+05

*Initial sample taken to failure

**Separate sample tested

Figure 4—Young's modulus testing of 10-lb/gal foamed cement

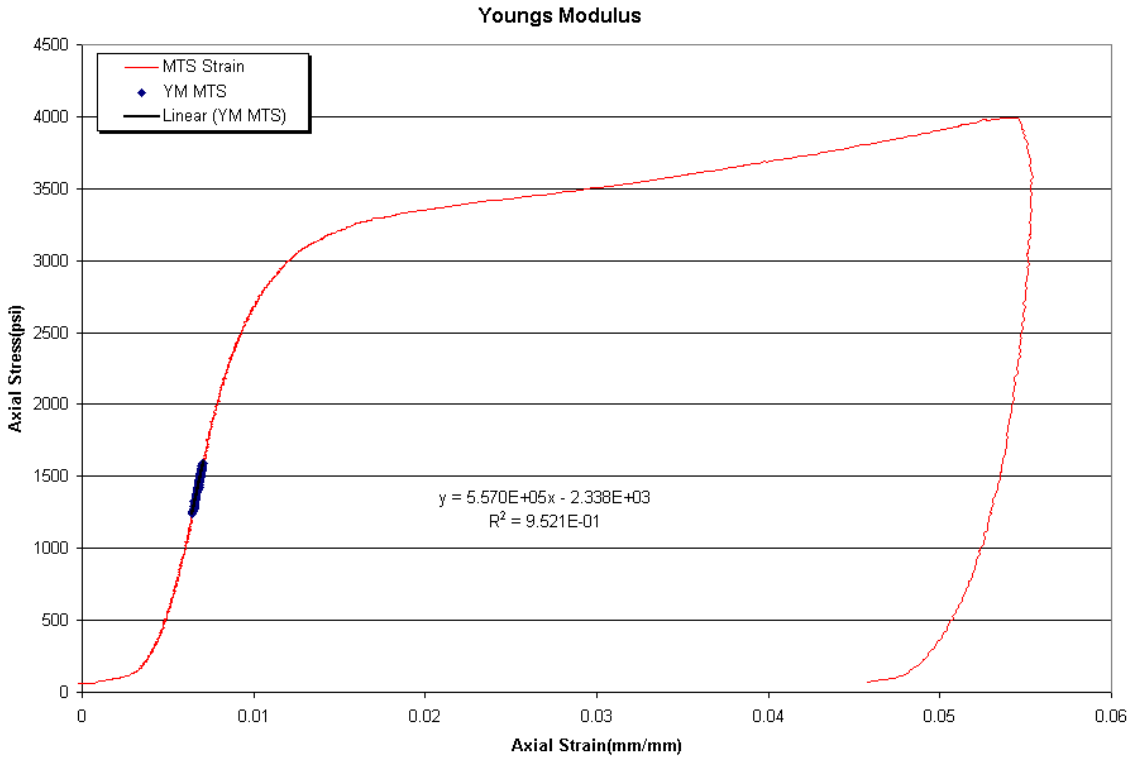

Figure 5—Young's modulus testing of 10-lb/gal foamed cement during hydrostatic cycling

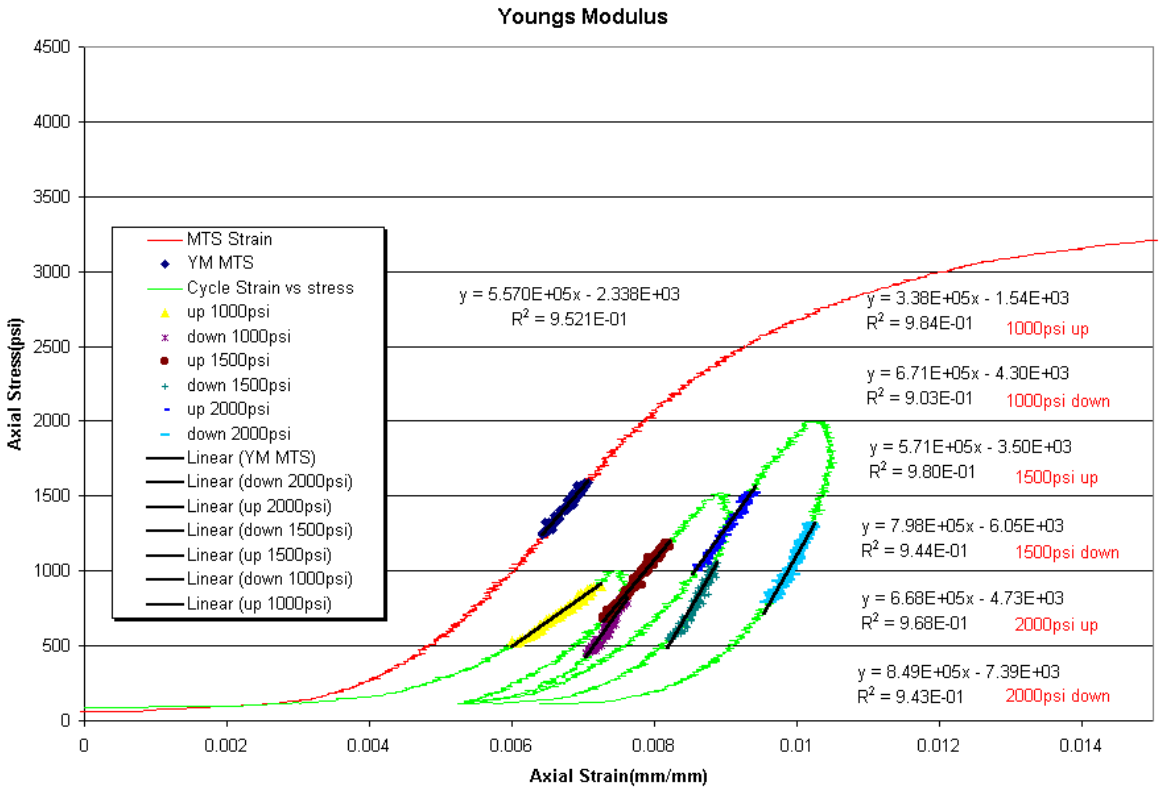

Figure 6—Deformation of 10 lb/gal foamed cement during hydrostatic cycling

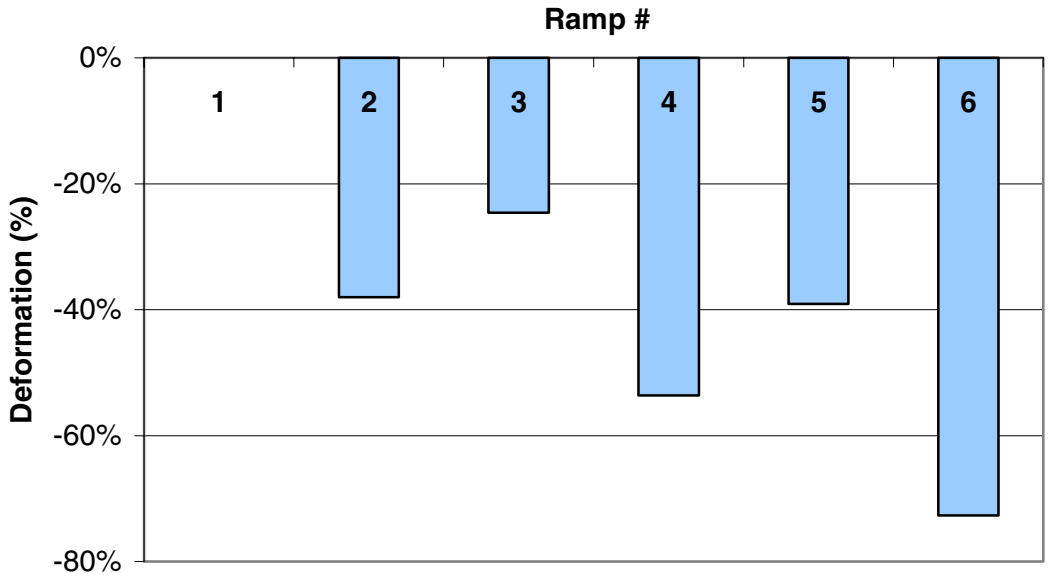

Figure 7— Young's modulus testing of 12-lb/gal foamed cement (Composition 2)

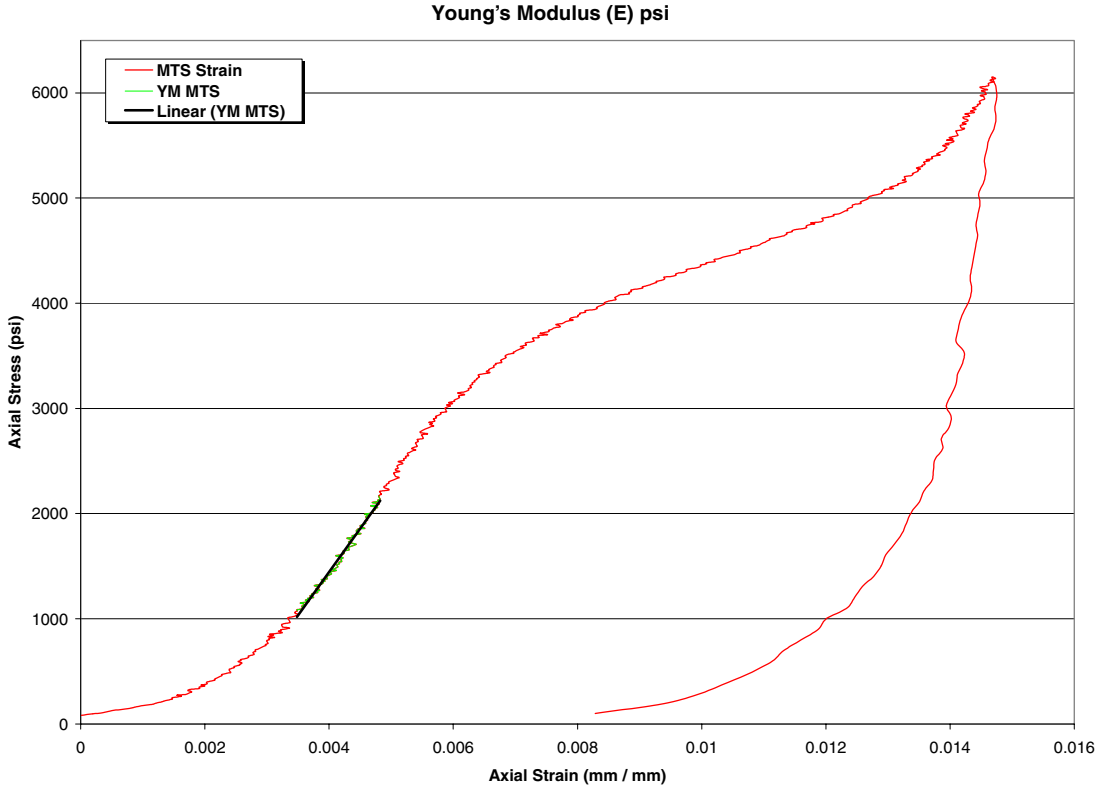

Figure 8—Young's modulus testing of 12-lb/gal foamed cement (Composition 2) during hydrostatic cycling

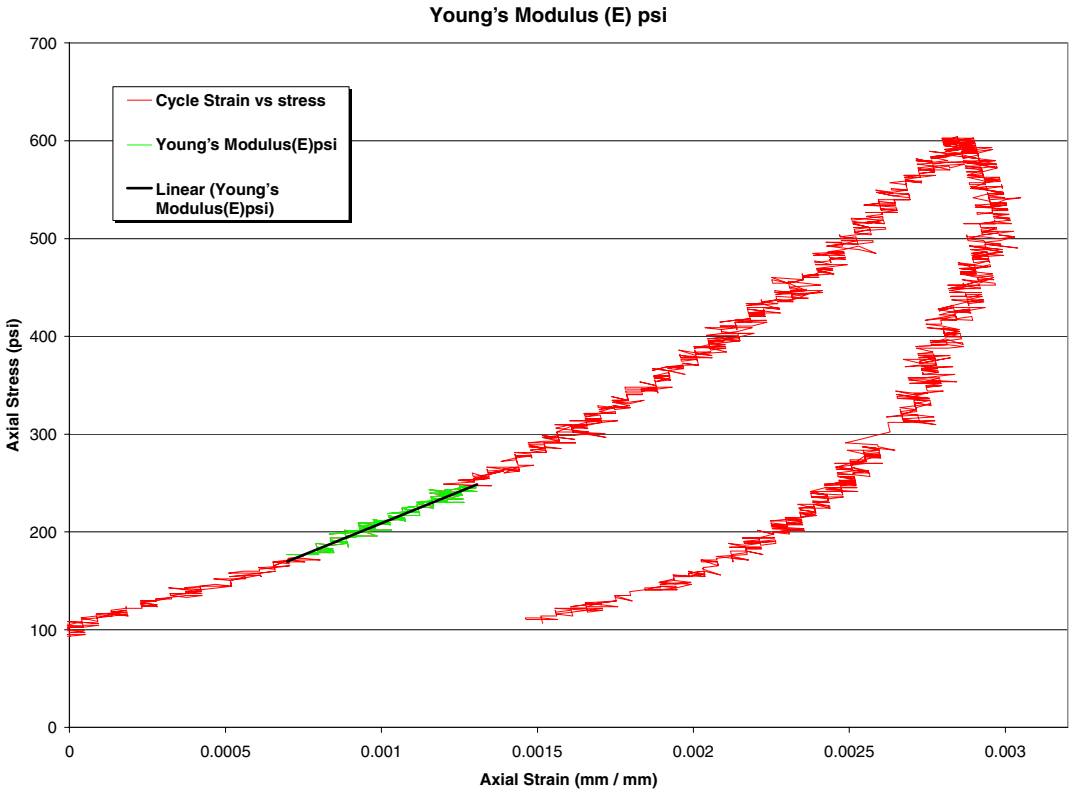

Figure 9—Deformation of 12-lb/gal foamed cement (Composition 2) during hydrostatic cycling

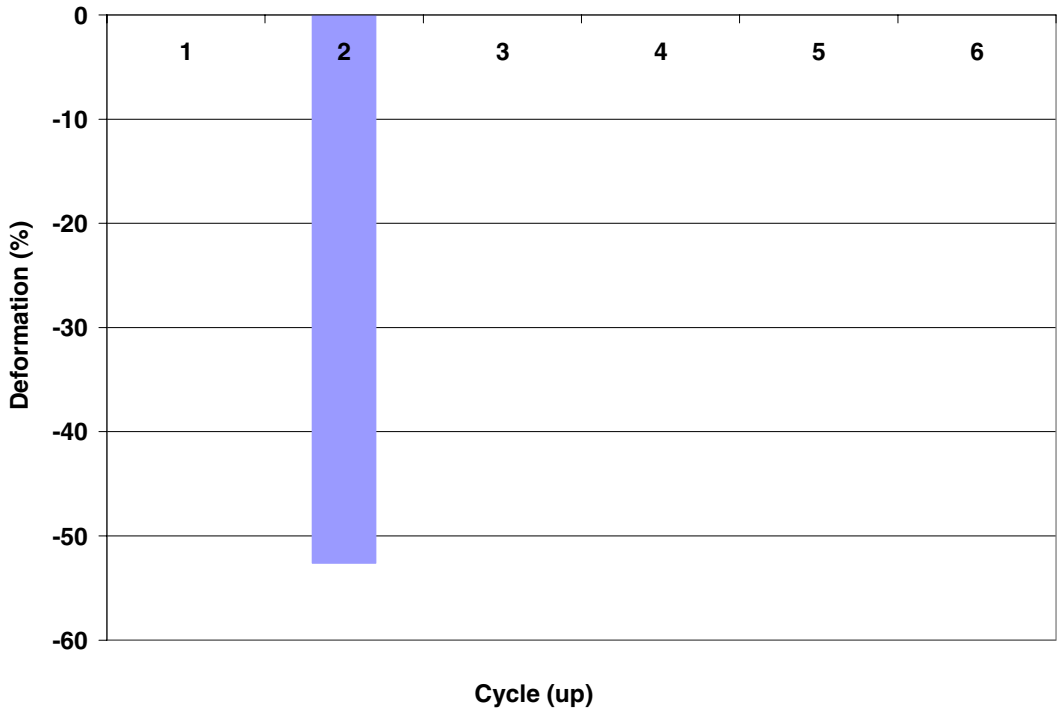

Chandler Engineering, Inc. Mechanical Properties Device

For comparison purposes, Chandler Engineering, Inc. and CSI have agreed to exchange data generated by two different systems – the rock mechanics system at Westport Laboratory and an acoustics-based system operated by Chandler. The same six slurries were tested in each device, and the comparative data is presented in **Tables 10 and 11**.

Initial results of Poisson's ratio testing on these lightweight cement compositions are not interpretable. The majority of tests yielded a negative Poisson's ratio, indicating a negative radial strain resulting from a positive axial strain. Several possible explanations for this phenomenon are under investigation. However, until the question is resolved, no Poisson's ratio data will be reported.

The Young's modulus values for latex cement with fibers, Class H cement, and Class H cement with fibers were not available at the time this report was prepared.

Like the UCA, Chandler's new analyzer measures the Young's modulus and compressive strength of a slurry as it cures at elevated temperatures and pressures, eliminating the

potentially damaging effects of depressurization and cooling involved with traditional core testing. For more information on this device, see Appendix F.

Table 10—Chandler Device

Composition	Poisson's Ratio	Compressive Young's Modulus
1	0.20	2.3 E 6
4	0.31	1.5 E 6
5	0.39	1.4 E 6
6	0.19	2.5 E 6
7	0.24	2.2 E 6
8	0.25	2.3 E 6

Table 11—Rock Mechanics Data

Composition	Poisson's Ratio	Compressive Young's Modulus
1	—	1.7 E 6
4	—	9.5 E 5
5	—	5.6 E 5
6	—	—
7	—	—
8	—	—

Unconventional Performance Testing

Shear Bond Testing

Table 12 presents results of shear bond strength tests performed with temperature and pressure cycling on Compositions 1, 3, 4, and 5. For more information on test procedures, see Appendix C.

Table 12—Shear Bond Strengths (psi)

System	Simulated Formation	Comp. 1	Comp. 3	Comp. 4	Comp. 5
Baseline	hard	1194	127/98	109/78	—
	soft	198	233	143	223
Temperature-Cycled	hard	165	299/215	191/269	—
	soft	72	7	56	149
Pressure-Cycled	hard	194/106	276/228	294/170	—
	soft	23	22*	23*	11

* Visual inspection revealed samples were cracked.

Shrinkage Testing

Information on test procedures for shrinkage testing is provided in Appendix D.

Annular Seal Testing

Table 13 presents the results of annular seal tests performed on Compositions 1, 3, and 4. For information on test procedures for annular seal testing, see Appendix E.

Table 13—Annular Seal Tests

Condition Tested	Formation Simulated	Composition 1	Composition 3	Composition 4
Initial Flow	Hard	0 Flow	0 Flow	0 Flow
	Soft	0 Flow	0.5K (md)	0 Flow
Temperature-Cycled	Hard	0 Flow	0 Flow	0 Flow
	Soft	0 Flow	123K md / (2200 md)	43K (md)*
Pressure-Cycled	Hard	0 Flow	0 Flow	0 Flow
	Soft	27K (md)	0.19K (md)*	3K (md)

* Visual inspection revealed samples were cracked.

Pipe-in-Pipe Testing

A pipe-in-pipe test was designed to simulate the shrinkage of cement that can lead to fluid leakage when no external fluid is present outside the cement. Four models were tested:

- 6-in. flange
- 6-in. flange with 200-psi pressure
- 5-ft flange with vacuum
- 5-ft flange with 200-psi pressure

In all cases, no leaks were observed. The cement provided a tight seal to gas flow.

Mathematical Modeling

The graphs in this section represent an average of test results obtained in testing the performance of a neat cement (baseline), latex cement, and foamed cement. The compressive and tensile strengths and shear bond strength of the cements are shown in **Table 14**.

The abbreviations “PIP” and “PIS” are used in the following graphs to differentiate between test conditions that simulate hard formations (pipe-in-pipe) and those that simulate soft formations (pipe-in-soft).

Table 14—Compressive Strength

Cement	Compressive Strength After 10 Days (psi)	Tensile Strength (psi)	Shear Bond	
			PIP	PIS
Composition 3	3436	578	321	147
Composition 5	3630	504	432	237
Composition 1	4035	673	519.6	203

Compressive Failure

Figures 10 and 11 show the results of tests used to predict the effect of casing pressure and confining pressure on the radial stress experienced by the inner pipe, the cement sheath, and a hard formation.

The model showed that annular cement retains its integrity at high casing pressures and at high confining pressures in a hard formation.

When casing pressure was varied (**Figure 10**), and no confining pressure was applied, virtually no variation in the radial stress was observed for the cement or the formation. All variation, rather, was limited to the internal casing.

When confining pressure was varied (**Figure 11**), and casing pressure was fixed at 5,000 psi, the greatest variation in radial stress was observed in the inner casing and outer pipe (representing the formation), with very little variation observed in the cement. This is because of the differences in the Young's modulus properties of the cement vs. the Young's modulus of the steel pipe.

Figure 10—Compressive failure, simulated hard formation (1 of 2)

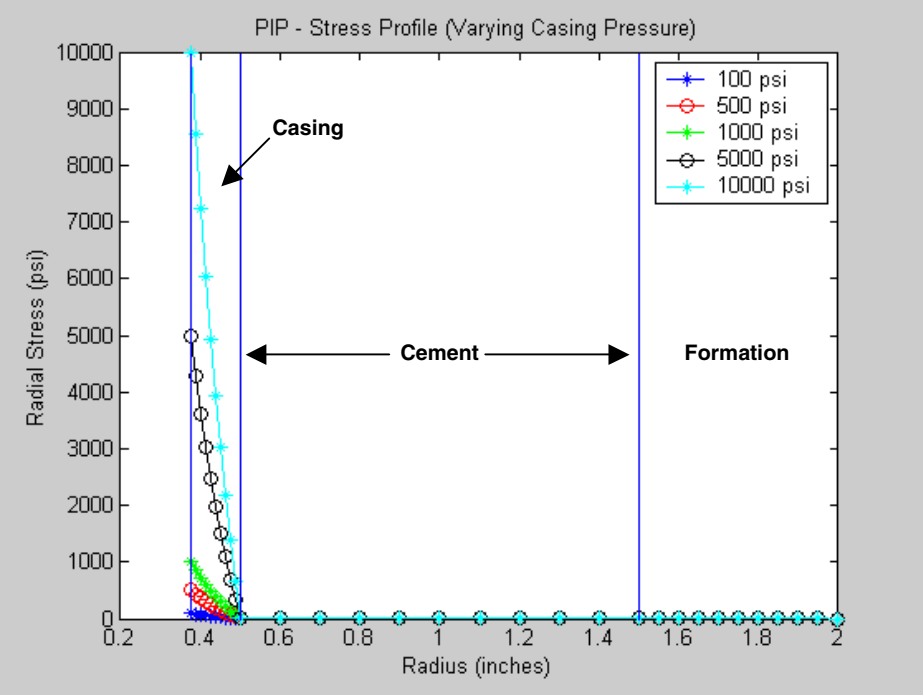

Figure 11—Compressive failure, simulated hard formation (2 of 2)

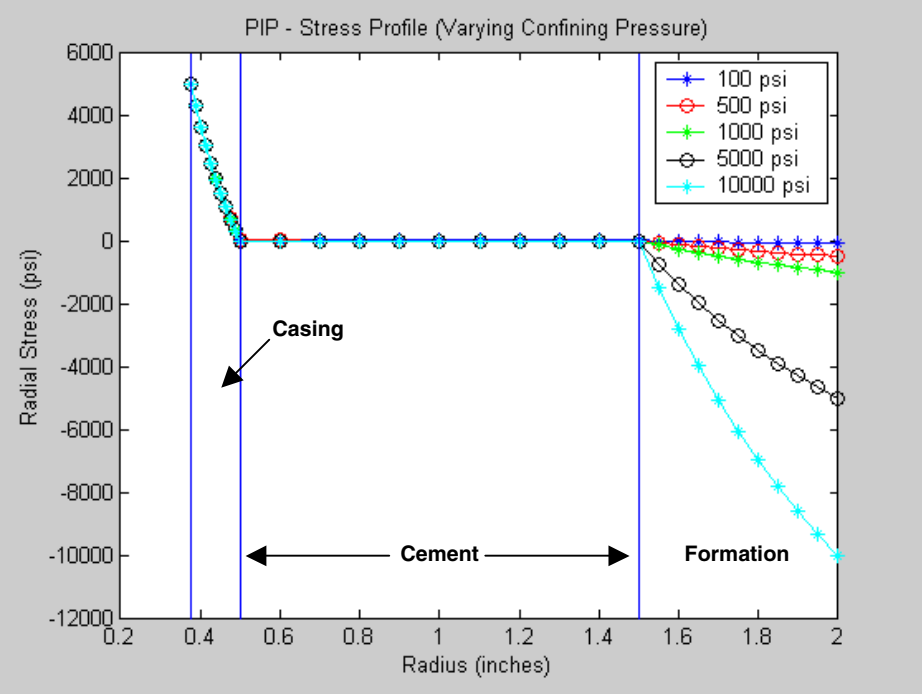

Cements were then tested to determine the effects of varying casing pressure and confining pressure in a soft formation scenario. Without confining pressure (**Figure 12**), the cement and the formation experience no variation in radial stress as casing pressure increases. As in the test with the hard formation, the variation is limited to the inner casing.

However, when the casing pressure is fixed at 500 psi, and the confining pressure is increased from 100 psi to 10,000 psi (**Figure 13**), the radial stress in the cement layer increases accordingly, to a point beyond which the sheath can withstand. At pressures of 5,000 psi and above, the cement sheath will almost certainly fail.

The positive and negative values shown in Figure 13 are used to differentiate radial stress (positive values) from the opposite of radial stress (negative values).

Figure 12—Compressive failure, simulated soft formation (1 of 2)

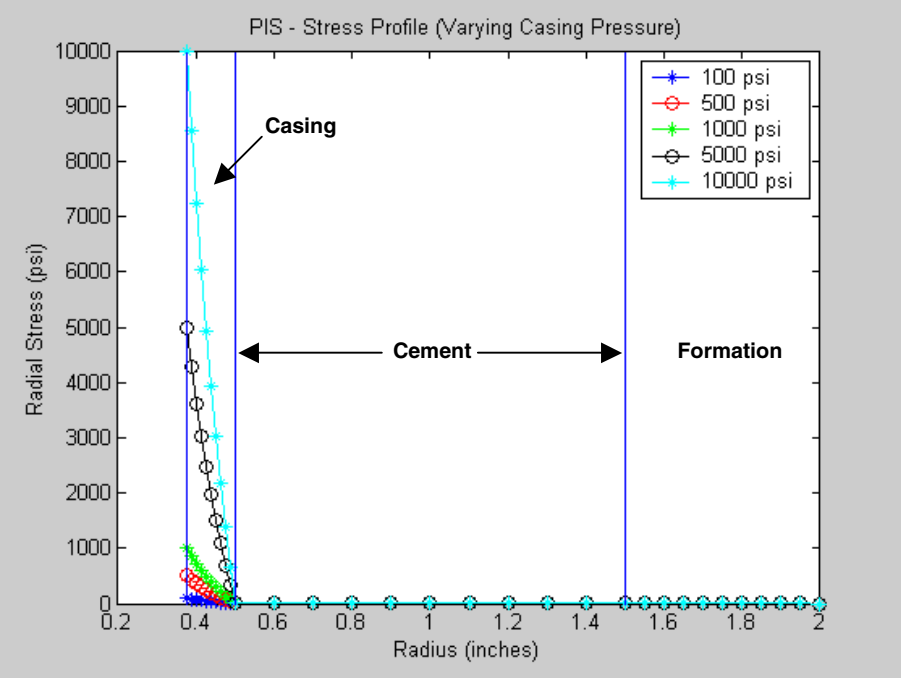

Figure 13— Compressive failure, simulated soft formation (2 of 2)

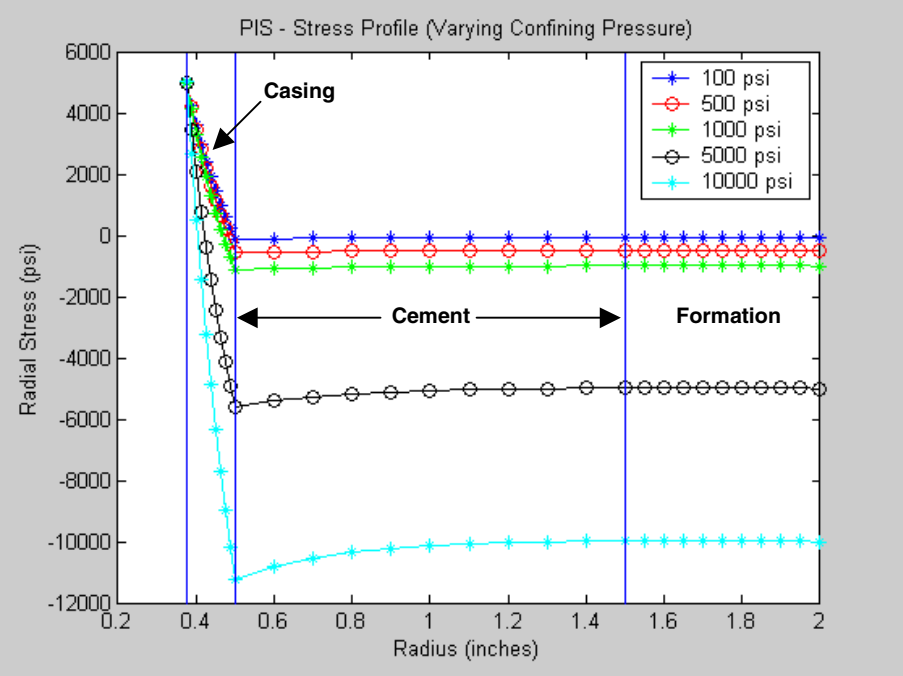

Shear Failure (Hoop Stress)

In a simulated hard formation (**Figure 14**), the variation in hoop stress at the pipe-cement interface is significantly less than that at the cement-formation interface. No significant variation in hoop stress is observed in the cement layer. Therefore, if failure occurs, it will most likely occur at the cement-formation interface.

In a simulated soft formation (**Figure 15**), there is almost no variation in the formation hoop stress, and there is slightly more variation in the hoop stress of the cement sheath. While the magnitude of variation between the pipe-cement interface and the cement-formation interface is significant, it is not as great as in the simulated hard formation shown in Figure 14. That is because the soft formation is more flexible and does not create the high stress contrast during displacement.

If failure occurs, it will most likely be at the pipe-cement interface.

Figure 14—Shear failure, simulated hard formation (1 of 2)

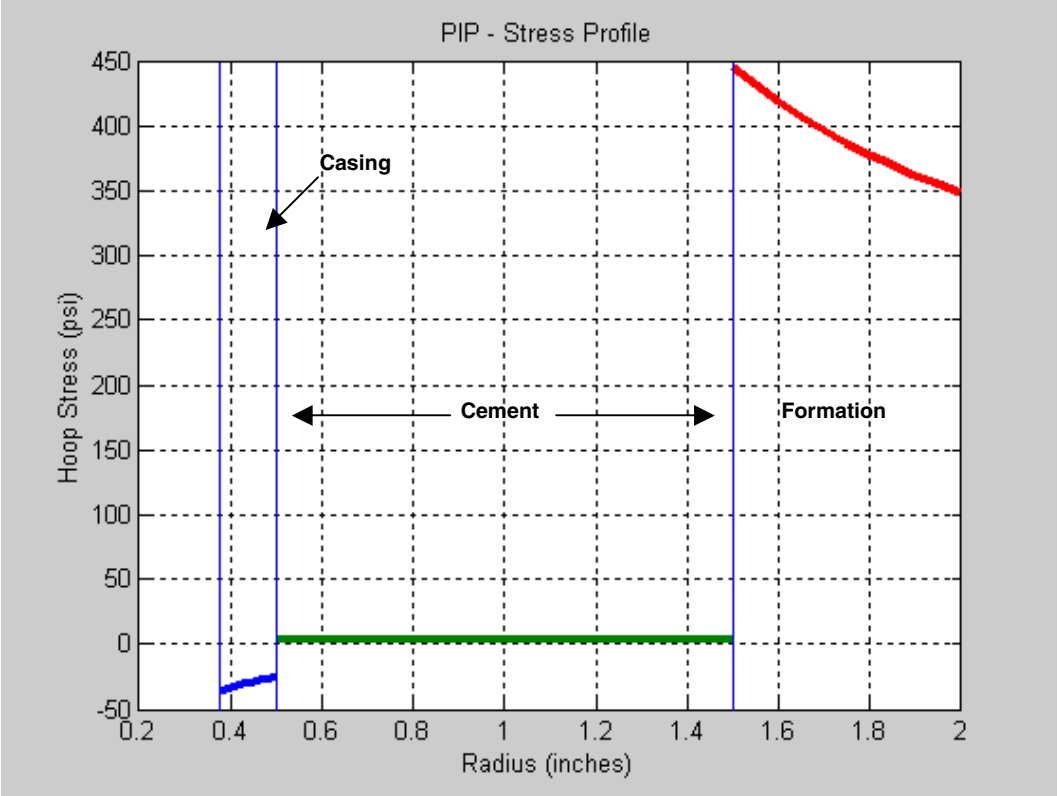

Casing Pressure	15 psi
Confining Pressure	100 psi
Hoop Stress Contrast	~ 450 psi

Figure 15—Shear failure, simulated soft formation (2 of 2)

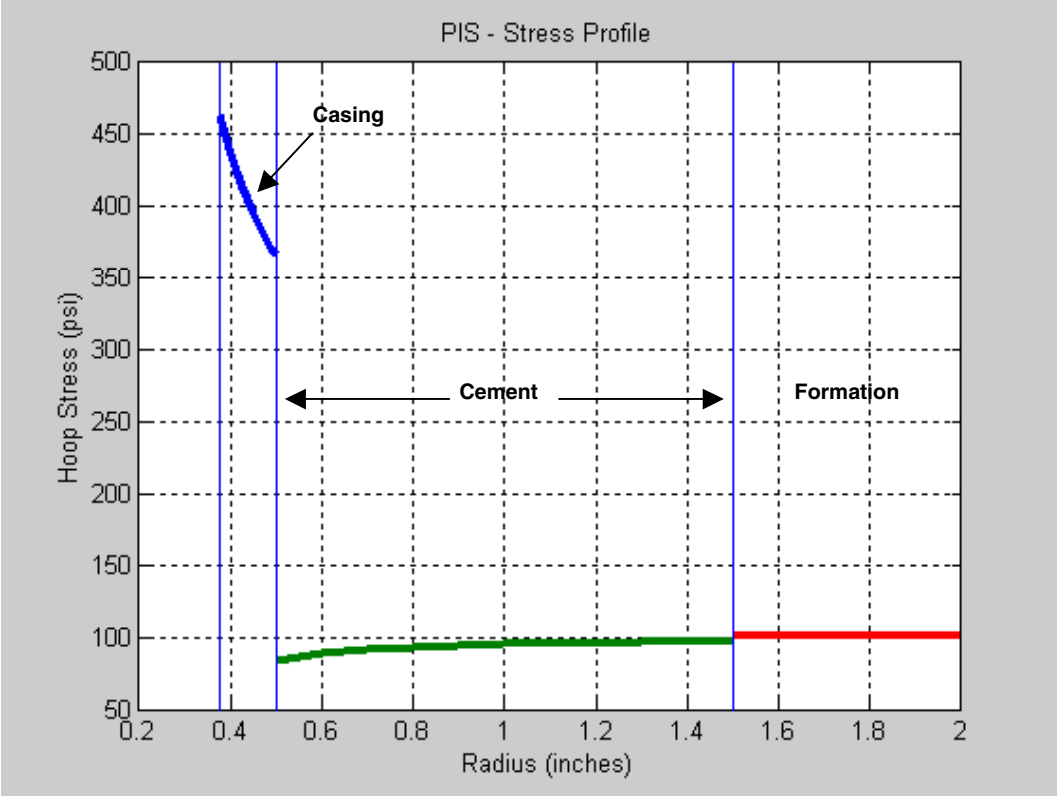

Casing Pressure	15 psi
Confining Pressure	100 psi
Hoop Stress Contrast	~ 300 psi

Heat of Hydration

Cements were tested for the effect of heat of hydration on the cement integrity. First, the borehole temperature was increased from 300K to 400K, and the heat of hydration rate was held constant (**Figure 16**). As the temperature increased, the peak temperature moves closer to the pipe-cement interface. Because the steel pipes conduct heat very well, little if any variation is seen in the inner casing or outer pipe.

With a fixed borehole temperature (**Figure 17**), increasing the heat of hydration rate causes an increase in the temperature of the cement sheath. At the peak heat of hydration rate, the temperature is increased by nearly 30C, which can cause considerable stress on the cement system.

When viewed as a radial stress profile (**Figure 18**), the highest heat of hydration rate creates a radial stress of 600 psi on the cement sheath, but little variation of radial stress is observed within the cement.

Figure 16—Heat of hydration, temperature profile (1 of 2)

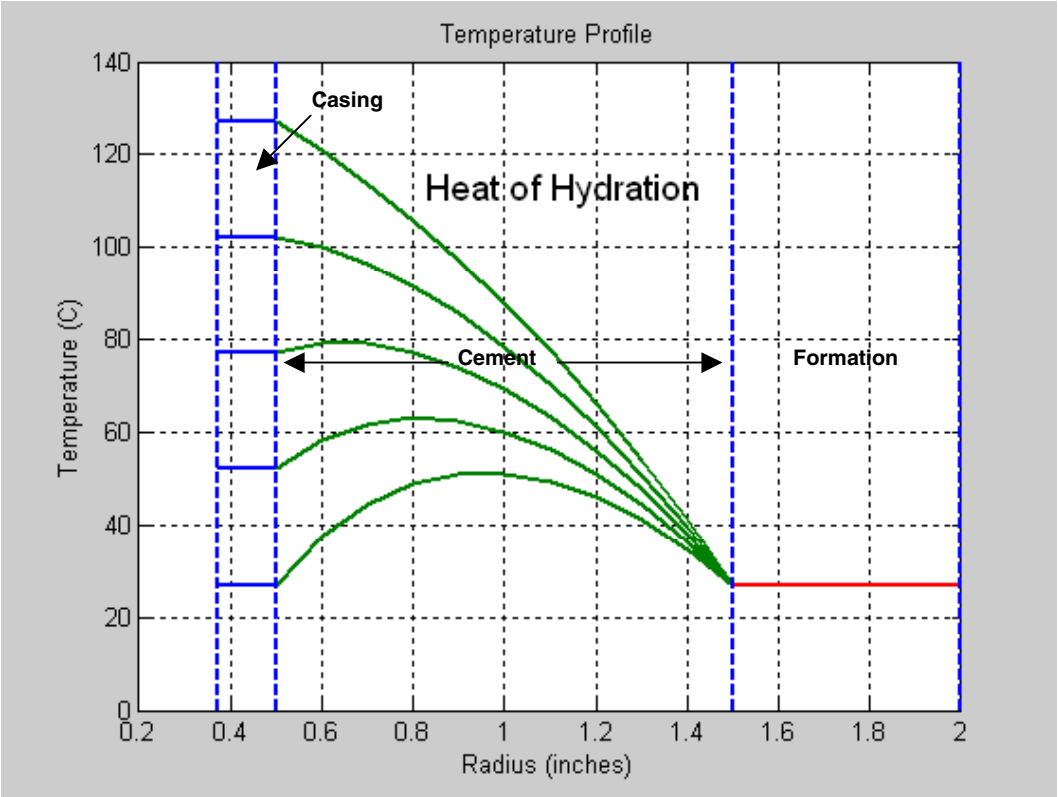

Borehole Temperature	300 K to 400 K
Heat of Hydration Rate	3.5 KJ/Kg.sec

Figure 17—Heat of hydration, temperature profile (2 of 2)

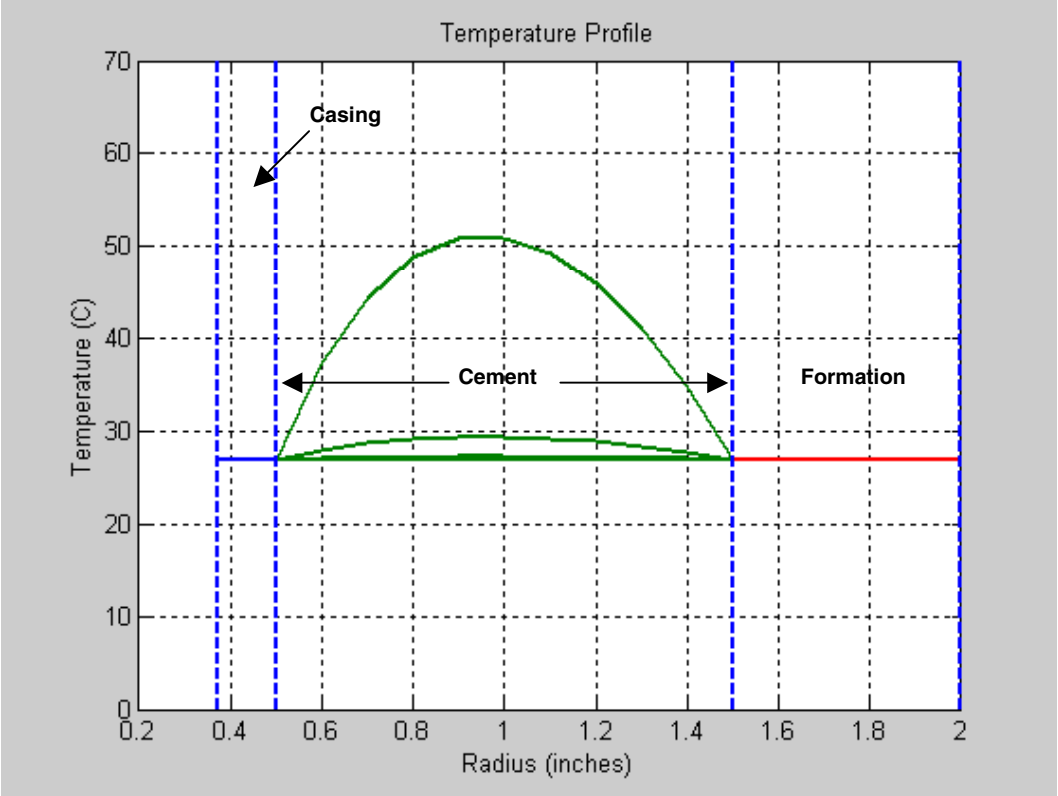

Borehole Temperature	300 K
Heat of Hydration Rate	3.5 KJ/Kg.sec - 3.5 KJ/Kg.sec

Figure 18—Heat of hydration, radial stress profile

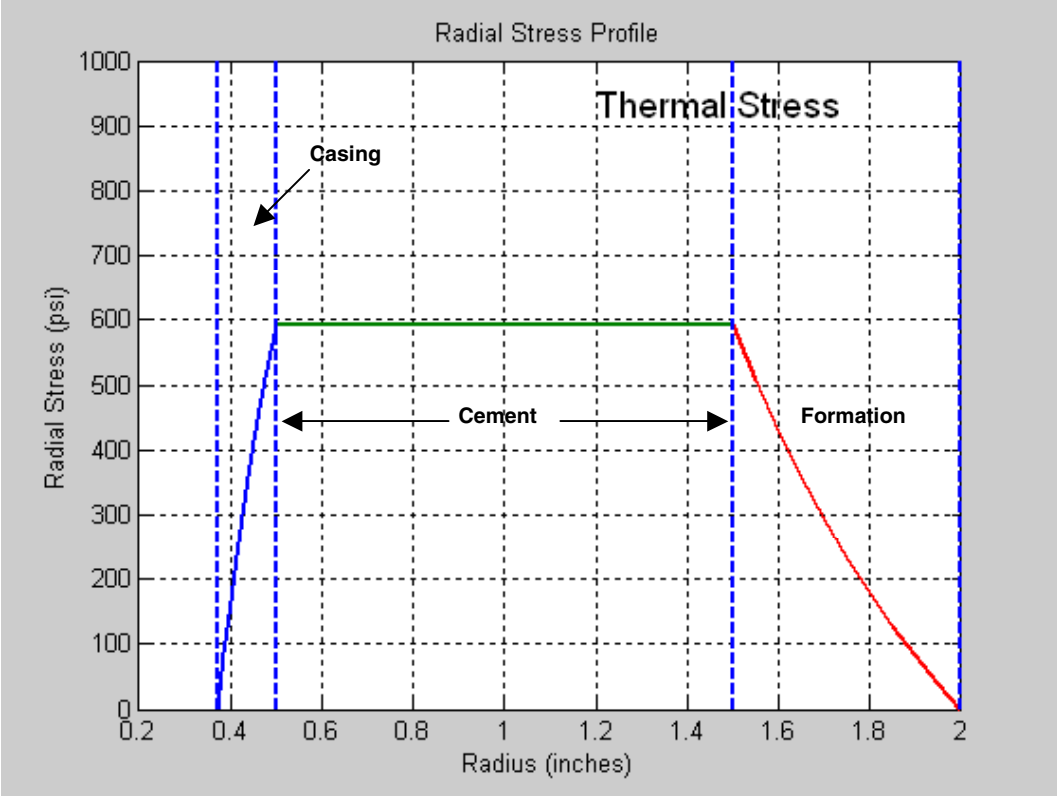

Borehole Temperature	300 K
Reservoir Temperature	300 K

Linear Superposition with Elastic Stress

Thermal Stress

Thermal stress tests were performed to evaluate the effect of thermal stress on the cement. **Figure 19** plots the differences between the borehole temperature and two different reservoir temperatures.

The large temperature contrast between the inner casing and formation can cause significant radial stress (as much as 700 psi in **Figure 20**), which can affect the integrity of cement. However, the radial stress does not vary greatly within the cement.

Figure 19—Thermal stress, temperature profile

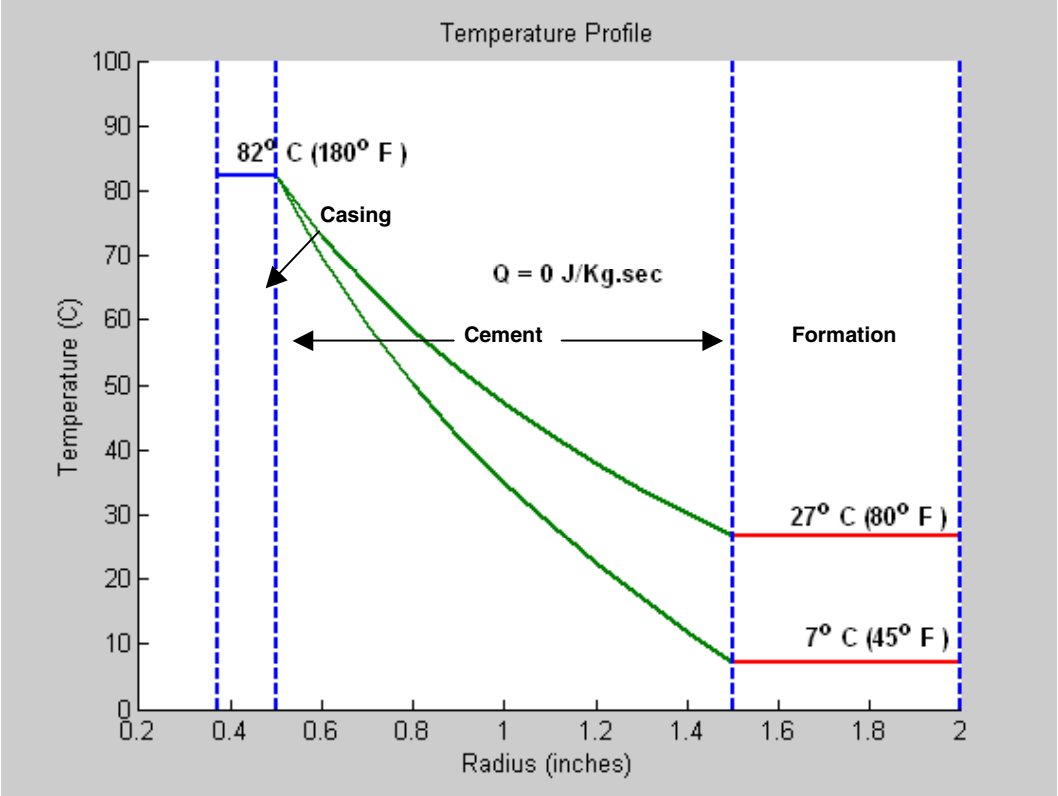

Borehole Temperature	180°F
Reservoir Temperature	45°F, 80°F
Heat of Hydration Rate	0 J/Kg.sec

Figure 20—Thermal stress, radial stress profile

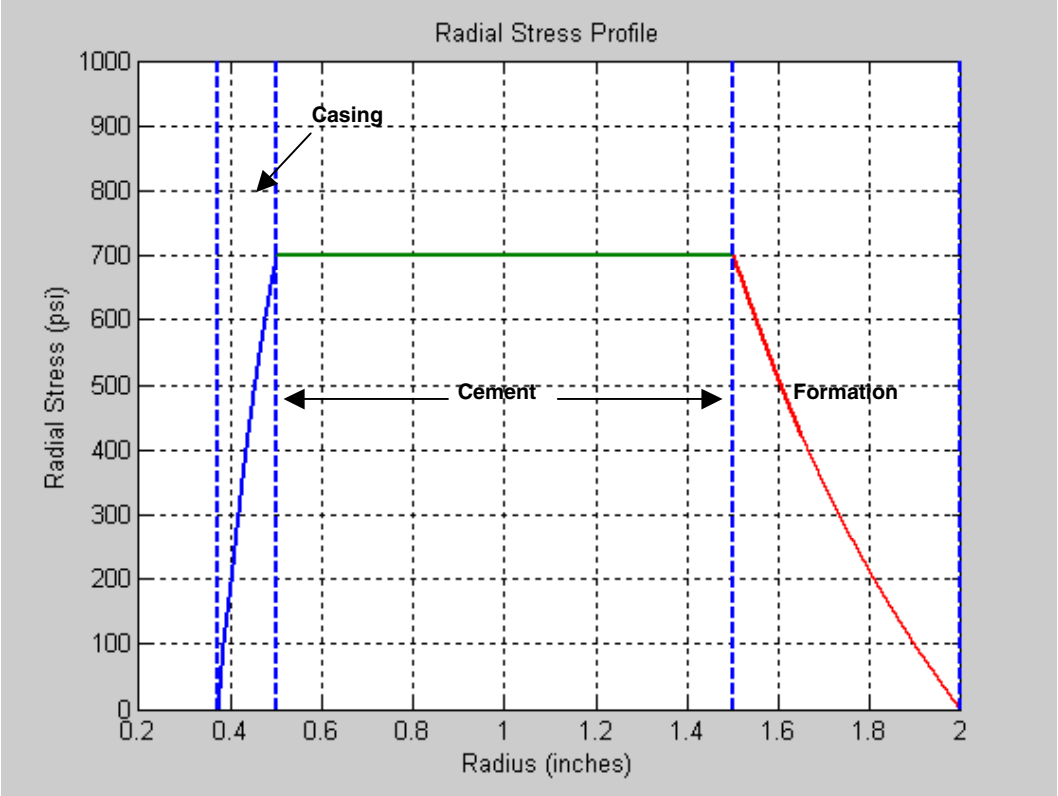

Borehole Temperature	180°F
Reservoir Temperature	45°F, 80°F
Heat of Hydration Rate	0 J/Kg.sec

- Higher thermal stress
- No significant variation within cement

Hoop Stress (Tensile) without Confining Pressure

Cements were tested to determine how hoop stress would affect the cement, given a specific casing pressure. No hoop stress variation was observed in either the cement or the outer pipe in simulated hard formations (**Figure 21**) and soft formations (**Figure 22**). The only contrast in hoop stress was apparent at the pipe-cement interface. This can be attributed to the difference in the elastic Young's modulus properties of the pipe and the cement.

Figure 21—Hoop stress (tensile), simulated hard formation, 0-psi confining pressure

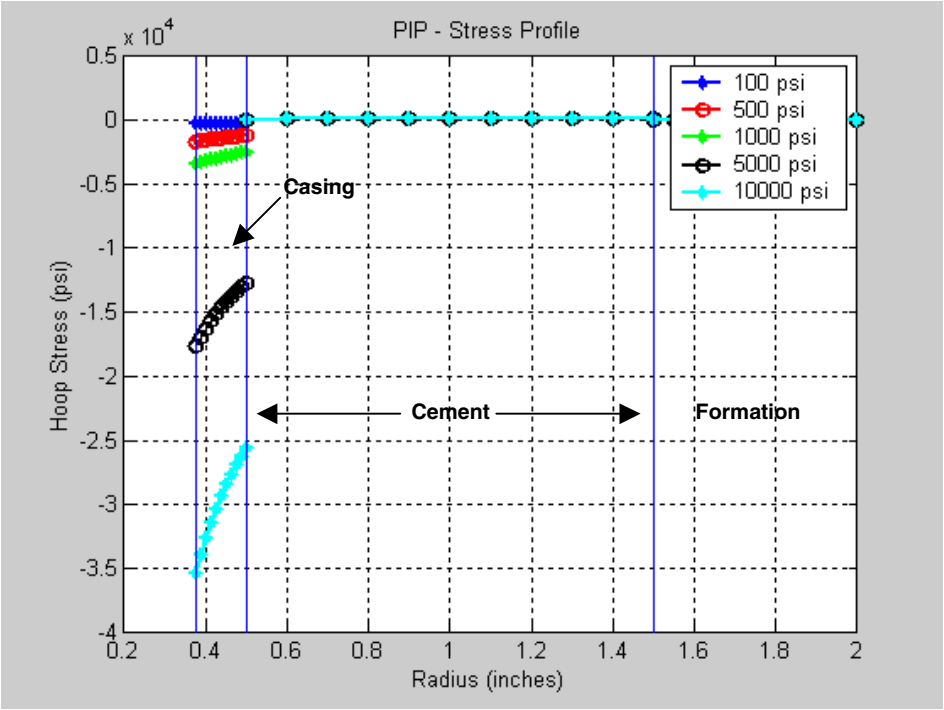

Figure 22— Hoop stress (tensile), simulated soft formation, 0-psi confining pressure

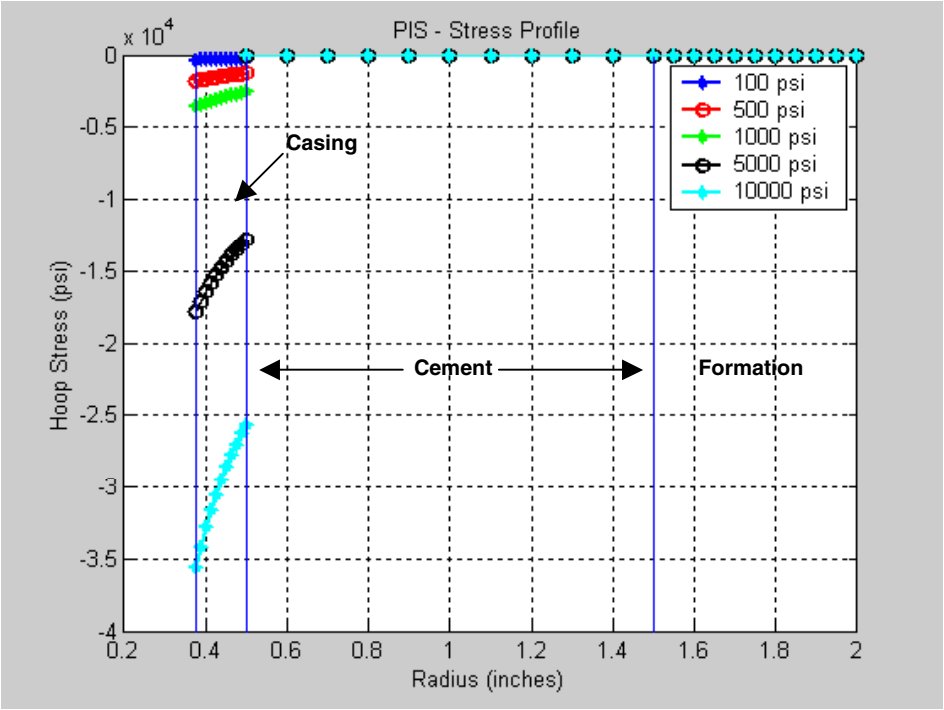

Displacement (No Confining Pressure)

The next set of simulations was conducted to determine the effect of varying casing pressures on displacement, in both hard and soft formations with no confining pressure. In hard formation tests, a larger displacement, and incidentally, a larger variation in displacement, was observed within the cement (**Figure 23**). The displacement of the cement is significantly large to absorb the load.

In simulated soft formations (**Figure 24**), a large displacement (and variation in displacement) was observed for both the cement and the formation.

Figure 23—Displacement profile, simulated hard formation, 0-psi confining pressure

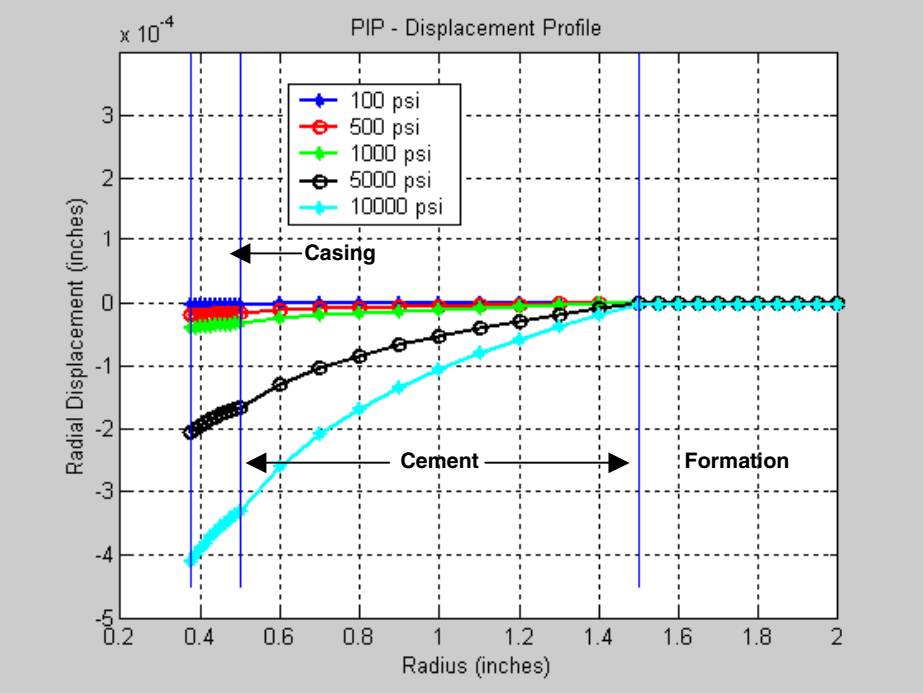

Figure 24—Displacement profile, simulated soft formation, 0-psi confining pressure

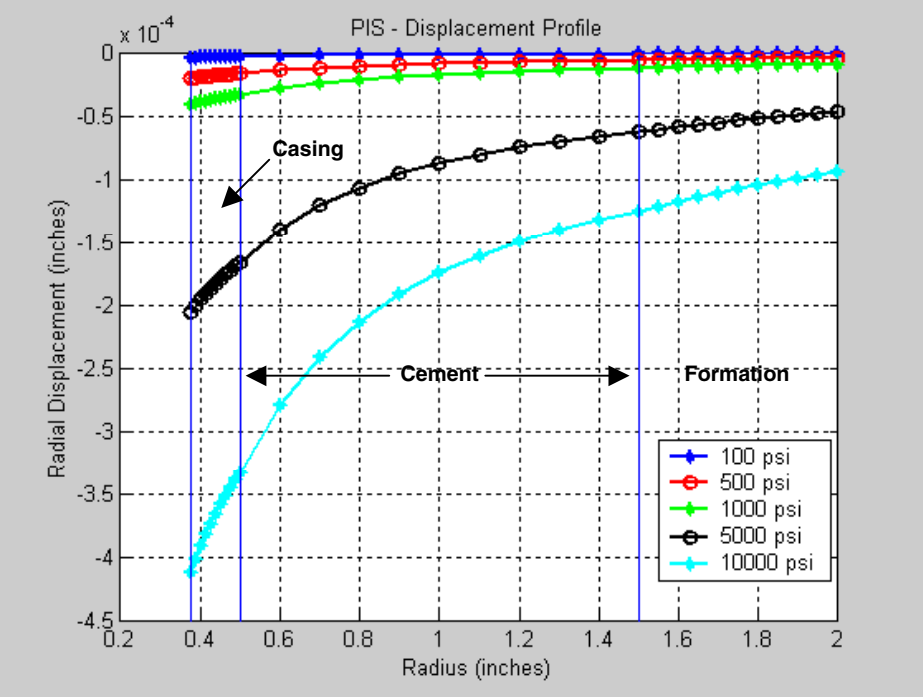

Hoop Stress (Tensile) with Confining Pressure

Tests were also performed to determine the effect of varying casing pressures on hoop stress with 500-psi confining pressure.

When applied to a simulated hard formation configuration (**Figure 25**), the test indicated that increasing casing pressures result in an increase in hoop stress at the cement-outer pipe interface; yet, the cement itself does not experience much hoop stress.

Increasing casing pressures in the simulated soft formation test (**Figure 26**) revealed a slightly higher hoop stress in the cement and the formation, but no significant contrast in hoop stress at the cement-formation interface.

Figure 25—Hoop stress (tensile), simulated hard formation, 500-psi confining pressure

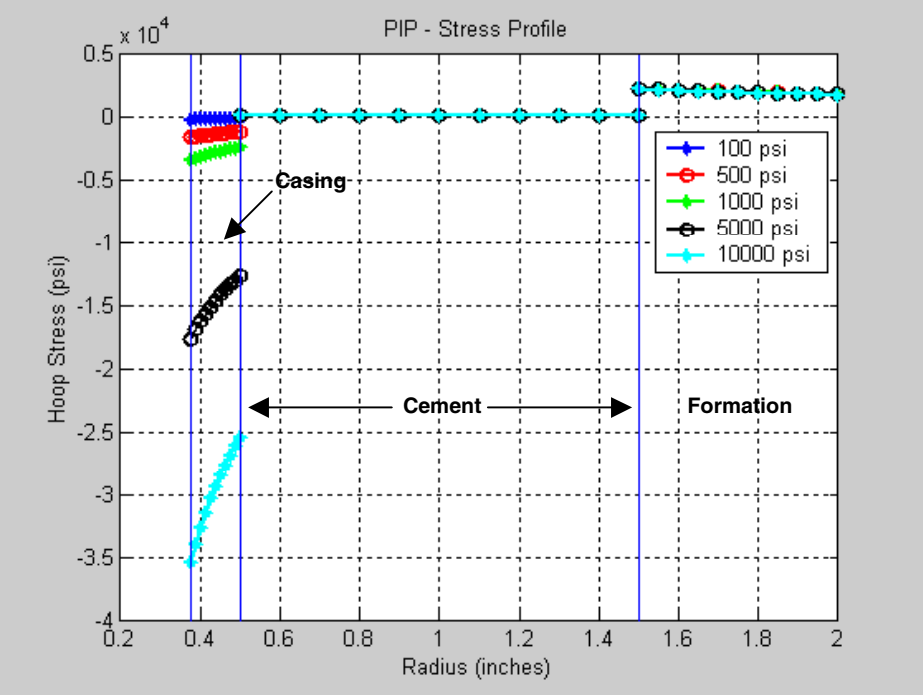

Figure 26—Hoop stress (tensile), simulated soft formation, 500-psi confining pressure

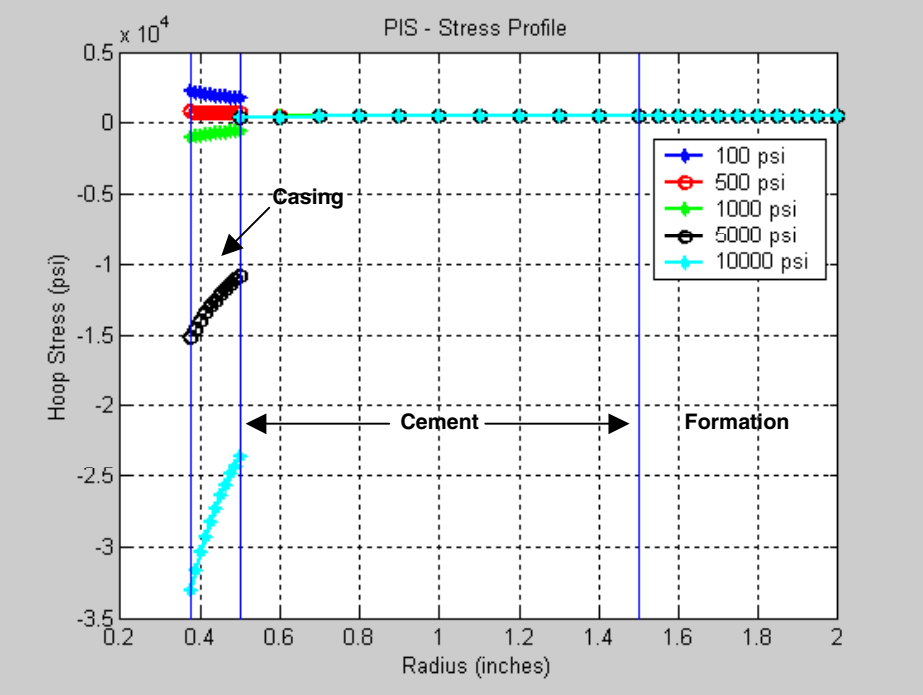

Displacement with Confining Pressure

As casing pressures vary and confining pressure is held constant in a hard formation, hoop stress increases in the formation, and stays constant in the cement. Displacement, rather, varies within the cement, and is almost constant in the formation (**Figure 27**).

As casing pressures are varied and confining pressure is held constant in a soft formation, hoop stress is slightly greater than that of the hard formation, and remains constant through the cement-formation interface. Displacement varies significantly in both the cement and the formation (**Figure 28**). This variation helps explain why no significant difference in hoop stress values is seen at the cement-formation interface in Figure 26.

Figure 27—Displacement profile, simulated hard formation, 500-psi confining pressure

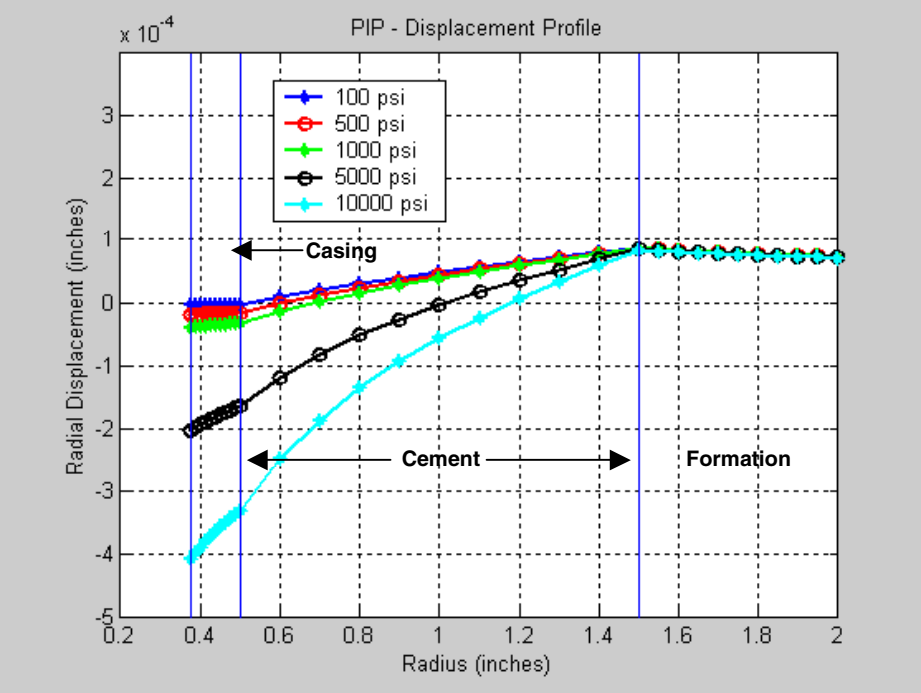

Figure 28— Displacement profile, simulated soft formation, 500-psi confining pressure

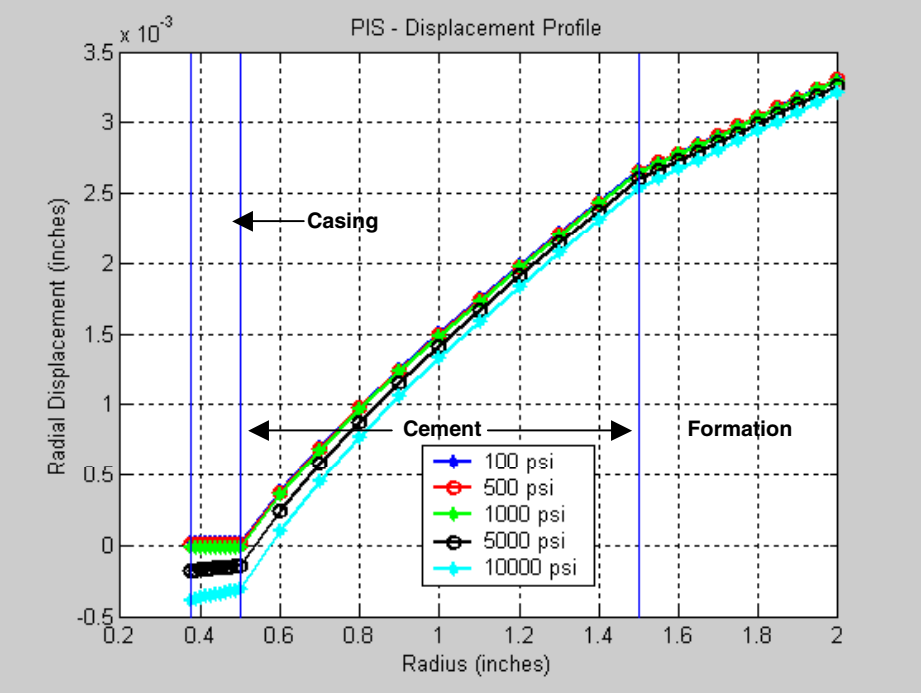

Appendix A—Young's Modulus Testing

Traditional Young's modulus testing was performed using ASTM C469[1], Standard Test Method for Static Modulus of Elasticity (Young's Modulus) and Poisson's Ratio of Concrete in Compression.

The following procedure is used for the Young's modulus testing.

1. Each sample is inspected for cracks and defects.
2. The sample is cut to a length of 3.0 in.
3. The sample's end surfaces are then ground to get a flat, polished surface with perpendicular ends.
4. The sample's physical dimensions (length, diameter, weight) are measured.
5. The sample is placed in a Viton jacket.
6. The sample is mounted in the Young's modulus testing apparatus.
7. The sample is brought to 100-psi confining pressure and axial pressure. The sample is allowed to stand for 15 to 30 min until stress and strain are at equilibrium. (In case of an unconfined test, only axial load is applied.)
8. The axial and confining stress are then increased at a rate of 25 to 50 psi/min to bring the sample to the desired confining stress condition. The sample is allowed to stand until stress and strain reach equilibrium.
9. The sample is subjected to a constant strain rate of 2.5 mm/hr.
10. During the test, the pore-lines on the end-cups of the piston are open to atmosphere to prevent pore-pressure buildup.
11. After the sample fails, the system is brought back to the atmospheric stress condition. The sample is removed from the cell and stored.

Appendix B—Tensile Strength Testing

Tensile strength was tested using ASTM C496[2] (Standard Test Method for Splitting Tensile Strength of Cylindrical Concrete Specimens). For this testing, the specimen dimensions were 1.5 in. diameter by 1 in. long. **Figure B1** shows a general schematic of how each specimen is oriented on its side when tested. The force was applied by constant displacement of the bottom plate at a rate of 1 mm every 10 minutes. Change in the specimen diameter can be calculated from the test plate displacement. The (compressive) strength of the specimen during the test can be graphed along with the diametric strain (change in diameter/original diameter) to generate the tensile Young's modulus.

Figure B1—Sample Orientation for ASTM C496-90 Testing

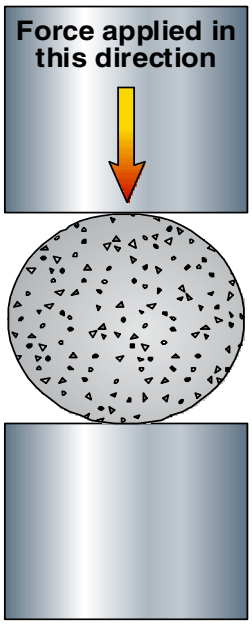

Appendix C—Shear Bond Strength Testing

Shear bond strength tests are used for investigating the effect that restraining force has on shear bond. Samples are cured in a pipe-in-pipe configuration (**Figure C1**) and in a pipe-in-soft configuration (**Figure C2**). The pipe-in-pipe configuration consists of a sandblasted internal pipe with an outer diameter (OD) of $1\ ^{1}/_{16}$ in. and a sandblasted external pipe with an internal diameter (ID) of 3 in. and lengths of 6 in. A contoured base and top are used to center the internal pipe within the external pipe. The base extends into the annulus 1 in. and cement fills the annulus to a length of 4 in. The top 1 in. of annulus contains water.

For the pipe-in-soft shear bonds, plastisol is used to allow the cement to cure in a less-rigid, lower-restraint environment. Plastisol is a mixture of a resin and a plasticizer that creates a soft, flexible substance. This particular plastisol blend (PolyOne's Denflex PX-10510-A) creates a substance with a hardness of 40 duro.

The pipe-in-soft configuration contains a sandblasted external pipe with an ID of 4 in. A molded plastisol sleeve with an ID of 3.0 in. and uniform thickness of 0.5 in. fits inside this external pipe. With the aid of a contoured base and top, a sandblasted internal pipe with an OD of $1\ ^{1}/_{16}$ in. is then centered within the plastisol sleeve. The pipes and sleeve are 6 in. long. The base extends into the annulus 1 in. and cement fills the annulus to a length of 4 in. between the plastisol sleeve and the inner $1\ ^{1}/_{16}$ -in. pipe. The top inch of annulus is filled with water.

Figure C1—Cross-Section of Pipe-in-Pipe Configuration for Shear Bond Tests

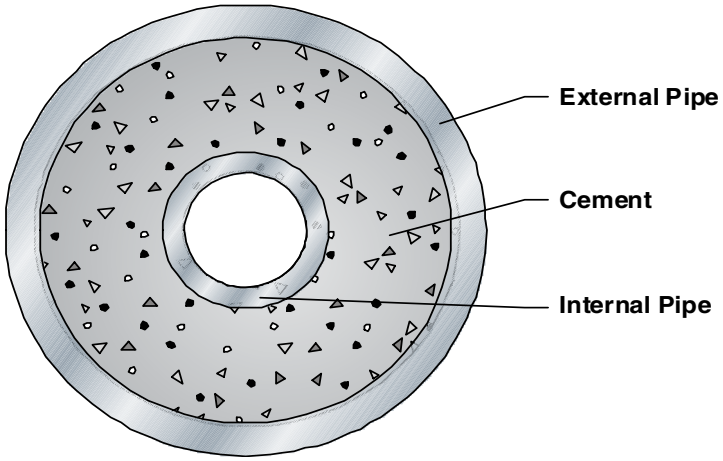

Figure C2— Cross-Section of Pipe-in-Soft Configuration for Shear Bond Tests

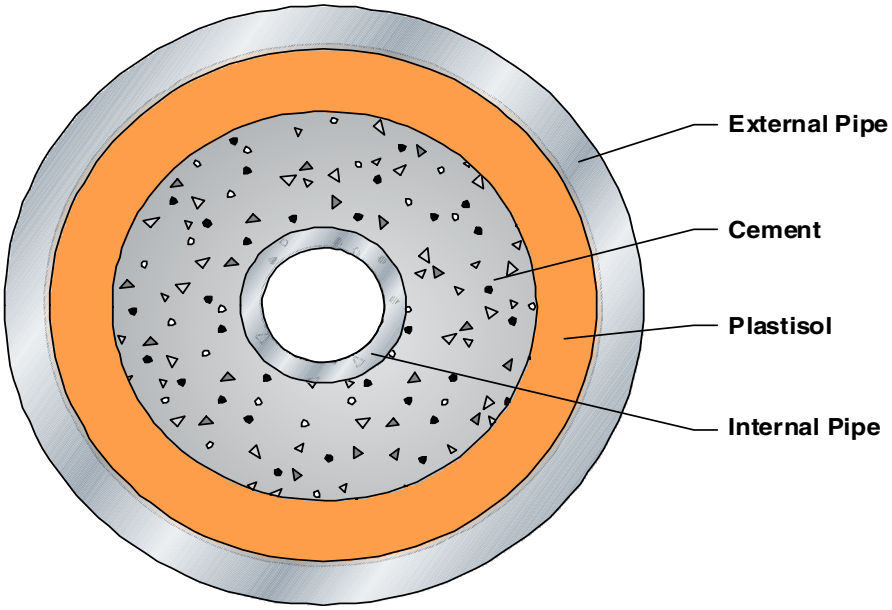

The shear bond measures the stress necessary to break the bond between the cement and the internal pipe. This was measured with the aid of a test jig that provides a platform for the base of the cement to rest against as force is applied to the internal pipe to press it through. (**Figure C3**) The shear bond force is the force required to move the internal pipe. The pipe is pressed only to the point that the bond is broken; the pipe is not pushed out of the cement. The shear bond strength is the force required to break the bond (move the pipe) divided by the surface area between the internal pipe and the cement.

Figure C3—Configuration for Testing Shear Bond Strength

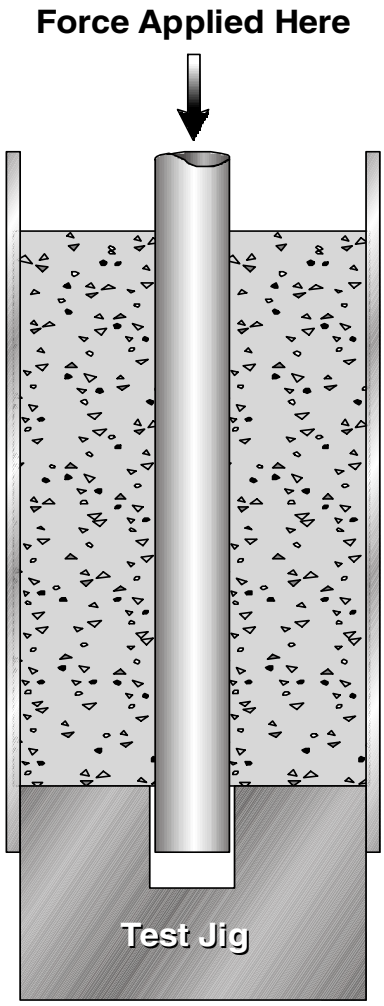

Temperature Cycling

The effect that temperature cycling has on shear bond is tested as follows.

The temperature cycling procedure is designed to simulate temperature conditions that might be encountered during production of a well. The samples are first cured for 14 days in a 45°F water bath at atmospheric pressure. They are then subjected to five days of temperature cycling. During each of these five days of temperature cycling, the cured samples are cycled as follows.

1. Samples are removed from 45°F water bath and placed in 96°F water bath for one hour.
2. Samples are placed in 180°F water bath for four hours.
3. Samples are placed in 96°F water bath for one hour.

4. Samples are placed back in 45°F water bath.

Pressure Cycling

The effect that pressure cycling has on shear bond is tested as follows.

The pressure cycling procedure is designed to simulate pressure conditions that might be encountered during production of a well. Because these samples will be dealing with high pressures, the interior pipe of each sample was made from 1-in. diameter, 40/41 coiled tubing pipe that can withstand 10,000 psi. Each end of the pipe is threaded. One end will have a pressure-tight cap on it during pressure cycling and the other end of the pipe will be connected to the pressure source.

The samples are first cured for 14 days in a 45°F water bath at atmospheric pressure. They are then subjected to five periods of pressure cycling in which the interior pipe is pressured to 5,000 psi for 10 minutes and then allowed to rest at 0 psi for 10 minutes.

Appendix D—Shrinkage Testing

Using a modified Chandler Model 7150 Fluid Migration Analyzer, tests are performed to determine shrinkage of the neat Type I cement. The following procedures are used for performing the shrinkage testing.

1. Fill the test cell with 180 cm^3 of the cement slurry.
2. Place 40 mL of water on top of cement slurry.
3. Place the hollow hydraulic piston into the test cell and on top of the water.
4. Close off the test cell and attach the pressure lines and piston displacement analyzer.
5. Close all valves except valve on top of test cell cap. Purge air out of system.
6. Apply 1,000-psi hydrostatic piston pressure to the test cell and begin recording data (time, piston displacement, and pressure).
7. Run test and gather data for desired amount of time.

Appendix E—Annular Seal Testing

The following procedures are for the use of the Pipe-in-Soft annular seal apparatus (for simulating soft formations) and the Pipe-in-Pipe annular seal apparatus (for simulating hard formations). The Pipe-in-Soft apparatus is to be used with cores that were formed using a soft gel mold surrounding the cement slurry to form a core that was cured to set by using a semi-restricting force on the outside of the core. The Pipe-in-Pipe apparatus is to be used with cores that were made inside steel pipes, giving the cement slurry a restricting force outside of the core.

Simulated Soft Formation Test Procedure

1.) After the core is cured, place the core inside the gel mold sleeve.
2.) Place the core and sleeve inside the Pipe-in-Soft steel cell.
3.) Once inside, both ends of the core are supported with o-rings.
4.) The o-rings are then tightened to close off air-leaks that might be present.
5.) Using water, pressurize the exterior circumference of the sleeve to 25 psi. Once the pressurized water is applied to the cell, check for leaks on the ends of the cell.
6.) Using the cell's end caps, cap off both ends of the steel cell. One end cap has a fitting that allows for N_2 gas to be applied into the cell, and the other end cap allows for the gas to exit the cell.
7.) Attach the pressure in-line to one end and then attach the pressure out-line to the other end.
8.) Apply pressure to the in-line. (Do not exceed 20 psig.) Measure the output of the out-line with flowmeters.

Simulated Hard Formation Test Procedure

1.) After the core is cured inside the steel pipe, using steel end caps, cap off each end of the pipe. Each end cap has a fitting that allows for gas to be applied into the pipe on one end, and also allows for the gas to exit the pipe on the other end.
2.) Attach the pressure in-line to one end, and then attach the pressure out-line to the other end.
3.) Apply pressure to the in-line. (Do not exceed 20 psig.) Measure the pressure output of the out-line with flowmeters.

Appendix F—Chandler Engineering Mechanical Properties Analyzer

See the attached brochure for a detailed description of the Chandler Engineering Mechanical Properties Analyzer, its applications, and its benefits.

MECHANICAL PROPERTIES ANALYZER

In recent years the oil/gas industry has begun to understand the implication of cement sheath mechanical properties on the ability of the cement to perform its zonal isolation function long term. With computer modeling capabilities, the mechanical compliance of the cement sheath relative to the deformation of the contacting rock and casing can be optimized to improve wellbore sealing. Cement formulations are being developed to address the need for flexure of the cement, rather than say the need for high compressive strength. However, the measurement of cement mechanical properties at elevated pressure and temperature has limited the implementation of cement mechanical properties as a design protocol.

With a technological breakthrough (patent applied), Chandler Engineering has developed the first high-pressure, high-temperature instrument designed specifically to measure the mechanical properties (elastic moduli and compressive strength) of oil/gas-well cements. Like the Ultrasonic Cement Analyzer (UCA), testing with the new Mechanical Properties Analyzer (Model 6265 MPro) begins with a cement slurry, which is placed into a pressure vessel. Measurements are then taken directly from this sample as it cures at elevated temperature and pressure.

The ***CHANDLER*** Model 6265 MPro has several advantages over routine mechanical properties testing. First, by providing continuous measurements, a single test with the MPro can provide more information about the cement properties than one would get from a series of routine tests. Second, samples for routine testing are typically cured in one vessel returned to room conditions, and then cored and/or cut, before testing begins in a different pressure vessel. With the MPro the sample conditions and integrity are maintained for the duration of the test (which may be days, weeks, or even months). Thus,

MODEL 6265 MPro

the MPro samples are neither subjected to damage from preparation, and handling, nor from unrealistic cooling and depressurization.

The ***CHANDLER*** Model 6265 MPro is optionally configured to perform UCA (compressive strength) Analyses in addition to the elastic mechanical properties measurements - thus providing a suite of information from a single sample and single test, and optimizing laboratory efficiency.

The new Model 6265 MPro includes programmable temperature control which provides the capability to investigate the impact of temperature variations on the cement mechanical properties. With the Chandler Model 6265P programmable pressure control module, the user can simulate realistic pressure conditions to evaluate the impact on the mechanical properties of the cement sample.

Combining the programmable pressure control module with programmable temperature control, will allow the investigator to replicate realistic pressure and temperature conditions.

Using Chandler Engineering's state-of-the-art 5270 Automation System, complex-testing protocols can be easily set up and run using a standard PC. The 5270 System can be optionally configured to control and collect/display/analyze data from several Model 6265 MPro's.

MODEL 6265P
PROGRAMMABLE PRESSURE
CONTROL MODULE

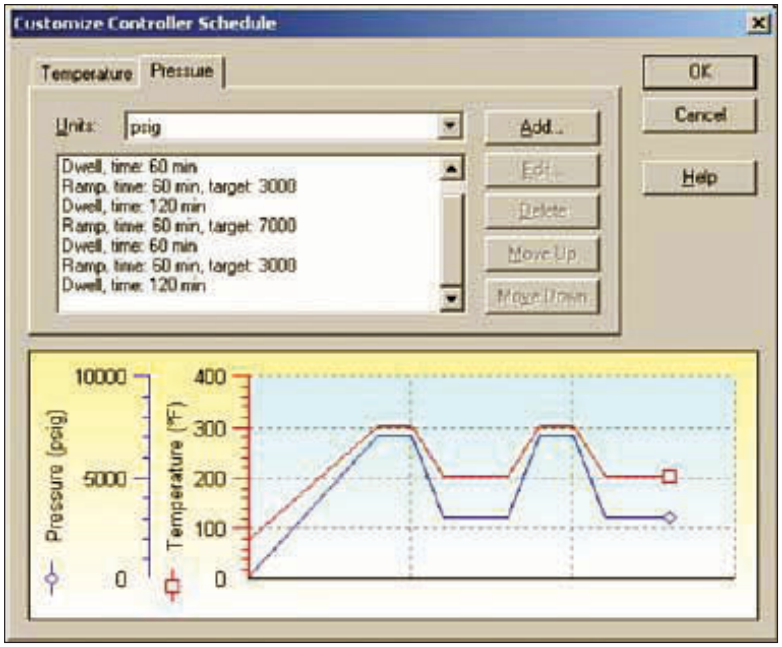

Cement Mechanical Properties Testing
Chandler Engineering Model 6265 Data
Young's Modulus vs Time

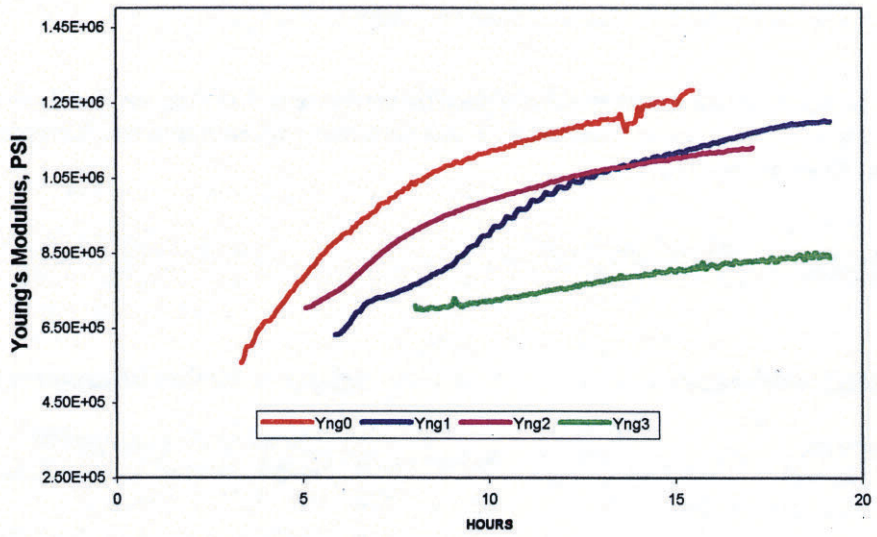

Cement Mechanical Properties Testing
Chandler Engineering Model 6265 Data
Poisson's Ratio vs Time

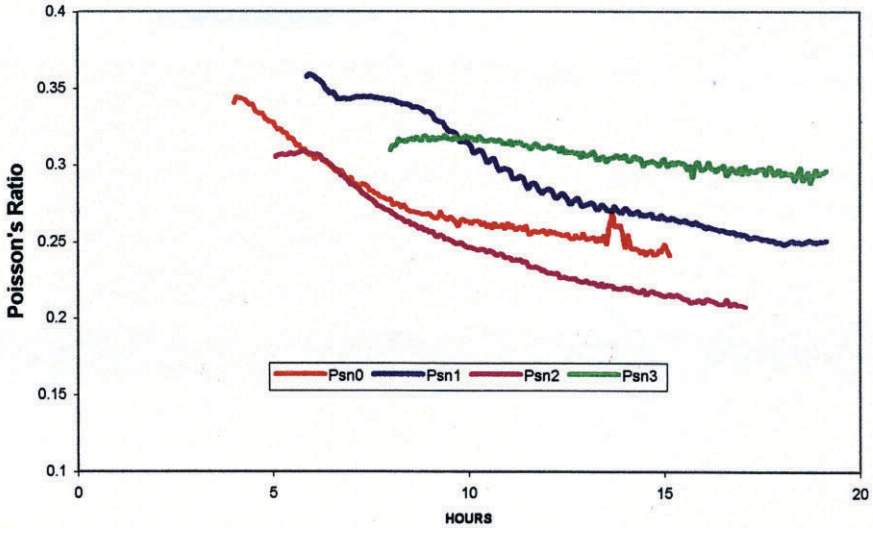

All Chandler Engineering products are covered by a full one-year warranty against defects in materials and workmanship. Sales terms, conditions and warranty statements are included with each quotation or confirmation of order.

More than 50 years ago, Chandler Engineering pioneered High Pressure and High Temperature Equipment. Today, Chandler Engineering is the leading manufacturer of a broad range of innovative and extremely reliable Measurement Instruments for the Energy Industry.

Chandler Engineering specializes in outfitting laboratories designed for testing cement, drilling muds and stimulation fluids. Through Research & Development, experienced manufacturing and worldwide logistic operations, Chandler Engineering provides for your complete laboratory requirements.

DRILLING AND COMPLETION INSTRUMENTS

- Cement Consistometers
- Cement Curing Chambers
- Cement Gas Migration Instruments
- Compressive Strength Testers
- Computer Automated Core-flow Instruments
- Constant Speed Mixers
- Corrosion Test Apparatus
- Data Acquisition System
- Liquid/Slurry HPHT Rheometers
- Portable Mud/Cement Laboratories
- Static Gel Strength Analyzer (SGSA)
- Stirred Fluid Loss Cells
- Ultrasonic Cement Analyzer (UCA)
- Viscometers (Atmospheric and Pressurized)

PIPELINE AND INDUSTRIAL INSTRUMENTS

- Carle Gas Chromatographs
- Hydraulic Pressure Testers and Gauges
- Liquid Densitometers
- Natural Gas Heating Value Analyzers
- Natural Gas Moisture Analyzers
- Ranarex Gas Gravitometers

RUSKA FLUID TECHNOLOGY INSTRUMENTS

- PVT Systems
- Digital Gasometers
- Digital High Pressure Pumps
- Phase Detection Systems
- Sample Cylinders

Plus a full range of replacement parts and accessories for all our instruments.
Contact us for our latest catalog of Cement Testing Laboratory Equipment, and other instruments for testing Oil Well Cements, Drilling Fluids, and Precision Physical Property Measurement Instrumentation for the Natural Gas Industry.